NAVAL POSTGRADUATE SCHOOL

MONTEREY, CALIFORNIA

THESIS

FABRICATION AND CHARACTERIZATION OF SURROGATE GLASSES AIMED TO VALIDATE NUCLEAR FORENSIC TECHNIQUES

by

Ken G. Foos

December 2017

Thesis Advisor: Claudia C. Luhrs
Co-Advisor: Chun-Hsien Wu

THIS PAGE INTENTIONALLY LEFT BLANK

REPORT DOCUMENTATION PAGE	*Form Approved OMB No. 0704-0188*

1. AGENCY USE ONLY *(Leave blank)*	**2. REPORT DATE** December 2017	**3. REPORT TYPE AND DATES COVERED** Master's thesis

4. TITLE AND SUBTITLE
FABRICATION AND CHARACTERIZATION OF SURROGATE GLASSES AIMED TO VALIDATE NUCLEAR FORENSIC TECHNIQUES

5. FUNDING NUMBERS

6. AUTHOR(S) Ken G. Foos

7. PERFORMING ORGANIZATION NAME(S) AND ADDRESS(ES)
Naval Postgraduate School
Monterey, CA 93943-5000

8. PERFORMING ORGANIZATION REPORT NUMBER

9. SPONSORING /MONITORING AGENCY NAME(S) AND ADDRESS(ES)
DTRA

10. SPONSORING / MONITORING AGENCY REPORT NUMBER

11. SUPPLEMENTARY NOTES The views expressed in this thesis are those of the author and do not reflect the official policy or position of the Department of Defense or the U.S. Government. IRB number ____N/A____.

12a. DISTRIBUTION / AVAILABILITY STATEMENT
Approved for public release. Distribution is unlimited.

12b. DISTRIBUTION CODE

13. ABSTRACT (maximum 200 words)

The aim of this study was the fabrication and characterization of surrogate glasses to support validation of a nuclear forensic technique called Laser-Driven Hydrothermal Processing (LDHP). Previous examination of inhomogeneous natural materials obsidian and tektite confirmed potential benefits of the LDHP technique with regard to separation of elements of interest from the bulk silica structure during processing. However, natural materials are too inhomogeneous, making it difficult to clearly determine which features were present in the sample before LDHP and which were caused by it.

In this study, the sol-gel process involving acid or base catalysts was used as the fabrication method. The average elemental composition of tektite served as the target composition for surrogate material. Fe and Ti were introduced in solution as a salt and an alkoxide, respectively, to represent the presence of transition elements since no radioactive materials were used. Precursors for the remaining elemental components were then added to form the sol. Through variations in the hydrolysis, polymerization, drying and dehydration steps, the successful fabrication of xerogel products sharing the elemental composition of tektite but presenting a more homogeneous distribution of phases was achieved. Specimens like the ones produced herein, with greater homogeneity, will be more suitable to quantify the effects of applying novel forensic techniques such as LDHP.

14. SUBJECT TERMS laser-driven hydrothermal processing, surrogate glass, sol-gel, materials fabrication	**15. NUMBER OF PAGES** 161
	16. PRICE CODE

17. SECURITY CLASSIFICATION OF REPORT	**18. SECURITY CLASSIFICATION OF THIS PAGE**	**19. SECURITY CLASSIFICATION OF ABSTRACT**	**20. LIMITATION OF ABSTRACT**
Unclassified	Unclassified	Unclassified	UU

NSN 7540-01-280-5500 Standard Form 298 (Rev. 2-89)
Prescribed by ANSI Std. 239-18

THIS PAGE INTENTIONALLY LEFT BLANK

Approved for public release. Distribution is unlimited.

FABRICATION AND CHARACTERIZATION OF SURROGATE GLASSES AIMED TO VALIDATE NUCLEAR FORENSIC TECHNIQUES

Ken G. Foos
Lieutenant Commander, United States Navy
B.S., The Pennsylvania State University, 2004

Submitted in partial fulfillment of the
requirements for the degree of

MASTER OF SCIENCE IN MECHANICAL ENGINEERING

from the

NAVAL POSTGRADUATE SCHOOL
December 2017

Approved by: Claudia C. Luhrs
Thesis Advisor

Chun-Hsien Wu
Co-Advisor

Garth V. Hobson
Chair, Department of Mechanical and Aerospace Engineering

THIS PAGE INTENTIONALLY LEFT BLANK

ABSTRACT

The aim of this study was the fabrication and characterization of surrogate glasses to support validation of a nuclear forensic technique called Laser-Driven Hydrothermal Processing (LDHP). Previous examination of inhomogeneous natural materials obsidian and tektite confirmed potential benefits of the LDHP technique with regard to separation of elements of interest from the bulk silica structure during processing. However, natural materials are too inhomogeneous, making it difficult to clearly determine which features were present in the sample before LDHP and which were caused by it.

In this study, the sol-gel process involving acid or base catalysts was used as the fabrication method. The average elemental composition of tektite served as the target composition for surrogate material. Fe and Ti were introduced in solution as a salt and an alkoxide, respectively, to represent the presence of transition elements since no radioactive materials were used. Precursors for the remaining elemental components were then added to form the sol. Through variations in the hydrolysis, polymerization, drying and dehydration steps, the successful fabrication of xerogel products sharing the elemental composition of tektite but presenting a more homogeneous distribution of phases was achieved. Specimens like the ones produced herein, with greater homogeneity, will be more suitable to quantify the effects of applying novel forensic techniques such as LDHP.

THIS PAGE INTENTIONALLY LEFT BLANK

TABLE OF CONTENTS

LIST OF FIGURES

THIS PAGE INTENTIONALLY LEFT BLANK

LIST OF TABLES

THIS PAGE INTENTIONALLY LEFT BLANK

LIST OF ACRONYMS AND ABBREVIATIONS

Al	aluminum
ALARA	as low as reasonably achievable
Ca	calcium
C/D	cool down
Cl	chloride
cm	centimeter
Cu	copper
DI	deionized
DSC	differential scanning calorimetry
EDS	energy dispersive x-ray spectroscopy
EtOH	ethyl alcohol
Fe	iron
g	gram
HCl	hydrochloric acid
Hg	mercury
HT	heat treatment
in	inch
JADE	pattern processing, identification and quantification software
K	potassium
kV	kilovolt
LDHP	laser-driven hydrothermal processing
LLNL	Lawrence Livermore National Laboratory
mA	milliamp
Mg	magnesium
mm	millimeter
nm	nanometer
NPS	Naval Postgraduate School
Na	sodium
NH_4F	ammonium fluoride
O	oxygen

Pd	palladium
PDXL	integrated x-ray powder diffraction software
pH	potential of hydrogen
Pt	platinum
SEM	scanning electron microscope
Si	silicon
STA	simultaneous thermal analysis
STEM	scanning transmission electron microscopy
TEOS	tetra ethyl ortho silicate
TGA	thermogravimetric analysis
Ti	titanium
wt%	weight percent
XRD	x-ray diffraction
µm	micrometer

ACKNOWLEDGMENTS

I would like to express my profound appreciation for the effort and dedication that Naval Postgraduate School professors and support personnel display to their students. Special thanks to my advisors, Professors Dr. Claudia Luhrs, Dr. Chun-Hsien (William) Wu and Dr. Sarath Menon, for their professional support and personable natures. Without their guidance and training through classes and research, this thesis would not have been possible. I would also like to thank Dr. Ray Mariella, Jr. at Lawrence Livermore National Laboratory for explaining his work and providing insight into the LDHP process, and Ms. Ariana Rodd, who provided assistance as part of the SEAP intern program. To my fellow students, thank you for the fellowship and camaraderie that we shared; it was inspirational to go through this process with you. Special thanks to LT Patrick Stewart, whose partnership in navigating the waters of academia was critical through both support and motivation. This learning experience has been as enlightening and rewarding as it has been challenging.

I am grateful the United States Navy afforded me the exceptional opportunity to receive a higher education at Naval Postgraduate School. To the best of my ability, I will use the knowledge and understanding gained through this curriculum to benefit the U.S. Navy and our nation.

Most important of all, I would like to say thank you to my family, whose support and understanding made this effort possible. I dedicate this work to my wife, Charlene, and our two children, Alexandria and Jacob. Thank you for the love and fellowship that we share; it is the inspiration that drives me to succeed.

THIS PAGE INTENTIONALLY LEFT BLANK

I. INTRODUCTION

A. BACKGROUND

Collection and analysis of materials using nuclear forensics involves inherent levels of risk due to the nature and location of the materials [1], [2]. Often the samples of interest are radioactive or contaminated and are very likely located in areas where there is significant background exposure to the personnel gathering the samples [3]–[5]. Examples include post-nuclear event materials at site of incident, unexploded nuclear devices and/or the evidence left behind by such devices [3], [6]. Exposure could be mitigated by limiting the time that people and devices are close to the site, however, the half-life of major contributors to long term exposure levels are significant enough that delay to an investigation could be incurred since waiting for background levels to decay naturally takes time [1], [4], [5]. Investigating the signatures on the materials is important since through analysis of these materials physical, isotopic and chemical evidence is obtained that can result in identification of the material origin and processing techniques used [2], [6]–[8].

Nuclear forensic analytical methods used to determine material features include optical, mechanical, chemical, radioactive counting, spectroscopic and other techniques according to [2], [6]–[8]. Since small amounts of the source material may be available, the prioritized order of testing is an important decision making process since many of these techniques involve destructive testing as demonstrated in [6], [8]. The testing can also prove to be time consuming as the elements and isotopes of interest need to be separated from the bulk material so that the amounts can be concentrated enough for analysis as shown by [9].

The source material from a nuclear event would generally be inhomogeneous in nature since it will derive from natural minerals and not be suitable for use in validating new analysis techniques that show potential for improvement of both sample processing and safety of personnel [9]. Time, distance and shielding are the basic general methods to reduce personnel exposure to levels that are as low as reasonably achievable (ALARA)

[1], [4], [5]. Being able to collect the samples remotely and perform tests remotely would enable the exposure and risk to personnel to be kept ALARA.

B. LASER-DRIVEN HYDROTHERMAL PROCESSING (LDHP)

Laser-driven hydrothermal processing (LDHP) is an innovative method developed by Dr. Raymond P. Mariella Jr., a senior scientist at Lawrence Livermore National Laboratory. LDHP allows for the rapid comminution of a sample material without contamination from the container or loss of sample material as shown by [10], [11]. The technique can also be applied via remotely operated systems to reduce the hazard posed to personnel. Since the sample is processed while submerged and produces fine sized particles the exposure levels and risk of contamination from the samples is also greatly minimized (Figure 1) [4]. Initial trials using the LDHP method used DI water as the medium for submersion. Additional submersion mediums can be utilized such as alkaline and acidic aqueous solutions, as well as alcohols.

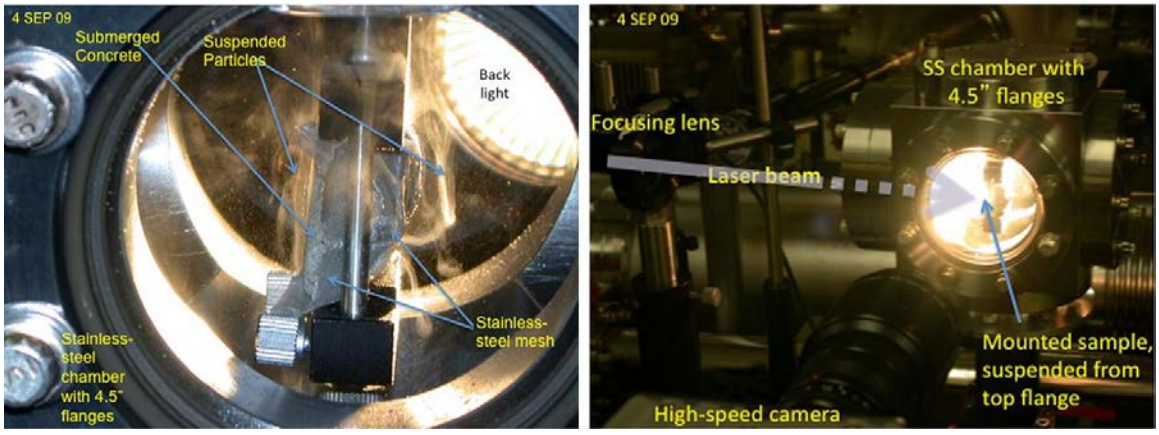

Left: LDHP holder for submerged sample. Technique developed and tested using natural materials including quartzite, obsidian and tektite. Right: General arrangement of submerged medium during LDHP processing.

Figure 1. Arrangement of Submerged Sample and Laser during LDHP Processing of Natural Material (Quartzite). Source: [12].

Preliminary material characterization of LDHP samples mentioned above was performed by Mariella et al using quartzite. Follow on work was conducted at NPS by Camargo et al. The later work focused on analyzing two natural materials that bear similarity in method of formation, such as high pressure and temperature, to a material

formed during a nuclear event [12]. Specifically, tektite and obsidian were the natural materials selected, which form as the result of high pressures and temperatures during meteoritic impact and volcanic activity respectively [13]. Tektite and obsidian have a high SiO_2 composition similar to the glass formed during a nuclear event, trinitite [14]. The SiO_2 composition is generally greater than 50% for trinitite and can vary appreciably between samples for tektite and obsidian due to their inhomogeneous nature [14]. These initial results seem to indicate that the LDHP technique is able to preferentially separate heavier elements of interest from the bulk material of the SiO_2 [15]. This could reduce or eliminate, until certain extent, the chemical processing needed to prior to the sample analysis. Moreover, the chemical processes currently employed to dissolve the specimens are a potential source of contamination from aggressive solution interaction with containers as well as a source of loss of sample material [6].

A basic theory for the mechanism of LDHP was postulated [16] as the energy in the laser light pulse being absorbed at the surface of the bulk material, causing a jump in temperature and, as a result, leading to a thermally driven expansion and pressure wave. The pressure wave and its reflection at the surface can result in fracture and spallation [17]. Modeling with ALE3D, as described in [16], showed that H_2O in contact with the surface of the illuminated material could experience hundreds of atmospheres in pressure in the form of a traveling pressure wave, along with a temperature increase. This short-lived increase in pressure and temperature in the adjacent H_2O was postulated to affect a transient hydrothermal dissolution of the silica-rich material [18], leading to some purification of the SiO_2, when the H_2O would return to ambient temperature and pressure of the room and the transiently-dissolved material precipitated/crystallized.

At lower laser fluences and intensities, the surface becomes enriched in SiO_2, but no visible crater is formed [19]; at higher fluences, craters are formed at the surface of the material as presented by [10], [12], [16]. Particles in the size range of 10 μm to 100 μm are ejected via fracture and spallation into the submersion medium. The transient hydrothermal process releases smaller particles (in the nanometer range) that become suspended in the medium while larger particles would settle to the bottom of the medium (Figure 2).

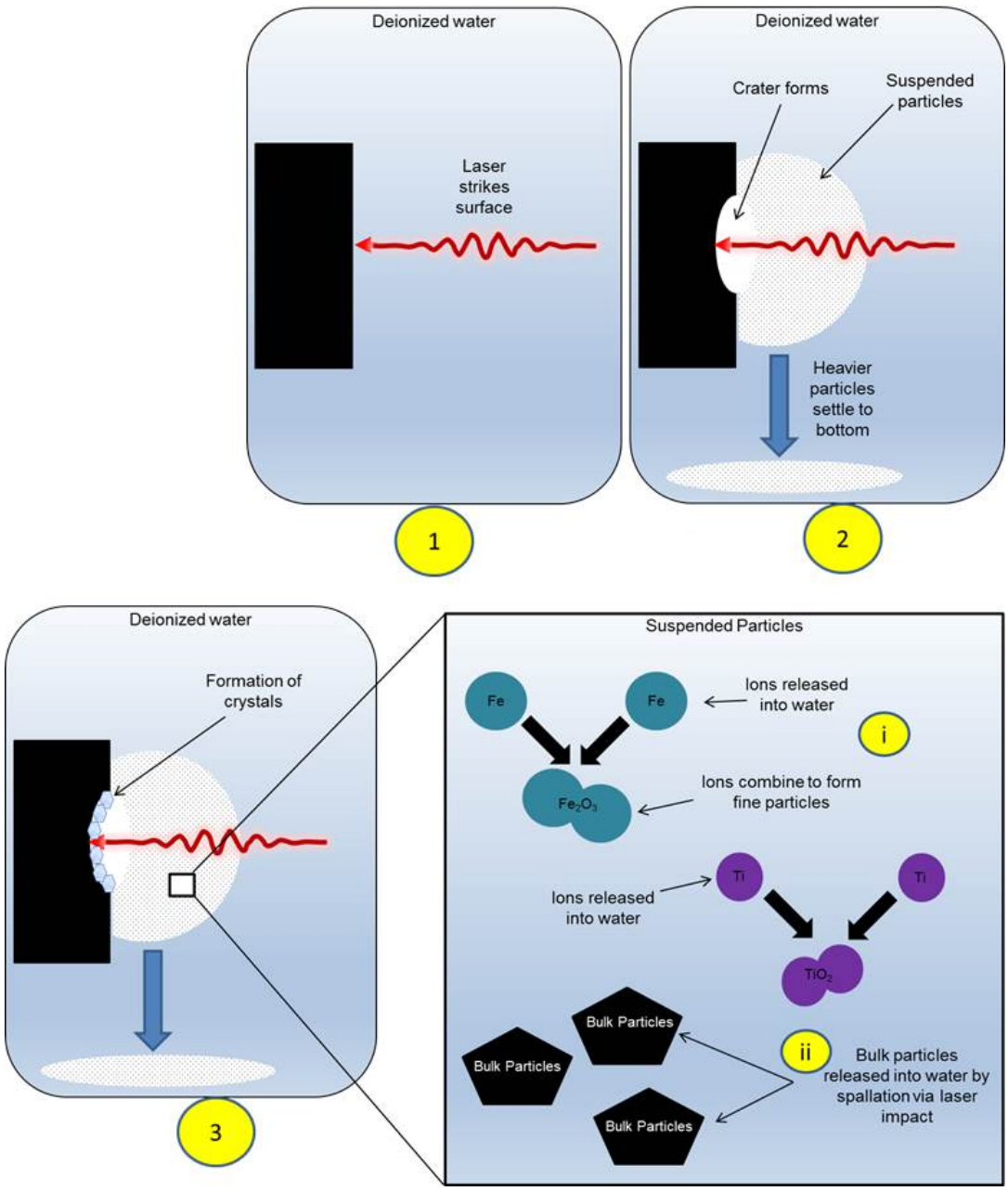

Top left: Laser impacts the material surface [12].

Top right: Crater is formed by laser impact and particles are ejected into the medium as ions and bulk particles. Heavier particles settle to the bottom of the medium while the fine particles become suspended in the medium [12].

Bottom left: Spallation of the material surface by laser impact [12].

Bottom right: Suspended particles formed from complex ions being released into the medium then combining to form fine sized particles and precipitates [12].

Figure 2. Mechanism of LDHP Postulated during Previous Characterization of Inhomogeneous Natural Materials. Source: [12].

The natural tektite and natural obsidian samples allowed for an evaluation of potential benefits of the LDHP technique [12]. However, due to the inhomogeneous nature of the natural material, it was difficult to make a direct correlation between the sample material characteristics before and after LDHP was performed, since the areas sampled were not identical in composition, even when taken from the same bulk sample material. Thus, the basic mechanism of the LDHP technique has been hypothesized, however, having a homogeneous sample to evaluate it would help validate the process, as proposed also by our team in a recent publication [15]. Since characterization has already been performed on these natural materials, the next step was clearly the use of a homogeneous material from which direct correlations between the pre and post treatment states could be established. The work presented in this thesis addresses that challenge and aims to create a synthetic homogeneous sample with features that approximate the structure and average composition of tektite.

C. OBJECTIVE OF THIS STUDY

The objective of this research was to create a surrogate glassy material that elementally resembled the average composition of tektite but that presented a homogeneous distribution of phases. Such a specimen could be used to quantify the effects of applying methods such as LDHP, since knowing the precise composition of the non-treated specimens will facilitate their comparison post-treatment.

The validation of a new material characterization technique, such as LDHP, is necessary to ensure that the hypotheses for the basic mechanism of the technique are sound as mentioned earlier [12]. Understanding the effect of process parameter variation on a sample being evaluated is paramount so that correlations can be made between source material and post-process material composition. These correlations can then be tested for repeatability and consistency to support development of a database for use with evaluation of future samples of unknown composition [2].

Homogeneous materials would be ideal for this purpose since the uniform composition of the source material allows for a more constructive analysis of the effects

of process parameter variations. Natural materials that are inhomogeneous introduce a level of uncertainty due to the sample being consumed during processing.

D. SOL-GEL METHOD

This study used the sol-gel fabrication approach, using hydrolysis and condensation/evaporation processes and utilizing precursors that contained the elements of interest to form tektite along catalysts mixed in a medium to form initial homogeneous solutions. The rationale was that once a uniform dispersion of the elements could be created such surrogate material could be used to help validate the LDHP process. Follow-on experimentation could then be focused on systematic adjustment of reactants stoichiometry and control of the fabrication parameters. The section below introduces the sol-gel process and the diverse steps required to render a solid product using such fabrication approach.

Surrogate materials can be made in a variety of ways. The sol-gel synthesis method was selected for this study based on previous reports of its usefulness creating silica based ceramics [20], [21]. Important steps for sol-gel synthesis are hydrolysis, polymerization, gelation, drying, dehydration and densification as explained in [21] and described later in this section [22]. Execution of these primary steps is the foundation for sol-gel synthesis. The term sol-gel is now applied to an assortment of processes and chemistries while the potential applications for sol-gel synthesis continue to grow as shown by [23], [24], [25]. The end product forms of the synthesis can be monoliths, patterns, fibers, powders and thin films emerged from both the sol and gel phases of the fabrication.

Initially, a sol is produced from the alkoxides of the element of interest (ca. silicon in most cases), a catalyst and solvents. The sol polymerizes and forms a gel, which upon drying will generate a solid phase. The procedure employed to dry/dehydrate the gel will determine the final porosity /microstructure/density of the solid product. The sol gel process steps are illustrated in Figure 3. Thermal energy input is critical to the sol-gel process throughout the steps mentioned in the figure and, in particular, during the drying stage that will generate the end product. The temperature, heating and cooling

rates, can greatly influence which morphology is produced. For example, supercritical drying of the gel will lead to an aerogel product while drying at ambient or near ambient temperatures will lead to a xerogel product [20], [23]. Indeed, xerogels are produced when solvents are removed from the gel under ambient conditions, what usually induces a collapse of the gel network and renders a finely divided solid. Aerogels require supercritical drying to remove the solvent without disturbing the gel tridimensional network, promoting the generation of a highly porous and extremely light structures. [26]. This difference in drying and dehydration leads xerogels to have a partially collapsed but strengthened gel network with preserved porosity while aerogels cease to be affected by capillary forces during solvent removal leading to a gel network with porosity as high as 99% [20], [26]. Sol-gel processing can be used to support the growing field of nanotechnology by producing nanowires, nanotubes, nanofibers and nanoparticles [24]. Properties of the products can be varied, including mechanical, electrical, optical and chemical [24]. Current applications include, but are not limited to, industries such as polymers, textiles, biotechnology, medical, cosmetic, construction, catalysis, agriculture, lithography, molding techniques, deposition techniques and UV patterning [23], [24].

During a sol-gel synthesis, the reaction media could be acidic or basic, and can act like a catalyst, having a significant impact on the speed of the reactions taking place. When combined with other variables, like the thermal input, a catalyst directly affects the rate and completeness of the hydrolysis and the polymerization of the sol as shown by [20], [21], [23]. Thus, when producing glass-like products by sol-gel, the control of the pH could promote the colloidal particles to form a branched network (basic solutions used as catalysts) or aggregates to form straight chained networks (solutions with acidic catalyst) [26]. The end product in both cases could be a xerogel according to the drying parameters. Steps used for the sol-gel synthesis during this study were derived from this known sol-gel methodology.

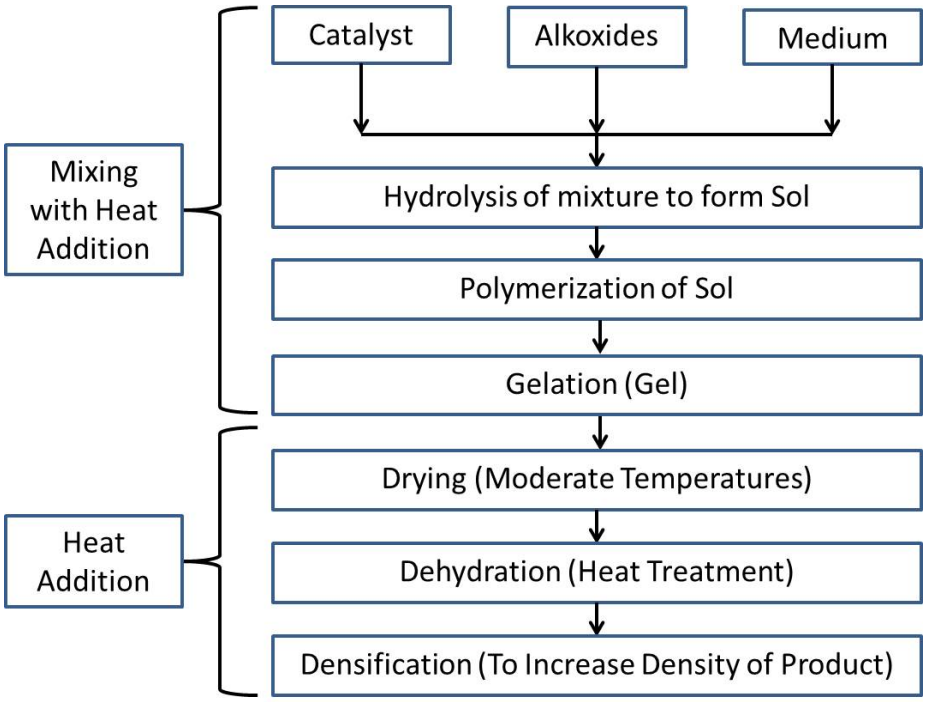

Figure 3. Important Steps of the Sol-Gel Process Applicable to General Synthesis and Followed by this Work

E. THESIS OVERVIEW

Glasses like natural tektite and obsidian are inhomogeneous and contain varied proportions of crystalline and amorphous material as shown by [27], [28]. Thus, in order to validate new processes like LDHP, instead of natural materials, this thesis focused on developing formulations and processes that could render surrogate glasses.

Our hypothesis is that a process such as the sol-gel method, combined with the right drying techniques and the correct combination of reactants, could create a homogeneous xerogel that, once annealed, will result in a homogeneous body with the appropriate chemical composition.

It was believed that by selecting reactants that could easily dissolve in the media used to carry out the sol-gel process (either in the alkoxide, ethanol or water solutions) and the right drying techniques, the elements would distribute uniformly within a matrix, rendering a homogeneous product. The elements added to the sol-gel synthesis were selected appropriately for the end product to elementally resemble one of the previously

characterized natural materials. Tektite was chosen as the material whose composition was to be reproduced.

The major challenge addressed by this work was to incorporate all elements into a solid product with a homogeneous phase distribution. The sol-gel process had been used before to create glassy materials but the compositions employed lacked the complexity that tektite presents.

Given that Fe and Ti naturally occur in tektite, those two elements were chosen to represent the elements of interest for the LDHP technique (when used for nuclear forensics) since no radioactive or contaminated material would be used for this study. Additionally, Fe and Ti are both transition metals with structural similarities to other elements of interest for nuclear forensics [29], [30].

Chapter II presents the materials, protocols, instrumentation and all experimental conditions followed to achieve the goals of producing and characterizing a surrogate glass.

Chapter III and Chapter IV contain the results of diverse fabrication approaches and the characterization data obtained along with discussions to explain it for the basic pH and acidic pH approaches respectively. Some of these are compared and contrasted with the known literature in the field.

Chapter V summarizes the milestones and major findings of this endeavor.

Chapter VI provides suggestions for future work to advance the development of surrogate materials from the lessons learned during the completion of this thesis.

THIS PAGE INTENTIONALLY LEFT BLANK

II. EXPERIMENTAL METHODS

The goal of this research, as mentioned in the previous chapter, was the manufacture of a surrogate material that would be elementally comparable to natural tektite but homogeneous in composition and phases distribution. The sol-gel process was selected as the route for creating this homogeneous matrix. Since tektite is a naturally occurring inhomogeneous material, the average composition of tektite determined from a previous study was selected as the target elemental composition for synthesis (Table 1). Protocols were developed to fabricate the surrogate material with the intent that a glass could be formed which would be homogeneous and similarly the gel produced would be homogeneous as well. Material characterization was performed on the results of these initial fabrication batches. Experimental parameters used for the fabrications were then adjusted and the samples re-examined to determine if the production path used would produce a homogeneous matrix with the target elemental composition.

Table 1. Average Composition of Tektite. Adapted from [15].

Oxide	Average Measured Composition wt%	Reference Composition wt%
SiO_2	73.04	72.00
Al_2O_3	12.34	12.00
FeO	5.98	5.32
K_2O	2.54	2.26
MgO	2.34	3.19
CaO	2.05	2.85
TiO_2	0.90	0.68
Na_2O	0.76	1.31

A. FABRICATION OVERVIEW

Although various parameters of the fabrication protocols were modified as necessary to support the synthesis of a homogeneous matrix, the primary parameter adjusted was the pH of the solution [20], [21], [23]. Two approaches were selected, one with an acidic pH during the production of the sol and the other with a basic pH. The protocols are a modified version of those published by [20], [21], [23]. Precursor salts or alkoxides were selected to introduce the elements needed: Si, Al, Fe, K, Mg, Ca, Ti, Na and O.

Iron (Fe) and Titanium (Ti) were included both as elemental components of tektite since they resemble the heavier elements left behind after a nuclear event and in their salt and alkoxide forms should dissolve into the sol-gel matrix for improved homogeneity. No radioactive specimens were produced, targeted or analyzed during this study. There was no risk of accidental exposure or contamination from the fabrication process or the samples produced.

As mentioned in the introductory chapter the six fundamental steps of the sol-gel methodology were applied, see Figure 4. However, these steps were modified to address the unique combination of reactants, the instruments used for drying/dehydration of the gel and to anneal the sample to induce the densification and crystallization needed to create a homogeneous surrogate.

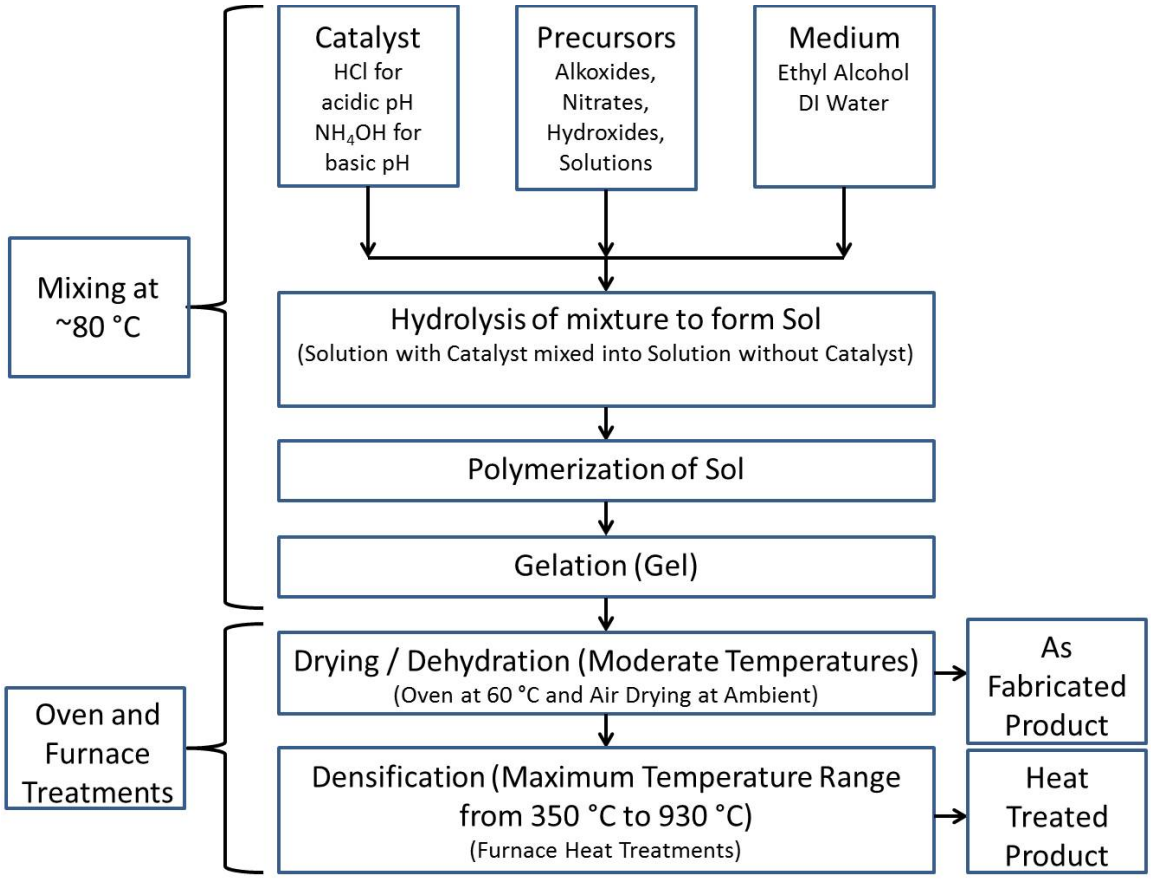

Figure 4. Steps of Sol-Gel Process Methodology Used for Sol-Gel Synthesis during this Study

B. STRATEGY ONE: BASIC PH CATALYST

1. Production Strategy

The first solution employed for the sol-gel synthesis had a basic pH, such will be referred to as the basic solution method. This basic solution method was used to create three different formulations: i) An initial fabrication was produced with Si, Al, Mg, K, Ca precursors as a baseline but without the elements Fe and Ti, ii) follow-on fabrications using this basic solution method added the elements Fe and Ti in the form of either solid oxides (Fe_2O_3 and TiO_2) or iii) added as reactants that could completely dissolve in the liquid sol-gel mixture (Fe nitrate and Ti isopropoxide). All the results generated from the use of a basic media will be presented in Chapter III. Segregation was anticipated for the fabrication using oxides which would adversely affect the ability to produce a

homogeneous product but was conducted for comparison with those in which Fe and Ti were added as molecular components. The analysis of samples produced by those 3 strategies, facilitated the comparison between products and illustrated the benefits of adding the elements of interest directly in solution.

Each of these variations i) basic solution containing Si, Al, Mg, K and Ca precursors, ii) same basic solution containing Si, Al, Mg, K and Ca precursors mixed with Fe_2O_3 and TiO_2 particulates and iii) solution in which all elements were added from components that completely dissolved in the starting media, was dried under different conditions to assess the effect of drying time in the composition and morphology on the final product. The drying conditions used were: gel dried in an oven, dried at ambient temperature, and dried under vacuum. The intention was to dry the fabricated gel specimens in a way that would prevent or minimize the creation of precipitates and occurrence of phase segregation.

The initial drying methods mentioned above are independent of the post-production heat treatments, which were employed to produce a denser and more crystalline product. For the purpose of this paper the term oven will be used to describe the apparatus used for drying. The term furnace will be used to describe a tubular furnace, able to reach much higher temperatures employed during the post-production heat treatment of all samples.

An overview of the initial basic solution production strategy is shown (Figure 5). These strategies were aimed at investigating the role of the various precursors and elemental constituents in the gels and glasses produced. The effects of gelation and drying in diverse conditions are also included. Figure 6 also highlights the characterization techniques used to determine if the features of the specimens were supporting the objective of this study.

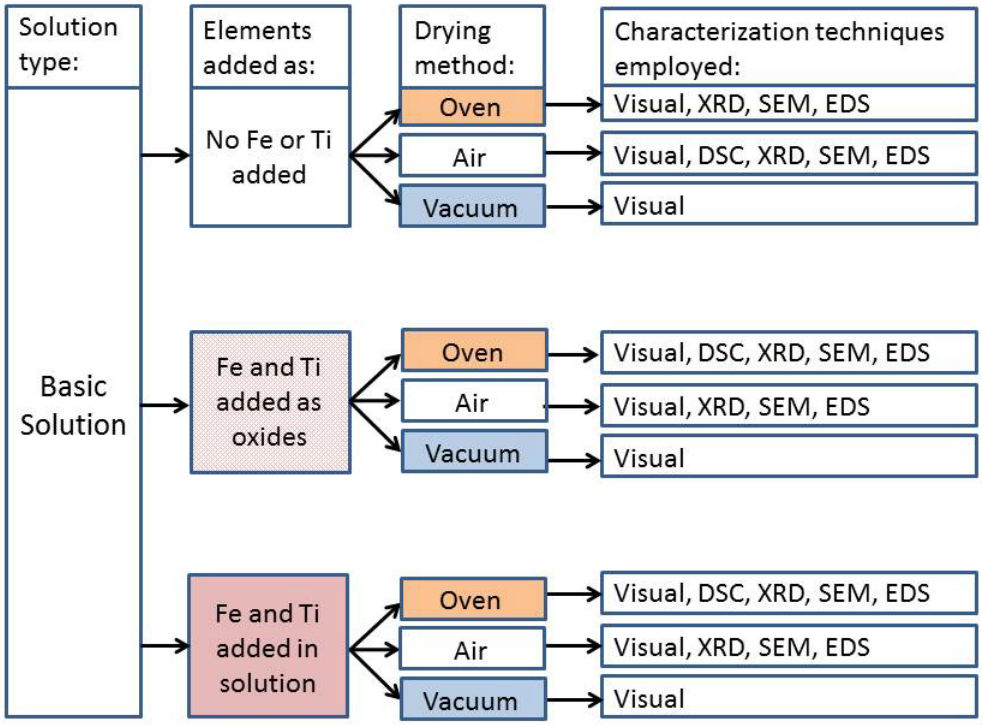

Figure 5. Flow Path for the Basic Solution Sample Production and Characterization

The basic solution production and characterization strategy presented above was followed by a heat treatment. Only the solution that contained all the elements of interest added as molecular components was post-processed as shown in Figure 6.

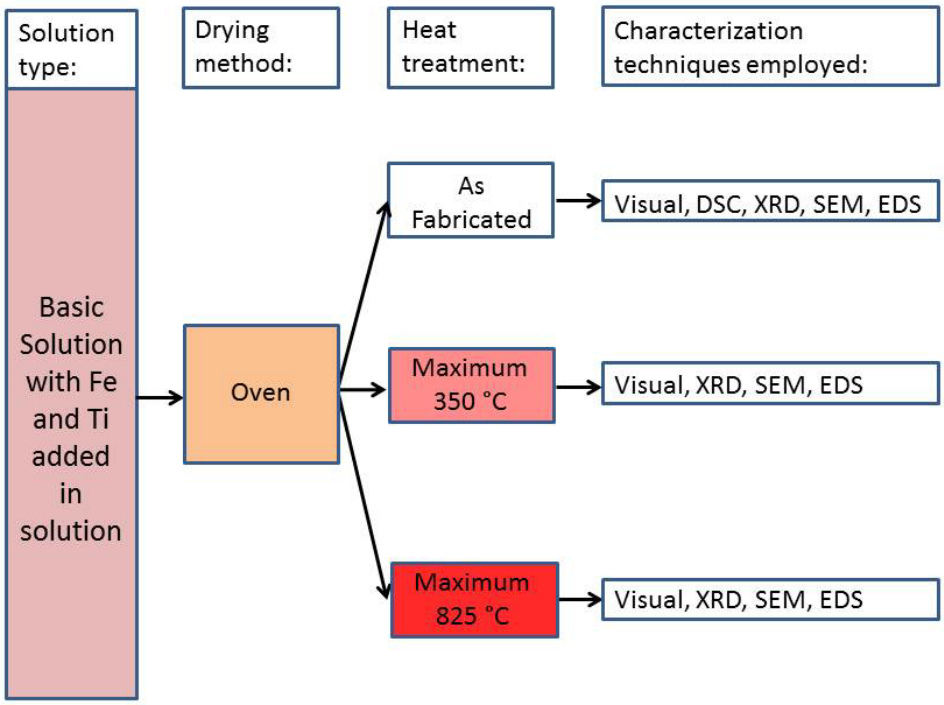

Figure 6. Basic Solution Production and Characterization Strategy, Heat Treatment Flow Path

2. Basic Solution Fabrications without Fe and Ti and with Fe and Ti Added as Oxides

a. Chemicals

Stoichiometric amounts of reactants to produce tektite were employed. Stoichiometric calculations were performed using MATLAB code generated for this project (Appendix A) [31]. Chemicals were selected based on their solubility in the basic pH solution components in order to achieve full integration into the solution with the exception of the oxides, when used. Fully dissolved chemicals allowed for thorough dispersion through stirring and provided an increased probability of product homogeneity after the gel synthesis.

The foundation for the basic solution production and the chemicals common to all the basic solution fabrications are listed (Table 2). Molar solutions calculated using Sigma-Aldrich website and chemical formula data from manufacturer [32].

Table 2. Precursor Chemicals Common to all Basic Solution Fabrications

Brand	Name	Formula	Manufacturer Molecular Weight (g/mol)	wt% due to element needed (%)
SIGMA-ALDRICH	Ethyl Alcohol (EtOH)	C_2H_6O	46.07	N/A
Weber Scientific	DI Water	H_2O	18.02	N/A
SIGMA-ALDRICH	30% Ammonia Aqueous Solution	NH_4OH	35.05	N/A
ALDRICH Chemistry	0.5M NH_4F Solution	NH_4F	37.04	N/A
ALDRICH Chemistry	Tetraethyl-Orthosilicate (TEOS)	$C_8H_{20}O_4Si$	208.33	13.48
Alfa Aesar Puratronic	Aluminum Nitrate Hydrate	$Al(NO_3)_3(H_2O)_9$	212.99	12.67
		$Al(NO_3)_3(H_2O)_9$	375.13	7.19
SIGMA-ALDRICH	Potassium Hydroxide	KOH	56.11	69.69
SIGMA-ALDRICH	Calcium Chloride	$CaCl_2$	110.98	36.11
SIGMA-ALDRICH	Magnesium Hydroxide	$Mg(OH)_2$	58.32	41.68
SIGMA-ALDRICH	Sodium Hydroxide	NaOH	40.00	57.48

The variation with Fe and Ti added as oxides utilized all the chemicals listed in Table 2 and the oxides listed in Table 3.

Table 3. Precursor Chemicals for the Basic Solution with Fe and Ti as Oxides

Brand	Name	Formula	Manufacturer Molecular Weight (g/mol)	wt% due to element needed (%)
ALDRICH Chemistry	Iron (II,III) Oxide	Fe_3O_4	231.53	77.73
ALDRICH Chemistry	Titanium (IV) Oxide Rutile	TiO_2	79.87	59.93

The majority of the constituent chemicals needed were solids of varying texture and form. We needed them all to be as close to fine particles as possible to aid in their thorough dissolution into the solutions as opposed to forming a precipitate within the solution. This was accomplished using a mortar and pestle to crush the ingredients.

b. Production

The basic solution production protocol was established from a pre-existing sol-gel processing methodology and then adapted for use with this project [20], [21], [23]. During production the primary ingredients were mixed as batches in two separate beakers and labeled as solution A and solution B (Figure 7). These solutions would then be combined into a final mixture to facilitate the hydrolytic reactions. As shown in Figure 5 an initial fabrication was performed where all the precursor chemicals were added with the exception of Fe and Ti.

For chemical and solution preparation since TEOS is one of the primary ingredients as well as the precursor chemical for the introduction of Si the amounts of the other elements and corresponding precursor chemicals were based off the amount of Si introduced due to the TEOS [Appendix A], [30]. TEOS was added to solution A along with EtOH for the fabrication using oxides for Fe and Ti. Solution B contained EtOH, DI water, ammonia aqueous solution and the aqueous solution of ammonium hydroxide. All the remaining constituent chemicals were added to solution B one at a time and allowed to dissolve into the solution. The Fe and Ti oxides were added after Solution B had been combined into Solution A.

Left beaker: Solution A with TEOS and EtOH.

Right beaker: Solution B with EtOH, DI water, ammonia aqueous solution, aqueous solution of 0.5M NH_4F and the precursors for Al, K, Ca, Mg and Na.

Fe and Ti were added as oxides after the solutions were mixed.

Figure 7. Basic Solution Initial Fabrication before the Addition of Precursor Chemicals, Initial Setup

Heating and continuous mixing of the solutions was maintained throughout the fabrication process. This thermal energy input aided the endothermic chemical reactions that dominated the process after the two solutions had been combined. Initial fabrications were only heated using conduction heat transfer through contact of the base of the beaker with the heated magnetic stirrer plate (Figure 7). This yielded an uneven temperature profile for the solution within the beaker and had a visible effect on the mixing and structure of the final product as it will be shown in the next chapter. Sol-gel synthesis is affected by the temperature used during fabrication so during the mixing process the protocol temperature of 80 °C, selected to maintain adequate thermal input while avoiding excessive boiling, was controlled using the dial setting on the front of the magnetic stirrer plate. However, this resulted in the system hunting excessively, both when heating and cooling, by as much as 15 °C to 20 °C. To resolve this issue a thermal bath was utilized with sand as the medium that allowed for a more uniform temperature distribution. A temperature controller was combined with a higher capacity hotplate that could generate the higher temperature differential needed between the plate and the sand

bath so that thermal losses could be quickly and efficiently replenished. The result was not only a more constant temperature throughout the fabrication but also a smoother temperature profile within the solution due to even heating from the bottom and sides (Figure 8). The effect of this change could be seen in the nucleation occurring during production as well as the time required to reach the final product as it will be discussed in the next chapter and observed by [26], [33]. These were positive enhancements to the process that would improve homogeneity due to the quicker change in viscosity while mixing was occurring which reduced the level of diffusion possible for the constituent chemicals, effectively helping to 'lock' the elements into the matrix [33], [34]. This quicker transition also resulted in a more gel like structure as opposed to the glass like appearance of the earlier fabrications.

The first fabrications were removed from the heat and mixing when the liquid samples were placed into containers for drying. Unfortunately, this allowed excessive time for sedimentation and phase segregation to occur while the liquid product dried into a glass like structure. The final production's gel like structure and quick drying time allowed for more continuous mixing to promote uniform dispersion of the ingredient chemicals into the solution.

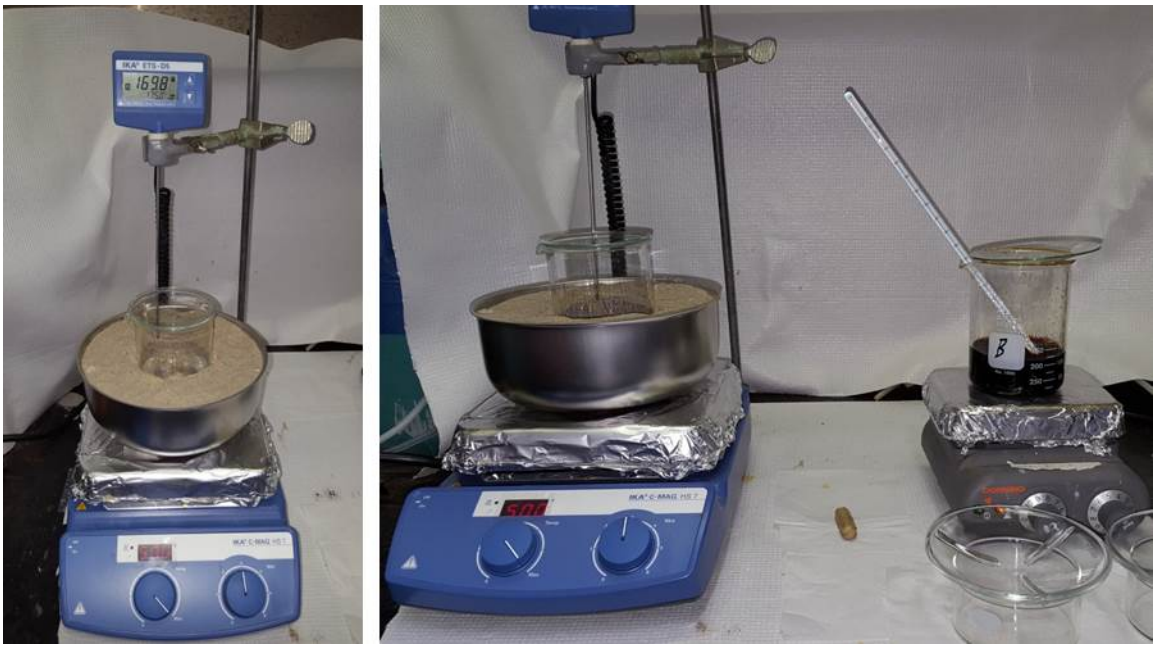

Left: Thermal bath with Solution A.

Right: Solution A in thermal bath (left) and Solution B (right).

Figure 8. Basic Solution Fabrication before combining Solutions A and B, Thermal Bath Setup

For the addition of Fe and Ti as oxides a quicker transition to gel formation would lower the risk of the oxide particles settling out as precipitates as they would during a longer drying period. The first fabrication was actually mixed together up until the point of Fe and Ti oxide introduction. At this point, the solution was divided into two separate beakers and the oxides were only added to one of the beakers. This was done so a direct comparison could be made between the surrogate material matrix formed with and without oxides added (Figure 9).

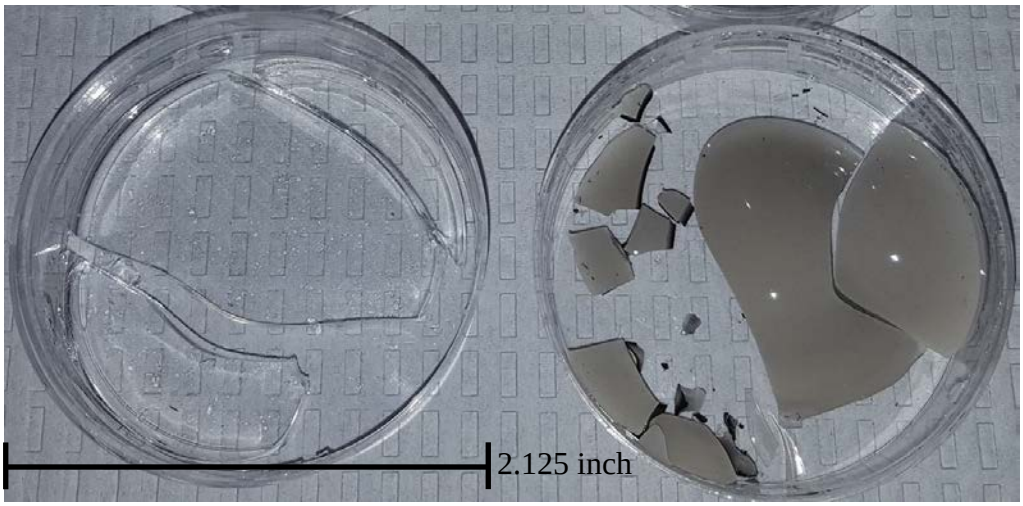

Left container: Top view of the basic solution without Fe and Ti added as oxides.

Right container: Top view of the basic solution with Fe and Ti added as oxides.

Figure 9. Visual Comparison of Basic Solution Product from Fabrication with and without Fe and Ti Added as Oxides

Following a hypothesis that precursor chemicals which resulted in ionized species during production would distribute more uniformly within the matrix the product without Fe and Ti added showed no visible phase segregation upon drying. Conversely, significant phase segregation was observed in the initial fabrication using the Fe and Ti oxides (Figure 10). This foreshadowed that even with improvement in product fabrication, it would be difficult to uniformly distribute the Fe and Ti as oxides and maintain this dispersion through to the final product.

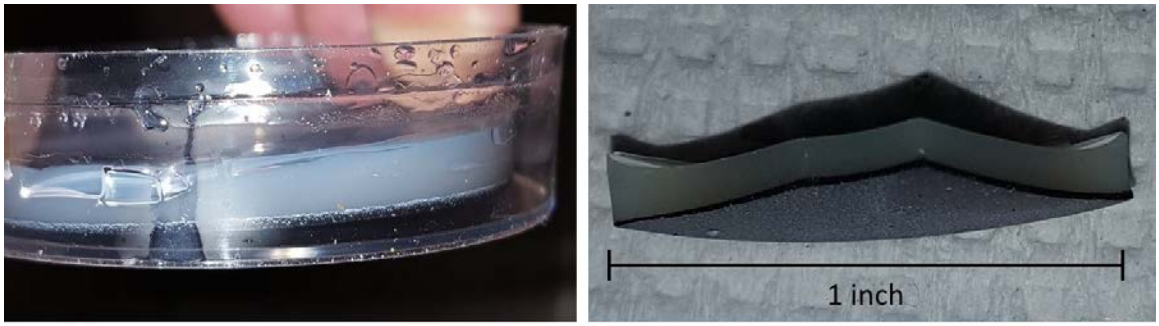

Left: Side view of the basic solution with Fe and Ti added as oxides dried in its container.

Right: Profile view of a piece of the basic solution with Fe and Ti added as oxides.

Figure 10. Basic Solution Product from Fabrication with Fe and Ti Added as Oxides

3. Basic Solution Fabrications with Fe and Ti Added as Soluble Precursors

a. Chemicals

For the basic solution fabrication with Fe and Ti added in solution all preparations were maintained the same with the exception of the Fe and Ti now being added in solution using a salt and an alkoxide respectively (Table 4).

Table 4. Precursor Chemicals for the Basic Solution with Fe and Ti in Solution

Brand	Name	Formula	Manufacturer Molecular Weight (g/mol)	wt% due to element needed (%)
SIGMA-ALDRICH	Iron (III) Nitrate Nonahydrate	$FeN_3O_9(H_2O)_9$	404.00	13.82
ALDRICH Chemistry	Titanium (IV) Isopropoxide	$C_{12}H_{28}O_4Ti$	284.22	16.84

b. Production

The basic solution production protocol was again utilized for the fabrications adding Fe and Ti in solution. The modification to the protocol is that the precursor chemicals from Table 4 were used instead of the previously mentioned oxides of Table 3. This involved adding the precursor Fe as a finely crushed solid to solution B and adding the precursor Ti as a liquid to solution A, prior to combining solution B into solution A. Adding Fe and Ti in this manner capitalized on the potential for more uniform distribution of the precursor chemicals through dissolution into the mixture. The probability of the elements coming out of solution as precipitates was also reduced. As with all the basic solution fabrications, the primary color change of the solution was due to the addition of the Fe (Figure 11).

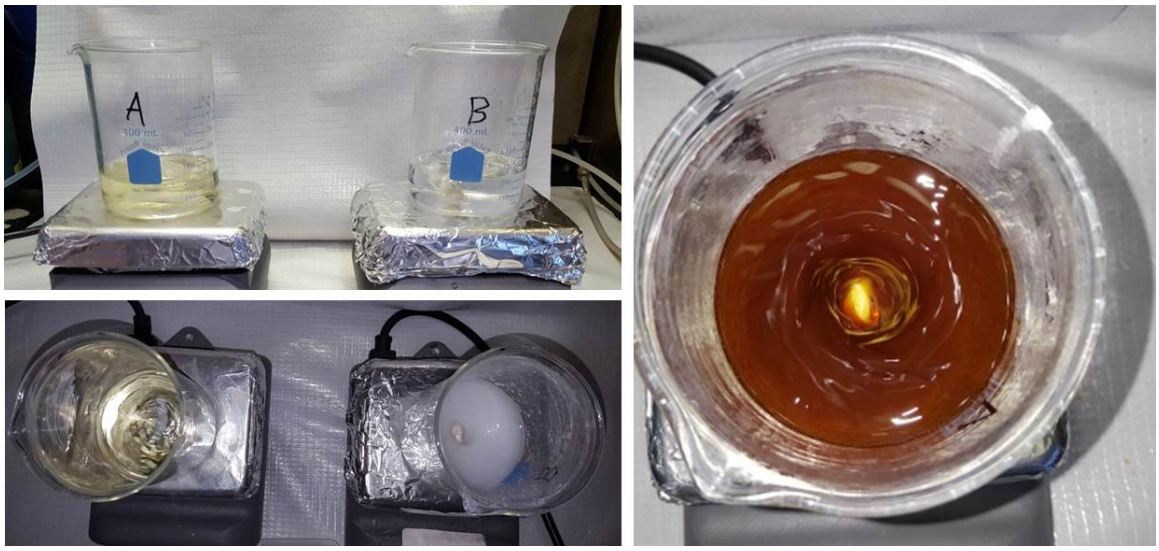

Top left: Front view of Solution A and Solution B before addition of Fe.

Bottom left: Top view of Solution A and Solution B before addition of Fe.

Right: Top view of Solution B after addition of Fe.

Solution A contained TEOS, EtOH and the Ti precursor for the fabrications adding Ti in solution.

Solution B contained EtOH, DI water, ammonia aqueous solution, aqueous solution of 0.5M NH_4F and the precursors for Al, K, Ca, Mg, Na and Fe for the fabrications adding Fe in solution.

Figure 11. Basic Solution Initial Fabrication Adding Fe and Ti in Solution

The final fabrication using this protocol was performed utilizing the thermal bath setup described for the fabrication using oxides. Due to the more controlled temperature during the synthesis, a difference in nucleation was observed and a gel like structure was formed instead of the previous glass like structure of the initial fabrications [21], [26], [33].

4. Post-production Drying Method and Heat Treatment

Following the hypothesis that the drying method used during sol-gel synthesis would affect the phase distribution of the product multiple drying methods were investigated.

a. Oven Drying Method

Samples were oven dried for 80 minutes at 60 °C using a Barnstead Lab-Line L-C Oven. Samples were covered with a concave glass cover with raised ridges along the bottom while in the oven to prevent debris from the inside of the oven chamber from falling into the sample while still allowing for convection heat transfer and minimal resistance to off-gassing. Following the initial drying period of 80 minutes the samples were left in the oven to finish drying under ambient conditions. Convection heat transfer was limited in the oven due to the enclosed volume of the space. Oven drying was performed on all the fabrications. The initial product resulted in a glass like structure and took approximately 2 days to solidify and dry. The final production only utilized this drying method for off-gassing due to a more gel like final form.

b. Air Drying Method

Samples were air dried at ambient temperature under a Hamilton Safeaire chemical hood with forced convection air flow. The same concave glass cover with raised ridges along the bottom was used to cover the samples. Air drying was performed for the first two fabrications with oxides and the first two fabrications with salts. These resulted in a glass like structure and could take approximately 3 days to solidify and dry. The final production did not utilize this drying method.

c. Vacuum Drying Method

Samples were placed under a vacuum dessicator dome and then moved to a Pelco 2251 Vacuum Dessicator at >762 torr. Vacuum drying was only performed for the first fabrication with oxides and the first fabrication with salts. These resulted in a glass like structure and took approximately 2 days to solidify and dry.

d. Furnace Heat Treatment

Samples were heat treated using a Thermo SCIENTIFIC, LINDBERG BLUE M furnace with programmable control which allowed heat up, dwell and cool down periods to be specified for target temperatures. The temperature profiles were based on material characterization data (Table 5). A SIGMA-ALDRICH Coors combustion boat, high alumina crucible was used to hold the sample within a tube that was exposed to air on one end and suction at the other end to allow for the flow of vapors from off-gassing to be continuously removed (Figure 12). HT used in this context represents a heat treatment. This furnace does not have a cooling function. C/D was through losses to ambient.

Table 5. Annealing: Furnace Heat Treatments

Segment	From 25 °C	HT #1	HT #2	HT #3	HT #4	HT #5	HT #6	HT #7
H/U	Temp °C	930	930	100	50	50	50	825
	Time	7 hr 30 min	9 hours	4 hours	2 hours	2 hours	4 hr 10 min	13 hr 20 min
Dwell	Temp °C	930	930	100	50	50	50	825
	Time	2 hours	4 hours	4 hours	2 hours	2 hours	2 hours	2 hours
H/U	Temp °C			930	100	110	110	
	Time			8 hours	4 hours	4 hours	10 hours	
Dwell	Temp °C			930	100	110	110	
	Time			4 hours	2 hours	2 hours	2 hours	
H/U	Temp °C				350	350	350	
	Time				6 hours	6 hours	20 hours	
Dwell	Temp °C				350	350	350	
	Time				2 hours	2 hours	2 hours	
H/U	Temp °C				930			
	Time				12 hours			
Dwell	Temp °C				930			
	Time				2 hours			
C/D	Temp °C	25	25	25	25	25	25	25
	Time	9 hours	9 hours	9 hours	9 hours	6 hours	6 hours	6 hours
	Temp °C	OFF	OFF	OFF	OFF	OFF	OFF	OFF

Metal connector on left side of glass tube is connected to Hamilton Safeaire chemical hood with forced convection air flow for removal of gas products emitted from samples in the furnace.

Figure 12. Heat Treatment Furnace (Acid Solution Sample in the Crucible)

C. STRATEGY TWO: ACIDIC PH CATALYST

1. Production Strategy

The second pH approach used a sol-gel solution with an acidic pH to form the surrogate material matrix [20], [21], [23]. This will be referred to as the acid solution method. All the results generated with the acid solutions are presented in Chapter IV. The evolution of the basic solution production strategy influenced the production strategy for the acid solution fabrications. The acid solution fabrication was only performed with the addition of the Fe and Ti in solution. Experimentation was performed to assess additional variations of the oven drying method while the air drying method was unchanged and the vacuum drying method was not used (Figure 13).

The temperature ranges during fabrication for this approach also produced a Xerogel. Longer chain formation was anticipated to occur with this method and the expected product was a gel instead of a glass based on the production strategy employed.

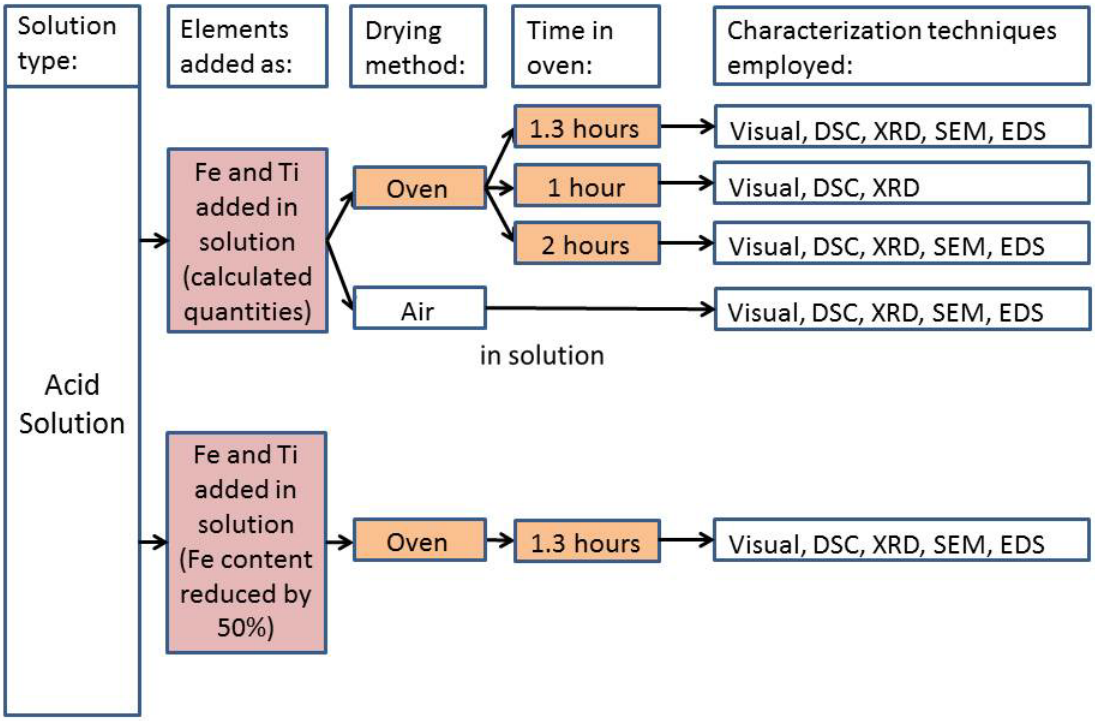

Production and characterization strategy to investigate the role of precursors and drying conditions on gel formation and the effect on final product homogeneity. A homogenous gel was the desired form of the product.

Figure 13. Acid Solution Production and Characterization Strategy, Overview of Flow Path

Characterization techniques were used to establish a baseline assessment of the samples and refine the production process. Post-production heat treatments of acid solution fabrication samples were conducted to further the understanding of final product characteristics (Figure 14).

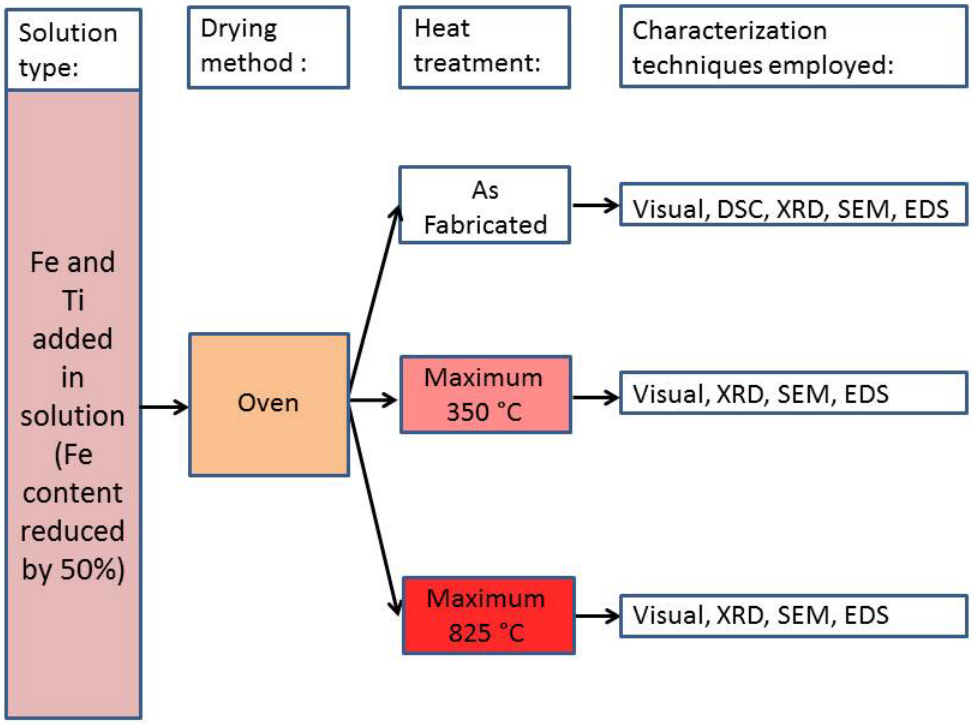

Production and characterization strategy to investigate the role of precursors and heat treatment on gel formation and the effect on final product homogeneity. Heat treatment temperatures were selected based on thermogravimetric analysis of antecedent samples. A homogenous gel was the desired form of the product.

Figure 14. Acid Solution Production and Characterization Strategy, Heat Treatment Flow Path

2. Acid Solution Fabrications with Fe and Ti Added as Soluble Precursors

a. Chemicals

Stoichiometric amounts of the individual precursors were once more calculated using MATLAB (Appendix B) [31] based on the average composition of tektite (Table 1) [30]. Precursor chemicals were selected given their solubility in the media used, that is, the acidic pH. Full integration and homogeneous distribution of the constituent chemicals into the solution was still an important desired attribute of the mixture. The focus was on introducing the elements as thoroughly mixed salts.

The chemicals used for the acid solution production are listed (Table 6). Notable differences are the replacement of the hydroxides with nitrates and the NH_4OH base

constituents with a 2M solution of HCl. Molar solutions calculated using Sigma-Aldrich website and chemical formula data from manufacturer [32].

Table 6. Precursor Chemicals for the Acid Solution with Fe and Ti in Solution

Brand	Name	Formula	Manufacturer Molecular Weight (g/mol)	wt% due to element needed (%)
SIGMA-ALDRICH	Ethyl Alcohol (EtOH)	C_2H_6O	46.07	N/A
Weber Scientific	DI Water	H_2O	18.02	N/A
SIGMA-ALDRICH	2M Hydrochloric Acid	HCl	36.46	N/A
ALDRICH Chemistry	Tetraethyl-Orthosilicate (TEOS)	$C_8H_{20}O_4Si$	208.33	13.48
Alfa Aesar Puratronic	Aluminum Nitrate Hydrate	$Al(NO_3)_3$~~$(H_2O)_9$~~	212.99	12.67
		$Al(NO_3)_3(H_2O)_9$	375.13	7.19
FISHER SCIENTIFIC	Potassium Bromide	KBr	119.00	32.86
SIGMA-ALDRICH	Calcium Chloride	$CaCl_2$	110.98	36.11
ALDRICH Chemistry	Magnesium Nitrate Hexahydrate	$Mg(NO_3)_2(H2O)_6$	256.41	9.48
SIGMA-ALDRICH	Sodium Nitrate	$Na(NO_3)$	84.99	27.05
SIGMA-ALDRICH	Iron (III) Nitrate Nonahydrate	$FeN_3O_9(H_2O)_9$	404.00	13.82
ALDRICH Chemistry	Titanium (IV) Isopropoxide	$C_{12}H_{28}O_4Ti$	284.22	16.84

b. Production

The acid solution production protocol used shared many similarities with the basic solution production protocol adding the Fe and Ti in solution. However, during the acid solution production the primary ingredients were also mixed as batches in two separate beakers and labeled as solution A and solution B. These solutions would then be

combined into a final solution to facilitate the reactions necessary for gel formation (Figure 15) [20], [21], [23].

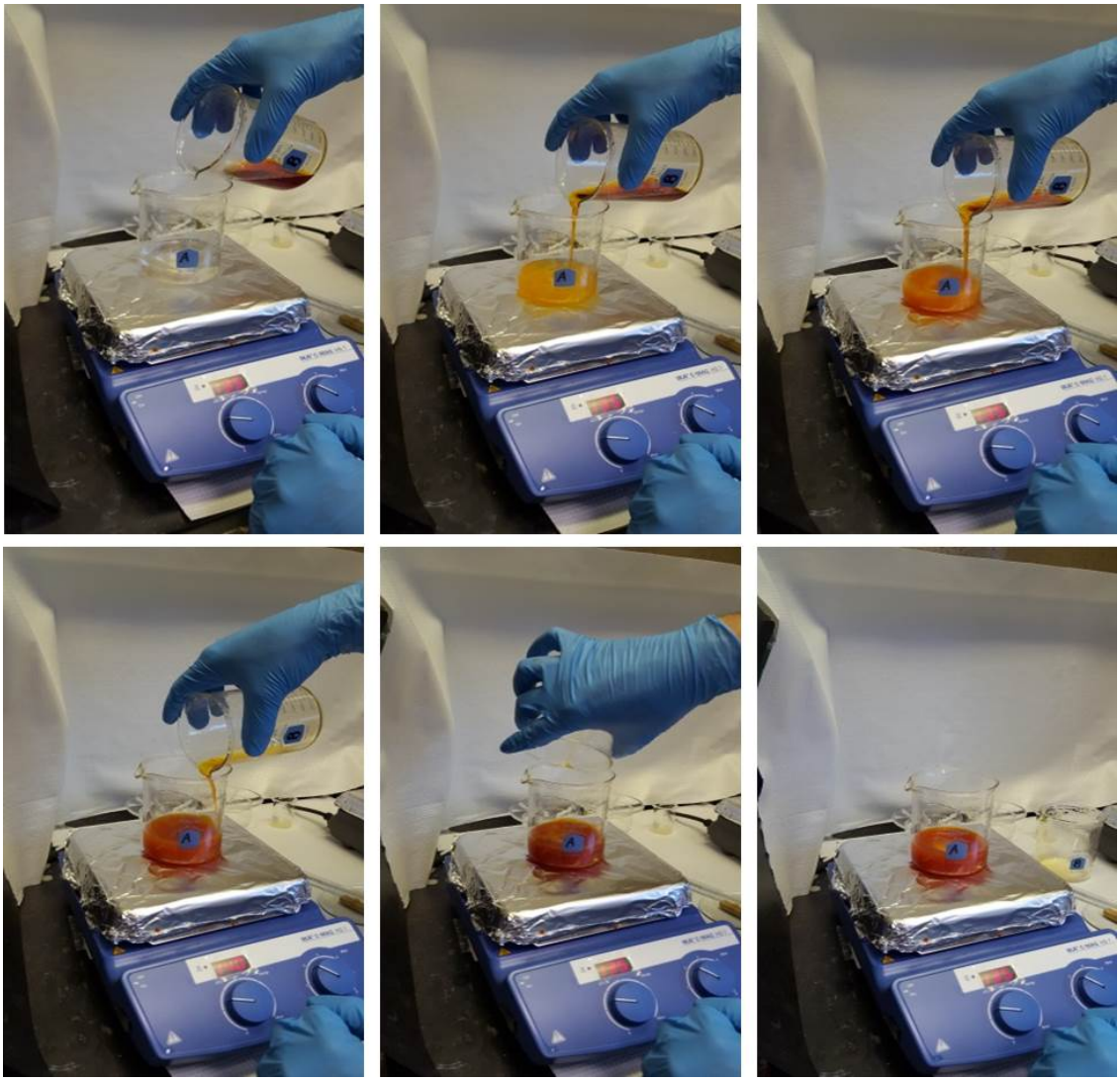

Left to right (top row to bottom row): Pouring Solution B into Solution A

Figure 15. Acid Solution Fabrication, Initial Hotplate Setup

A thermal bath setup was utilized for the two final acid solution fabrications and the effect of the additional thermal control during the sol-gel synthesis was observable during mixing and by the significant reduction in the time between pouring solution B into solution A and the start of gel formation (Figure 16) [21], [26]. The magnetic stirrer

was left in the solution as the gel formed, allowing for continuous mixing until the viscosity of the solution prevented further magnetic stirrer movement [34].

Left to right: Final mixing and rapid onset of gel formation.

Figure 16. Acid Solution Fabrication, Thermal Bath Setup

Due to the more homogeneous nucleation and rapid gel formation the acid solution fabrication was pursued as a primary path for satisfactory surrogate material production.

3. Post-production Drying Method and Heat Treatment

a. Oven Drying Method

Following production, the samples were oven dried at 60 °C for 60, 80 or 120 (minutes) using a Barnstead Lab-Line L-C Oven. Samples were covered with a concave glass cover with raised ridges along the bottom while in the oven to prevent debris from the inside of the oven chamber from falling into the sample while still allowing for convection heat transfer and minimal resistance to off-gassing. Following the initial drying period, the samples were left in the oven to finish drying under ambient

conditions. Convection heat transfer was limited in the oven due to the enclosed volume of the space.

Oven drying time was varied to allow for additional observation of potential changes in initial off-gassing and to document any subsequent changes in the final product. The 60 minutes and 120 minutes drying times were evenly spaced increments for comparison while the drying time of 80 minutes was performed for consistency between fabrications.

b. Air Drying Method

The first two fabrications were air dried at ambient temperature under a Hamilton Safeaire chemical hood with forced convection air flow. The same concave glass cover with raised ridges along the bottom was used to cover the samples. Air drying for the first fabrication which resulted in a gel like structure took approximately 2 days. Through control of thermal input during the production process air drying for the second fabrication which resulted in a gel like structure took approximately 1 day. All remaining fabrications did not utilize this drying method.

c. Furnace Heat Treatment

Samples were heat treated using a Thermo SCIENTIFIC, LINDBERG BLUE M furnace with programmable control which allowed heat up, dwell and cool down periods to be specified for target temperatures. The temperature profiles were based on material characterization data (Table 5). A SIGMA-ALDRICH Coors combustion boat, high alumina crucible was used to hold the sample within a quartz tube that was exposed to air on one end and directed to a hood at the other end to allow for the flow of vapors from off-gassing to be continuously removed (Figure 12).

D. CHARACTERIZATION, ANALYSIS AND TESTING

Multiple characterization techniques were utilized to gain understanding of the surrogate material created (Figure 17).

Top row (left to right): DSC, SEM and support equipment.
Bottom row (left to right): Sputtering in progress, Sputter Coater, XRD.

Figure 17. Characterization Equipment

1. Visual Observation

Visual observation was performed on all the samples during both fabrication and post-production. Production parameter variations could be seen to have affected the process in real time during follow-on fabrications. Certain visual characteristics helped guide the development of the fabrication process. The clearest example of this was during the basic solution fabrications using oxides for the Fe and Ti addition. Visual segregation of the Fe within the samples could clearly be seen under all the drying conditions and was a visible indicator of inhomogeneity within the samples.

2. Thermogravimetric Analysis (TGA) and Differential Scanning Calorimetry (DSC)

Simultaneous thermal analysis (STA) was performed using a high temperature platform 400 NETZSCH-Gerätebau GmbH STA 449 F3 Jupiter simultaneous Thermo-Balance (TG) with QMS 403C Aëolos Quadropole Mass Spectrometer. The data analysis was performed employing Proteus software [35]. Samples were placed in a crucible and heated from ambient to 35 °C. Data collection always started at the 35 °C threshold. A heat up rate of 2 °C/minute was applied until 1200 °C was achieved. A purge gas mixture of oxygen and argon was used during the measurement period. The data was used to gain understanding of the thermal properties of the samples. These insights aided the determination of adjustments to be made for the fabrication flow path and guided the creation of the heat treatment plans applied.

3. Scanning Electron Microscope (SEM)

Electron microscopy was performed using a Zeiss NEON 40 field emission SEM operated by Zeiss Smart SEM Software Version 5.07. Morphological features of post-production samples were collected for various locations in the samples. SEM micrographs were used to support investigation of visible discrepancies and look for indications of inhomogeneity within the samples. The SEM analysis was conducted from 2 kV to 20 kV. SEM systems also directly supported the determination of chemical composition for the post-production samples using EDS.

a. Energy Dispersive X-ray Spectroscopy (EDS)

EDS was performed utilizing EDAX Genesis Spectrum Software Version 6.53. EDS/SEM spectrum and images were collected at 20 kV with a 1.32×10^{-6} mA beam current and data collection runs of 300 seconds. EDS mapping was also utilized to provide another visual indication of sample homogeneity. Elemental weight percent (wt%) data was collected for multiple areas of each post-production sample using the oxygen by difference setting. This data was used to determine an average elemental composition of the post-production sample being analyzed and the corresponding

standard deviation was calculated to gage elemental distribution within the sample as another indicator of sample homogeneity.

b. Sputtering

Material coating of the samples prior to analysis was performed using a TED PELLA, INC. Cressington Sputter Coater 208HR with a Cressington Thickness Controller mtm20. Due to the electrically non-conducting nature of the post-production samples, a 3 nm layer coating of Cressington Pt 80% / Pd 20% with a density of 19.52 gm/cm^3 was applied.

4. X-ray Diffraction (XRD)

XRD was performed using a Rigaku MiniFlex 600 X-ray Diffractometer operated by Rigaku MiniFlex Guidance Software. This system operated at 40 kV and 15 mA and used Cu kα X-rays generated by a standard Cu X-ray tube. Post-production samples were prepared for analysis using a mortar and pestle to crush the samples prior to mounting onto Rigaku 906166 5 mm x 0.2 mm Well Si510 or 906165 Flush Si510 sample holders. Standard measurement conditions used were a 2θ angle range from 10° to 90° with a scan speed of 5 °/minute at a step width of 0.02°. Some final fabrication samples were run with a scan speed of 3 °/minute while maintaining the previous measurement parameters. XRD data was analyzed using the Integrated X-ray Powder Diffraction Software (PDXL) and XRD Processing, Identification and Quantification Software (JADE), version 9.

THIS PAGE INTENTIONALLY LEFT BLANK

III. RESULTS AND DISCUSSION FOR BASIC PH CATALYST APPROACH

A. OVERVIEW

The versatility provided by the sol-gel method is beneficial as mentioned by [22] but the development and implementation of application specific protocols was necessary to promote accuracy and repeatability of fabrications. The adaptability of the sol-gel process created trade space for the investigation of parameter variation to guide the optimization of a protocol using the sol-gel process. Applying characterization methods described in Chapter II allowed for the selective elimination of production paths and prioritization of the fabrication processes most likely to produce a homogeneous product using the basic pH catalyst (Figure 18 and Figure 19).

Figure 18 presents the specific steps followed to produce a solution with all elements except Fe and Ti and a solution with Fe and Ti added as oxides. That is, an initial solution was divided in two parts, one served as baseline for solution with no transition elements, referred as (i) in section 1b of previous chapter, and the other one as baseline containing segregated Fe and Ti oxides, represented as (ii). Figure 19, in contrast, presents the steps followed in order to generate a solution in which all the reactants were soluble either in the alkoxide or in the water media, referred as (iii) in previous chapter.

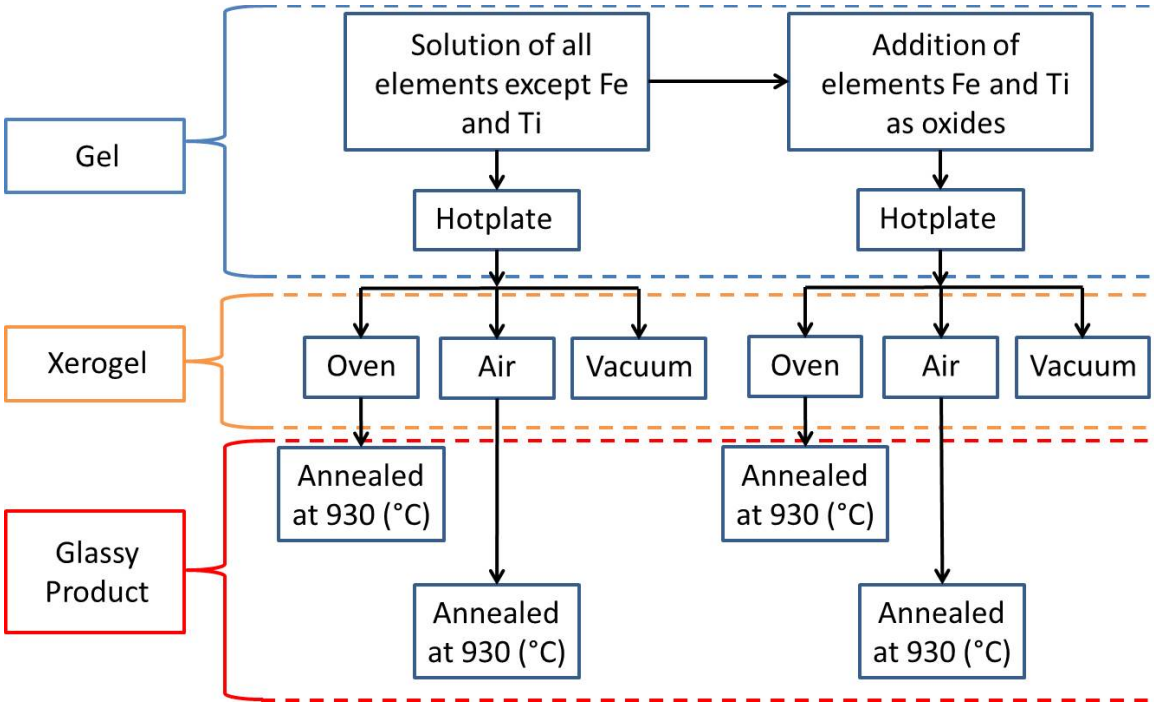

Precursor chemicals for the elements identified in Table 2.

Fe and Ti oxides identified in Table 3.

Figure 18. Overview of Basic pH Catalyst Fabrication Products Using a Solution with All Elements Except Fe and Ti and Using a Solution with Fe and Ti Added as Oxides

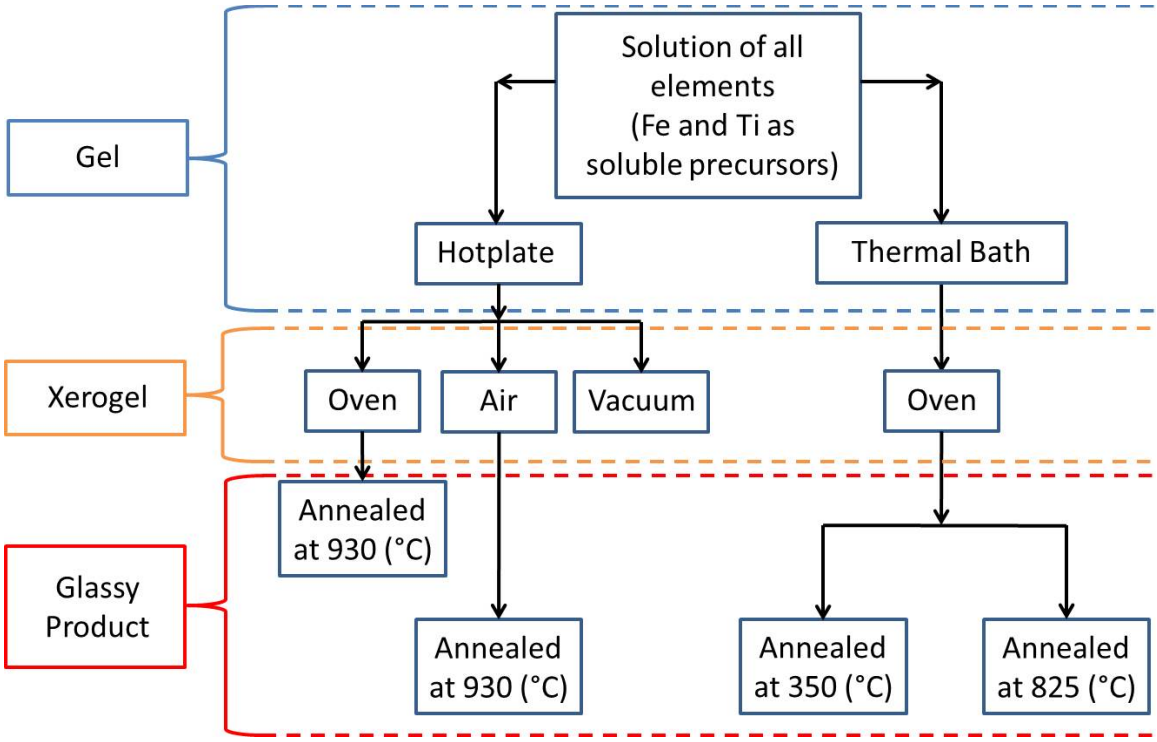

Precursor chemicals for the elements identified in Table 2.

Soluble precursors for Fe and Ti identified in Table 4.

Figure 19. Overview of Basic pH Catalyst Fabrication Products Using a Solution with All Elements with Fe and Ti Added as Soluble Precursors

As discussed in Chapter I and Chapter II the product underwent transitions during both production and post-production as, i) a sol formed using the selected catalyst, precursors and medium, ii) a gel which took form following polymerization of the sol, iii) a xerogel from evaporation of the solvents, primarily water and alcohol and iv) a glassy product following densification through heat treatment (Figure 20).

Multiple fabrications were performed using variations of the basic pH catalyst methods and the difference in effects of adding the Fe and Ti as oxides vice as soluble precursors was observed. Ultimately a path involving Fe and Ti being added as soluble precursors was pursued but based on improvements made during the process there is still potential for using oxides to introduce elements of interest to the surrogate material matrix to represent inclusions.

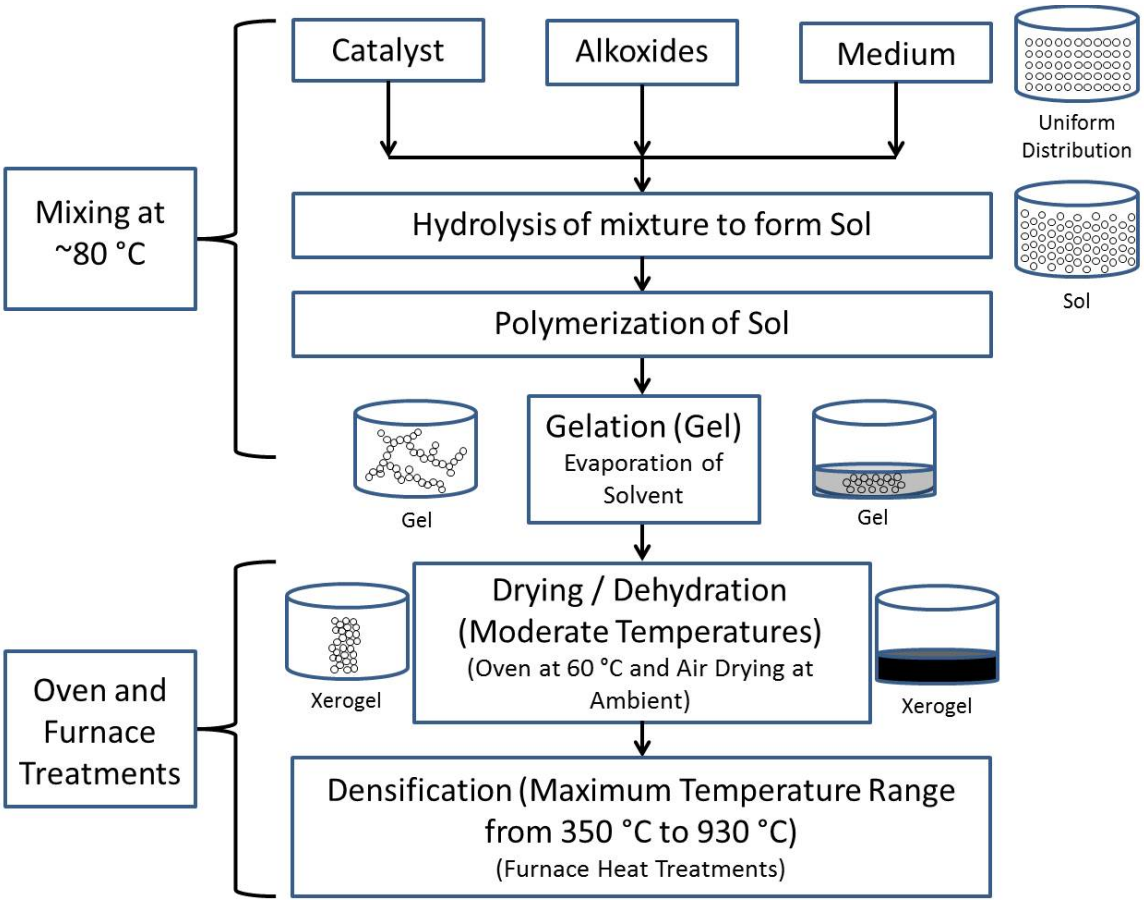

Densification included in strategy shows location of future work that could involve sintering or melting to produce a ceramic.

Figure 20. Sol-Gel Synthesis Strategy with Depictions of Product Forms throughout Fabrication Correlated to Process Steps

B. STRATEGY ONE: BASIC PH CATALYST

1. Basic Solution Fabrications without Fe and Ti and with Fe and Ti Added as Oxides

The basic solution containing only Si, Al, Mg, K and Ca precursors produced a russet color gel that upon drying turned into an opaque solid of glassy appearance. The observation of the solid by scanning electron microscopy revealed that the force applied to attach the specimen into a carbon tape substrate, which is a common step used for sample preparation for SEM observation, was enough to produce cracks that propagated in diverse directions. The surface of the solid presented two types of surfaces, one with no roughness presenting two different tones of gray and one with blisters, likely formed during the stage in which the sample was stored in vacuum and degas of solvents occurred (Figure 21).

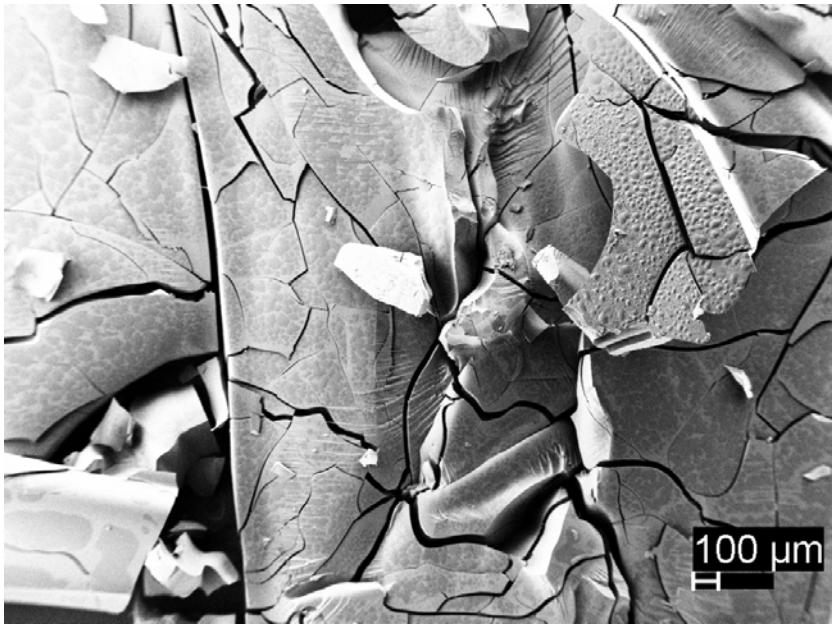

Figure 21. SEM Image: Hotplate Basic Solution Fabrication without Fe and Ti Added, as Fabricated

EDS analysis of the xerogel product with all the elements except Fe and Ti supported a fairly homogeneous dispersion of the constituent elements throughout a silicate matrix (Figure 22). This was support for the viability of the sol-gel process being able to achieve the objective of this study for such a complex formulation.

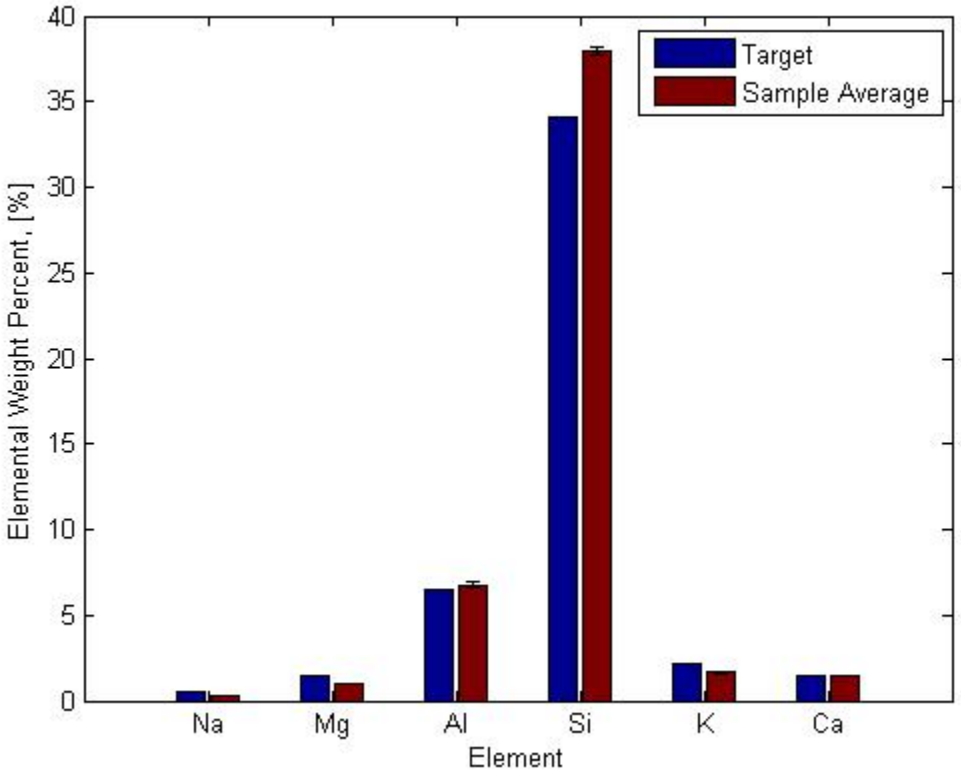

Note: The calculated standard deviation values are shown as line marker overlays on the top end of the Sample Average columns.

Figure 23. EDS Spectra Data Comparison for Hotplate Basic Solution with All Elements Except Fe and Ti, as Fabricated

When thermal analysis was performed, the surrogate material completed off-gassing and any remaining liquid within the matrix was evaporated. Heat exposure during the thermal analysis resulted in the physical breakup of the material due to the heat-up rate inducing the evaporation of volatiles components such as the EtOH and H_2O (Figure 23) [20], [22], [26].

Thermal analysis was performed after xerogel formation of the products so any diffusion would have to occur through the established matrix vice a liquid solution (Figure 24 and Figure 25). DSC-TGA data demonstrated the densification and crystallization steps reduced the particle size but maintained the glassy structure and appearance. This effort did not target the generation of a mechanically robust surrogate. In order to fabricate a glassy structure different protocols should be devised. Further discussion of this is provided in Chapter V and Chapter VI.

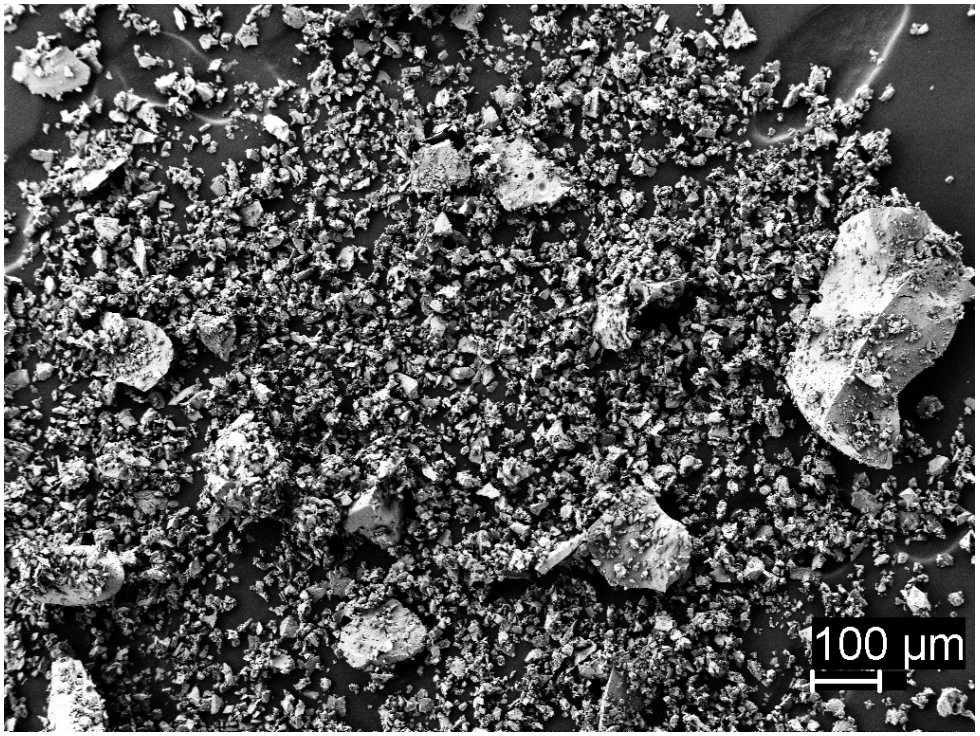

Figure 24. SEM Image: Hotplate Basic Solution Fabrication with All Elements Except Fe and Ti, Post-thermal Analysis

The rapid phase transformations from liquid to gas would lead to cracks forming to allow the gasses to escape. Endothermic activity was present leading up to the boiling point of the EtOH at 78.37 °C and while a volumetric expansion would occur it was not great enough to cause widespread cracking to allow for an increase in the rate of off-gassing (Figure 24). TG decrease was observed at a higher rate following reaching 100 °C since the volumetric expansion of H_2O into steam is much greater than that of EtOH

and more cracking would allow for increased off-gassing to occur (Figure 25). From this initial DSC data it was postulated that by adjusting the heat-up rate and providing for more time for diffusion the off-gassing might occur without severe detriment to the structural integrity of the sample and that the product might be maintained as a glass. Heat treatment #1 (HT #1) (Table 5) was performed using the furnace to obtain preliminary feedback on the effect of heating up the sample. The drying methods were also investigated for this reason since diffusion while in a liquid solution would be easier than through a solid. The reason for choosing the oven drying method as the path ahead was discussed in Chapter II. Additionally there was no significant mass loss observed above 800 °C (Figure 25).

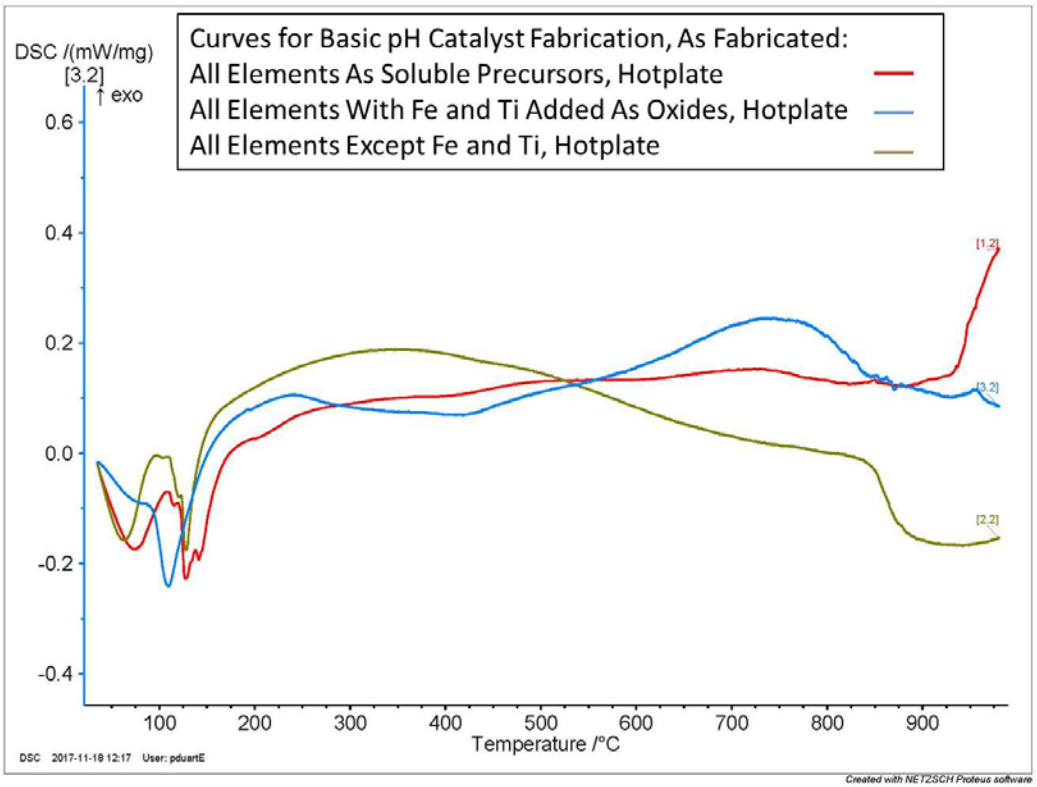

Figure 25. DSC Data Comparison for Hotplate Basic Solutions, as Fabricated

The basic solution with all the elements added as soluble precursors showed an additional change in off-gassing rate compared to the other basic pH catalyst fabrications, the loss of mass was also the highest out of the basic pH catalyst fabrications using the hotplate (Figure 25).

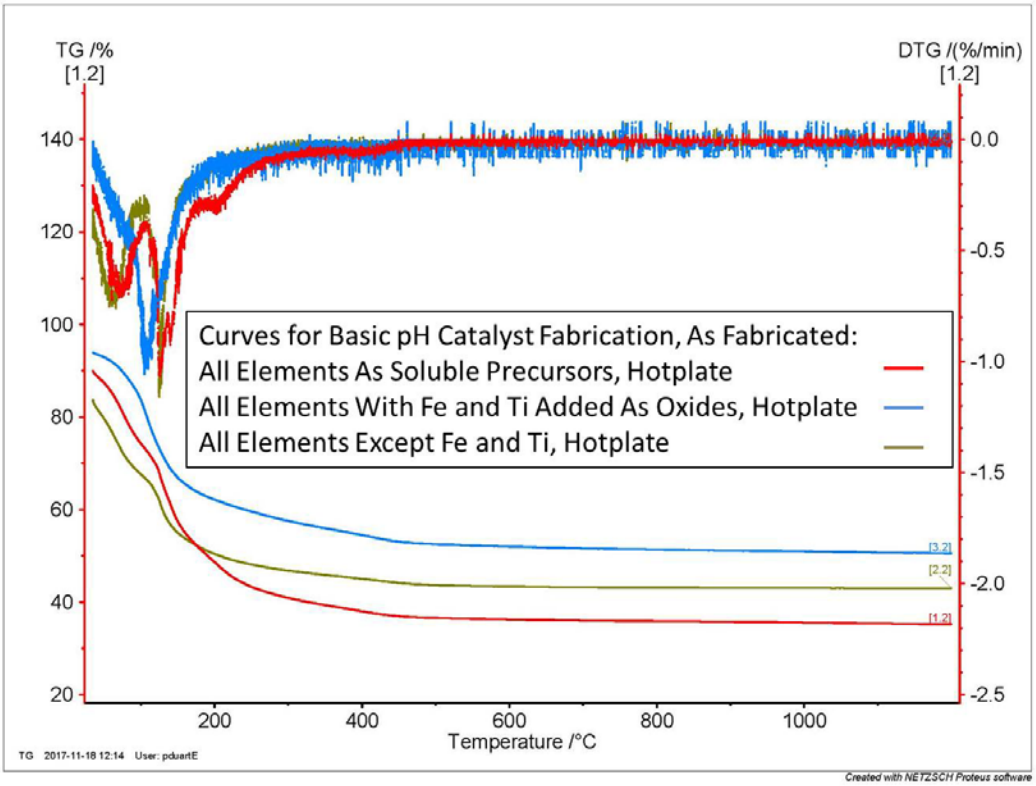

Figure 26. TGA Data for Hotplate Basic Solutions, as Fabricated

Despite the visual segregation of the un-dissolved oxides characterization was performed to assess the results of the production (Figure 26). SEM EDS spectra confirmed the visual assessment that the Fe oxide had settled excessively while the solution was drying due to gravity and simple diffusion through the liquid medium. The oxide particles were eventually locked into place within the matrix but not before the significant loss of uniform dispersion. Full homogeneity of the product would not be possible with the elements of interest added as oxides due to them being particulates suspended in the surrogate material matrix.

In contrast, as expected, the addition of Fe and Ti as oxides resulted in a markedly inhomogeneous product due to phase separation. The initial hotplate basic fabrication solution was divided mid-production into two equal halves by volume with oxides being added to one half and not the other. Target values for this fabrication were adjusted accordingly based on the reduced volume that the oxides would be added to [Appendix A]. The product, as shown in figure 10, consisted of a solid with two regions, one opaque grey and a darker one that solidified in the bottom. SEM observation of the sample, in Figure 26 presents a similar profile.

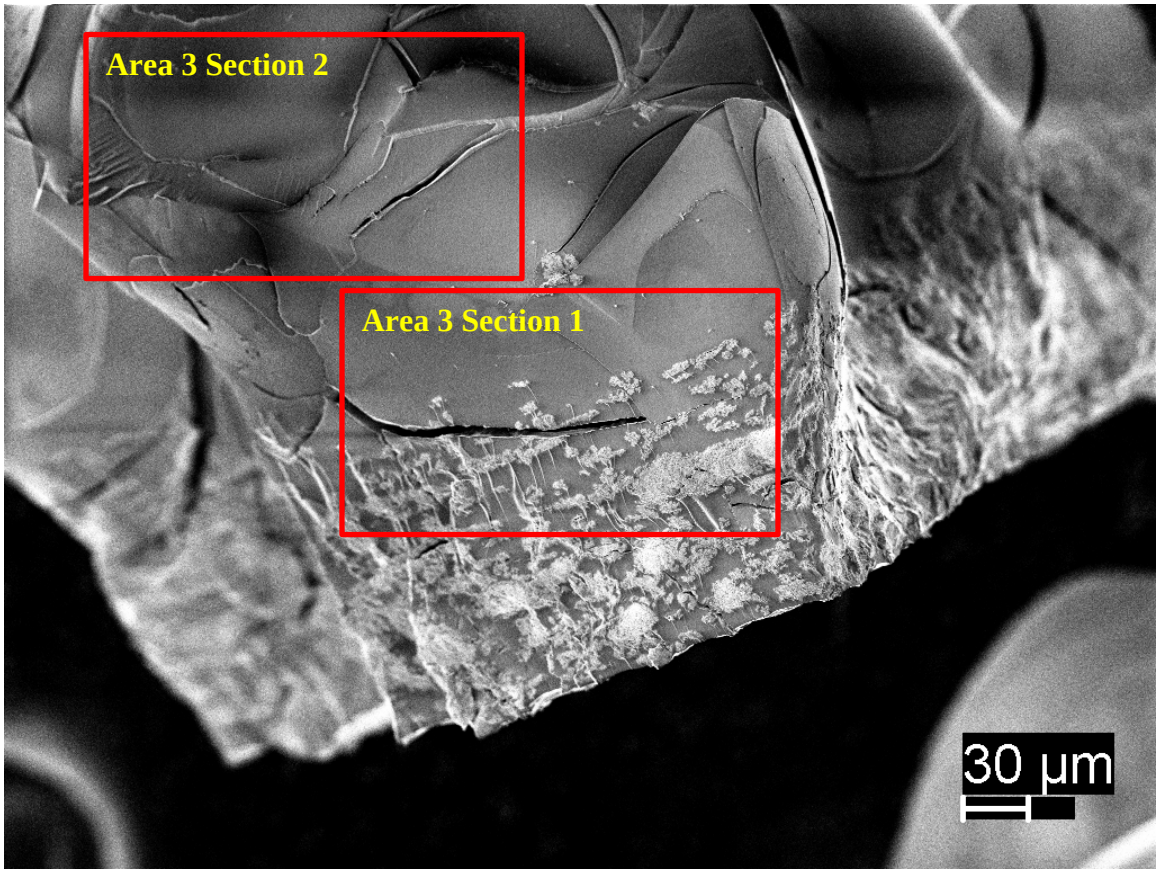

Area 3 Section 1: Lower portion of product showing Fe concentrations.

Area 3 Section 2: Upper portion of product.

Figure 27. SEM Image: Hotplate Basic Solution Fabrication with Fe and Ti added as Oxides, as Fabricated

By adding oxides the goal was to model the Fe and Ti added as inclusions instead of being part of the matrix generated by the sol-gel synthesis. SEM EDS spectra was collected from different areas of the samples to aid in the confidence level of the results as related to [2]. Some of the samples, the hotplate basic fabrication products with Fe and Ti added as oxides in particular, showed relative uniformity when large areas were analyzed but when these same areas were reviewed as smaller sections great disparities were observable. For the sample in Figure 26, the phase separation was visible so the sections were chosen to cover these different regions. The SEM EDS spectra data was plotted along with the standard deviation of the data population. While the sample average closely resembled the target composition, it was evident from the individual area EDS results and the calculated standard deviation for each element that the sample was inhomogeneous (Figure 27). This same approach was applied to all SEM EDS spectra data collection and analysis. Further EDS analysis was plotted using target composition and sample average with the standard deviation plotted coincidentally to provide an indication of homogeneity (Figure 28).

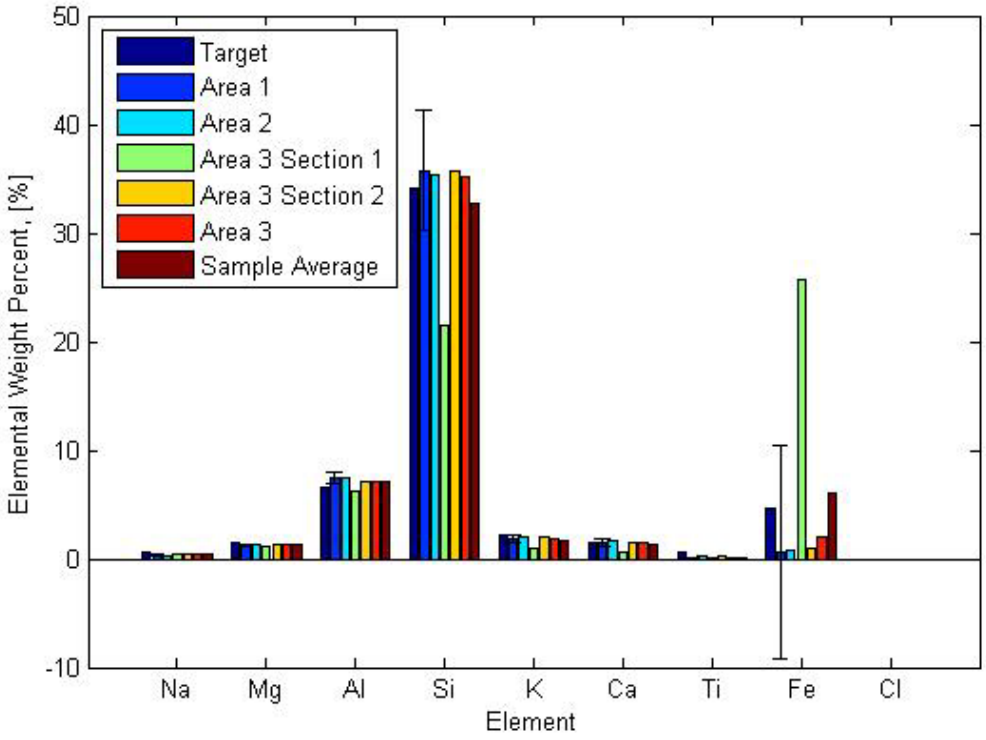

Note: The calculated standard deviation values are shown as line marker overlays on the top end of the column next to the Target column.

EDS spectra data for individual areas and sample average with standard deviation bar.

Figure 28. EDS Spectra Data Comparison of Individual Areas for Hotplate Basic Solution with Fe and Ti added as Oxides, as Fabricated

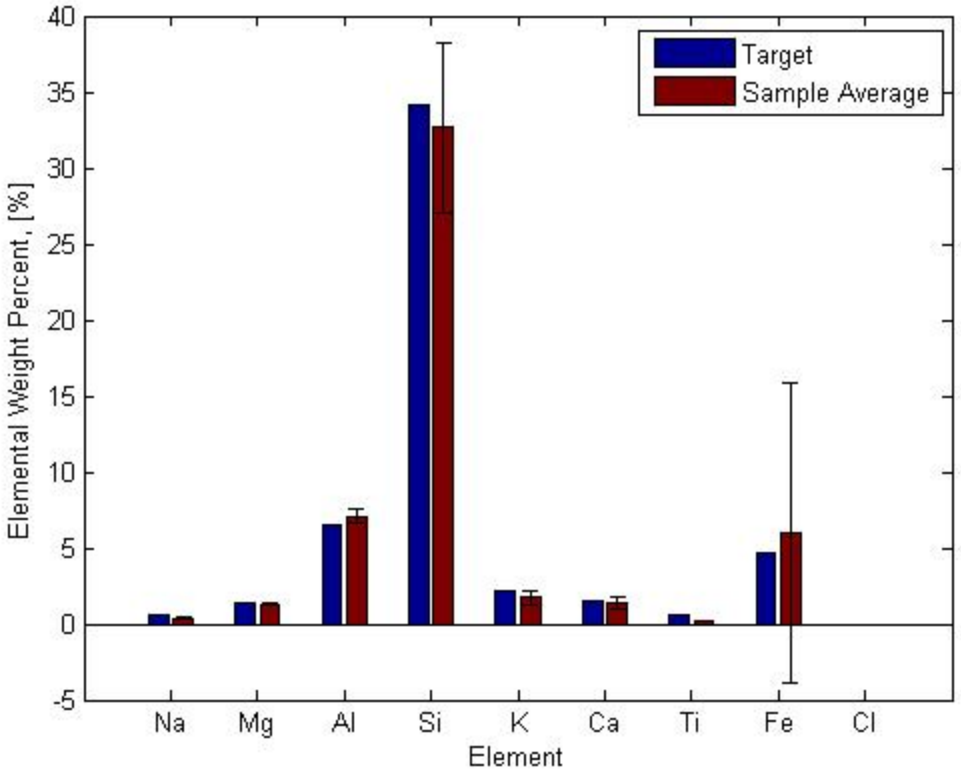

Note: The calculated standard deviation values are shown as line marker overlays on the top end of the Sample Average columns.

EDS spectra data sample average with standard deviation bar.

Figure 29. EDS Spectra Data Comparison for Hotplate Basic Solution with Fe and Ti Added as Oxides, as Fabricated

XRD analysis showed that the hotplate basic fabrication did produce the amorphous matrix that was expected following fabrication with peaks correlating to magnetite and rutile, which correlate to the oxides added for Fe and Ti respectively (Figure 29). Crystallization was noted to occur during post-production heat treatments in later analyses [36]. Further XRD investigation of the hotplate basic fabrication products with Fe and Ti added as oxides was limited due to previous observations and analyses (Visual, SEM EDS) indicating that the production with Fe and Ti added in solution as salts and alkoxides respectively would have more potential to produce homogeneity within the final product.

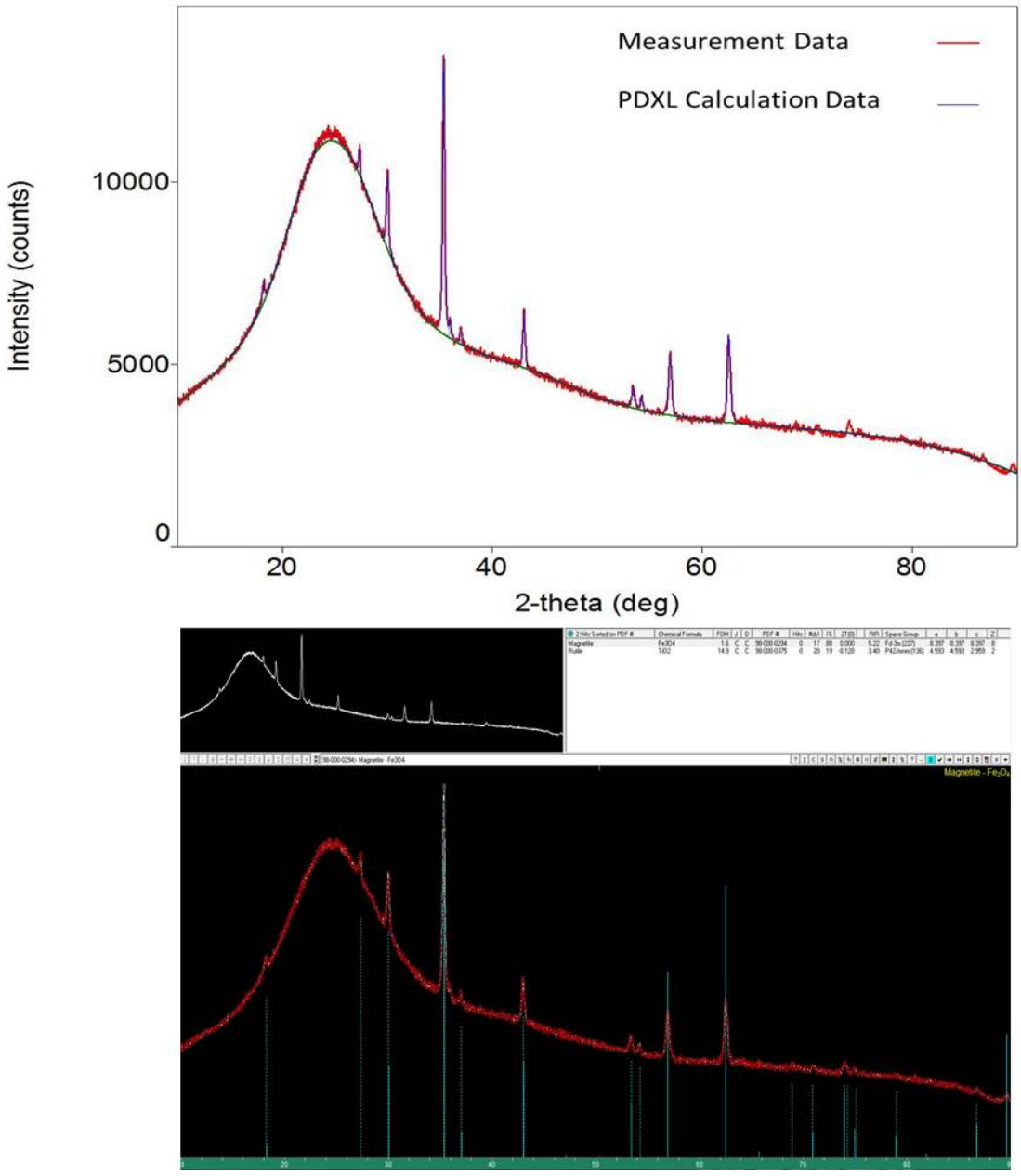

Top image: Results from Integrated X-ray Powder Diffraction Software (PDXL) allow for clearer image presentation.

Bottom image: XRD Processing, Identification and Quantification Software (JADE), version 9 allowed for greater refinement during investigation and identification of peaks.

While JADE was used to refine characterization of all XRD data, all further plots will be presented using PDXL.

Figure 30. XRD Analysis for Hotplate Basic Solution with Fe and Ti Added as Oxides, as Fabricated

Follow-on fabrication using oxides utilizing the thermal bath setup during production resulted in slightly improved visible homogeneity but still not to the level that adding the elements in solution would provide.

2. Basic Solution Fabrications with Fe and Ti Added as Soluble Precursors

Fabrication with the Fe and Ti added in solution (strategy iii) allowed for more even mixing during production with reduced potential for the elements to precipitate out and collect in one region due to gravity. A liquid solution (sol) was the result of the hotplate basic fabrications and took longer to dry. Therefore, these batches were more susceptible to diffusion of heavier elements during the formation of the surrogate material matrix through slower solidification [26].

Later fabrications were performed using the thermal bath setup from Chapter II. During thermal bath basic fabrication, the effect of the more uniform temperature profile was evident from visual observation and solidification time. Thermal energy provided from the thermal bath fueled hydrolysis within the combined solution with the basic pH catalyst contributing to the reaction [20], [21], [23]. A more uniform viscosity change was achieved during mixing as the solution experienced more homogenous nucleation [34]. This more rapid gelation produced the gel like structure expected from greater polymerization of the solution prior to gelation vice slow solidification producing the glass like structures from the earlier fabrications [20], [21], [23].

Hotplate basic fabrications took hours of mixing to observe the start of heterogeneous nucleation along the beaker walls where the temperature was more constant and the no slip boundary condition allowed for the solution near the wall to not be torn away back into the bulk solution where it would have been cooled down [34]. These hours of production were followed by additional hours (~24–48 hours) of drying time in order for solidification to finish. In contrast, the thermal bath basic fabrication experienced gel formation only 56 minutes 19 seconds from the combination of solution B and solution A with homogeneous nucleation of the bulk solution transforming it into a gel within a minute once gelation began.

The glassy structure achieved by the hotplate basic fabrications with Fe and Ti added in solution appeared uniform in color and texture with no visible phase segregation, which was advantageous over the hotplate basic fabrication method of adding the Fe and Ti as oxides (Figure 30). Analysis of the glassy products was central to the preliminary effort directed at maintaining the form of the product during heat treatment. The focus would later shift to producing homogeneous xerogels capitalizing on the improvement in thermal control during production and resulting products of gel formation. Faster gel formation would be more inclined to 'lock in' homogeneity during production. These improvements also provided support for the capacity of future fabrications being able to use oxides to represent selected elements of interest as uniformly dispersed inclusions in the future.

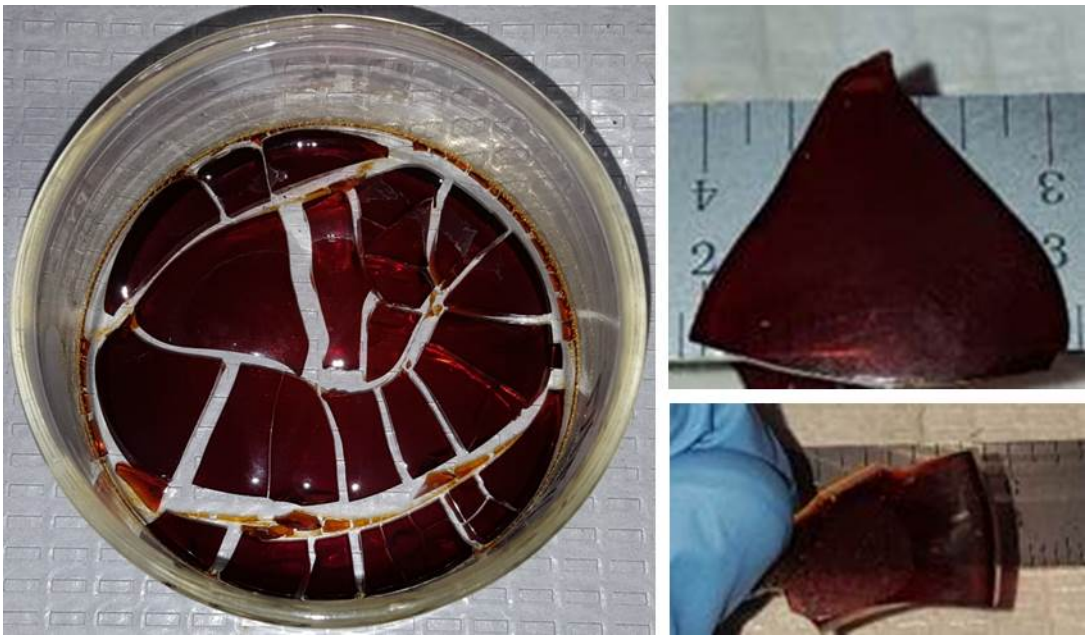

Left image: Glass container is 3.1 inches in diameter.

Figure 31. Hotplate Basic Solution Fabrication Adding Fe and Ti as Soluble Precursors, as Fabricated

Thermal analysis for the hotplate basic and thermal bath basic fabrications adding Fe and Ti in solution was performed. Analysis showed DSC reaction similarities below 200 °C related to the endothermic reactions for the phase changes and off-gassing of the

EtOH and H_2O (Figure 31). The thermal events start near the boiling points for EtOH and H_2O but are different shapes and magnitudes due to the hotplate basic fabrication producing a liquid solution that was present for a longer period during the drying process. Diffusion and subsequent evaporation of EtOH and H_2O would have been facilitated by this leaving less of these constituents held within the surrogate material matrix when DSC was performed. The sample temperature would likely lag behind the programmed temperature of the DSC machine due to the phase changes occurring and the isothermal nature of phase changes regardless of the ambient temperature. As the temperature differential increased so would the rate of the phase transformations which would also affect the depth and width of the endothermic event peaks. For the thermal bath basic fabrication a gel was formed and more volatile constituents would be contained within the surrogate material matrix. As opposed to the two distinct but similar peaks of the hotplate basic fabrication the thermal bath basic fabrication showed a much more pronounced first minimum followed by a smaller and narrower second minimum. This is potentially from the increased effect of volumetric expansion due to more EtOH being present in the thermal bath basic fabrication product. This would have led to larger mechanical damage during heating and allowed more off-gassing pathways and exposure when the H_2O underwent its phase transformation therefore producing a shallower and narrower second DSC minimum. Notable differences above 200 °C included upward peaks that projected the possibility of exothermic events such as crystallization and further decomposition (Figure 31). The exothermic event peak for the thermal bath basic fabrication occurred at ~325 °C.

TG analysis showed rate changes below 200 °C with increased off-gassing following 100 °C with a transition to minimal slope change by ~400 °C (Figure 31). By ~800 °C they was no longer an observable change in mass of the sample.

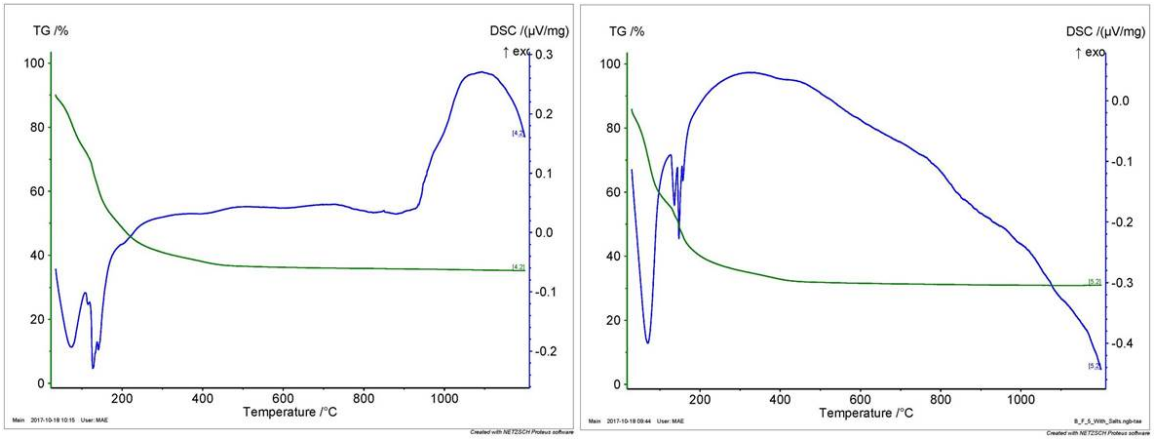

Left: DSC data for initial hotplate basic solution fabrication adding Fe and Ti as a salt and an alkoxide respectively.

Right: DSC data for final thermal bath basic solution fabrication adding Fe and Ti as a salt and an alkoxide respectively.

Figure 32. DSC-TGA Data for Hotplate Basic Solution with Fe and Ti Added in Solution, as Fabricated

Heat treatments, HT #1, HT #2 and HT #3 (Table 5), were performed with the hotplate basic fabrications to off-gas the product and allow crystallization to occur to attempt production of an intact glass product for LDHP (Figure 32). Thereby the LDHP procedure would only be processing the sample and not affecting phase changes and crystallization of the sample during the process. The temperature range of these heat treatments covered the estimated temperatures of the pulse and surrounding area noted during research by Mariella et al. [16].

Heat treatments, HT #6 and HT #7, were conducted with the hotplate basic fabrication to experiment with the effect on the end product of slow off-gassing of the product to just above the 325 °C exothermic peak noted in Figure 31 and to allow for crystallization to occur (respectively) (Table 5). These heat treatments failed to maintain the structural integrity of the products as a glass. HT #6 and HT #7 did provide slight improvement in the physical break up with the post-furnace samples still being cracked completely through and mechanically separated due to the off-gassing but with slightly larger pieces present (Figure 33).

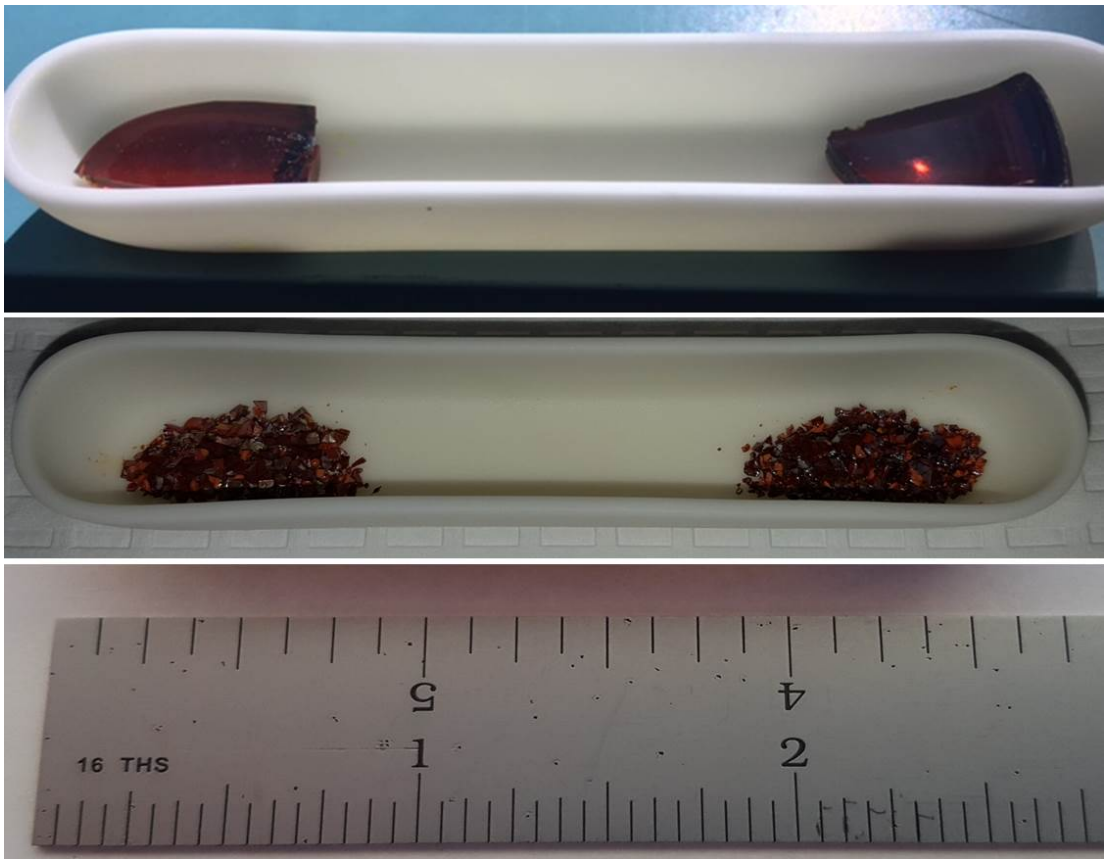

Top: Hotplate basic fabrication with Fe and Ti added in solution, as fabricated, left side is air dried and right side is oven dried.

Middle: Hotplate basic fabrication with Fe and Ti added in solution, post-furnace HT #3, left side is air dried and right side is oven dried.

Bottom: Ruler for scale.

Figure 33. Hotplate Basic Solution Fabrication with Fe and Ti Added in Solution, Pre- and Post-furnace

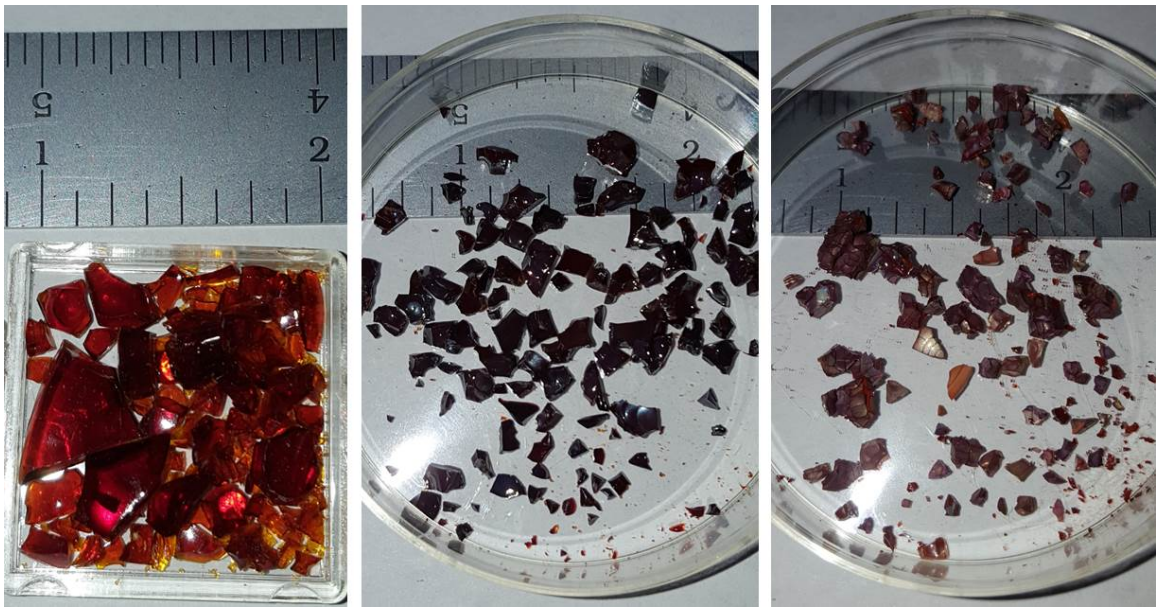

Left: Final thermal bath basic fabrication with Fe and Ti added in solution, as fabricated.
Middle: Final thermal bath basic fabrication with Fe and Ti added in solution, post-furnace HT #6.
Right: Final thermal bath basic fabrication with Fe and Ti added in solution, post-furnace HT #7.

Figure 34. Thermal Bath Basic Solution Fabrication with Fe and Ti Added in Solution, Final Fabrication

It was determined that the surrogate materials would be mechanically broken up went put through heat treatment. Sample homogeneity was prioritized over the final mechanical robustness of the xerogel product. Discussion began regarding the possibility of post-heat treatment crushing and sintering to utilize the product as a pellet provided that reasonable homogeneity could be achieved during fabrication [37].

SEM EDS analysis was performed on the hotplate basic solution with Fe and Ti added as soluble precursors. SEM imagery showed variations in texture along the different sides and profile of the product samples (Figure 34). These areas were reviewed to assess the distribution of phases for homogeneity.

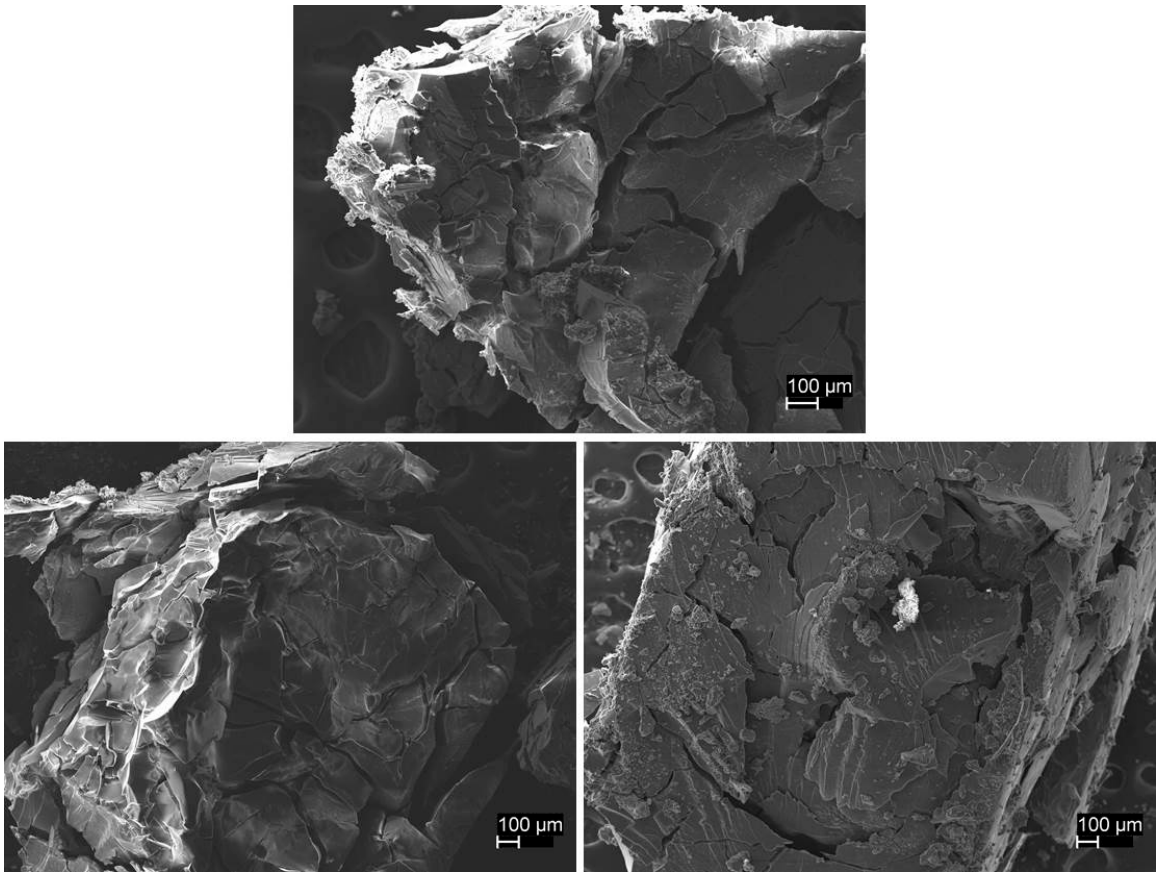

Top: Hotplate basic fabrication with Fe and Ti added in solution, as fabricated, profile.

Bottom left: Hotplate basic fabrication with Fe and Ti added in solution, as fabricated, side A.

Bottom right: Hotplate basic fabrication with Fe and Ti added in solution, as fabricated, side B.

Figure 35. SEM Image: Hotplate Basic Solution with Fe and Ti Added in Solution, as Fabricated

EDS spectra was collected and evaluated in comparison to the target composition with the standard deviation of the population being used as an indicator of homogeneity among the samples analyzed.

For the hotplate basic fabrication the largest standard deviations were calculated for the elements of Si and Fe (Figure 35). While many of the elements demonstrated a more even dispersion of the constituents the Fe and Si were displacing one another and affecting the homogeneity of the end product. Additionally, the elemental wt% of Al and K was noticeably off of the target composition even with a smaller calculated standard deviation among the samples. Cl continued to appear as a volatile element present that

could be reduced and eliminated through adequate post-production heat treatment of the fabricated sample [38].

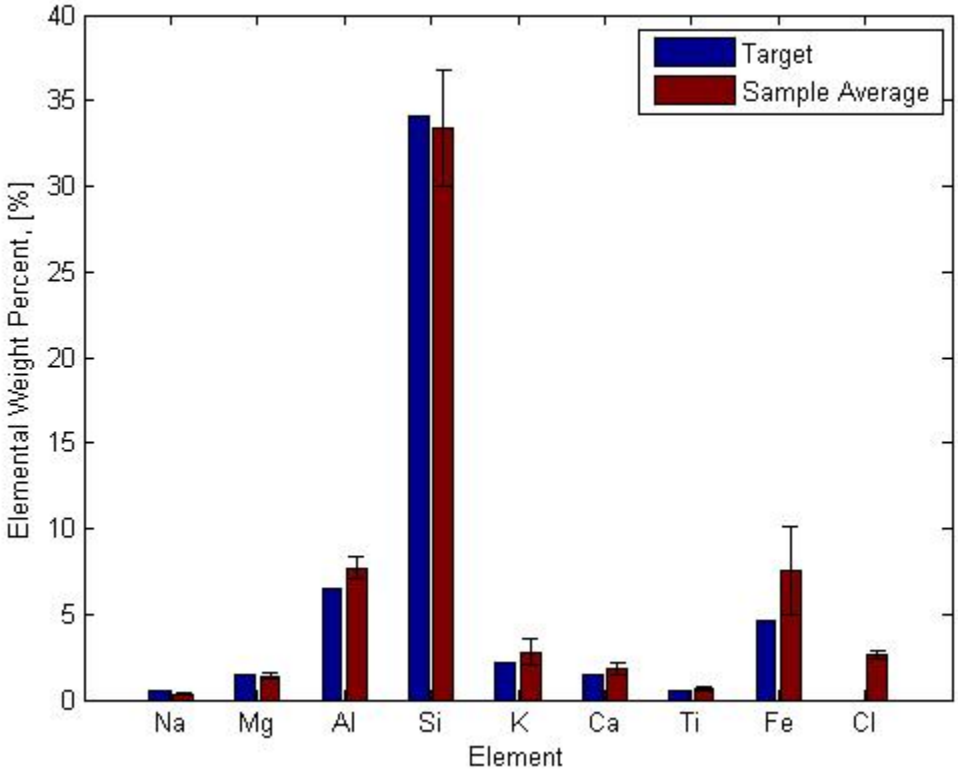

Note: The calculated standard deviation values are shown as line marker overlays on the top end of the Sample Average columns.

Figure 36. EDS Spectra Data Comparison for Hotplate Basic Solution with Fe and Ti in Solution, as Fabricated

EDS spectra for the thermal bath basic fabrication showed improvement with regard to the elements of interest Fe and Ti but at the expense of the precursors for Si and Al (Figure 36). The Fe showed a much smaller deviation between sampled areas and composition wt% was closer to the target composition. The Si content distribution variability was comparable to the hotplate basic fabrication as shown by the calculated standard deviation but the thermal bath basic fabrication wt% showed a greater departure from the target composition. The Al wt% for the thermal bath basic fabrication showed

an increased departure from the target composition with an increased variability among the samples as shown by the standard deviation.

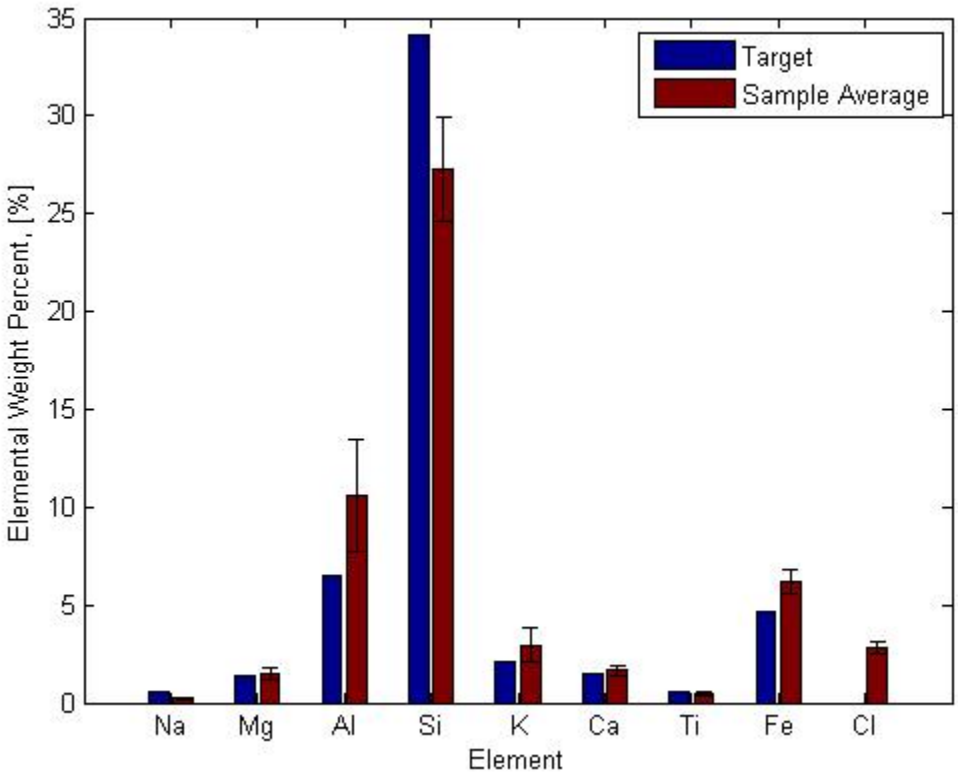

Note: The calculated standard deviation values are shown as line marker overlays on the top end of the Sample Average columns.

Figure 37. EDS Spectra Data Comparison for Thermal Bath Basic Solution with Fe and Ti in Solution, as Fabricated

EDS spectra collected for the post-heat treatment samples of the thermal bath basic fabrication showed a strong correlation to each other (Figure 37). This was anticipated based on the thermogravimetric analysis performed for the thermal bath basic fabrication (Figure 31, Right Image). The minimal slope change observed for TG between 350 °C and 825 °C had no observable effect on the elemental composition during the two heat treatments when compared to each other and these were the peak temperatures reached during HT #6 and HT #7 respectively.

Elemental wt% showed increased deviation from target composition values but this was not due to the introduction or removal of precursors or elements of interest, but rather the presence of volatiles still trapped within the porous networks of the xerogel.

SEM EDS analysis, while perfectly suited for this study to assess product homogeneity and dispersion of constituent elements, does not provide for a complete elemental breakdown of the composition of a specimen. A more accurate accounting of volatiles may prove useful due to their observed effects on post-production characteristics of the xerogel products. This could be performed using mass spectrometry techniques, but would result in both consuming of the specimen tested and a mere composition of the sample as a whole, not the dispersion of elements present. Due to these considerations regarding mass spectrometry and the nature of this study, the SEM EDS analysis was the perfect choice for this endeavor with only identified elements evaluated based on the prominent peaks observed. These were the precursors Na, Mg, Al, Si, K, Ca, Cl and the elements of interest Fe, Ti. The prominent peak for carbon was not included due to the sample containing no carbon and these readings being from the carbon tape background of the SEM sample holder. The difference between measurement values for the identified elements and the whole sample was consolidated and assigned to oxygen and was identified as the oxygen by difference method.

The change in wt%s can be attributed to the burn off of volatiles contained in the sample during heat treatment. The measurement for the precursor Cl shows evidence of this since Cl would also be one of the volatiles anticipated to burn off. Cl burn off was not complete and this was due to the need for longer exposure to thermal input during the heat treatment with an additional minor effect of the conversion of some iron oxide into the corresponding chloride thereby trapping some of the elemental Cl in the product [38].

A more in depth investigation into the effect of volatile burn off and anticipation of effect on elemental composition would require techniques that would yield a more precise composition of all elements present in the fabrication. Such techniques could include atomic absorption spectrometry and inductively coupled plasma atomic emission spectrometry. Through these analyses a correction might be made to the measurement values to account for the burn off bias. These resources were not available during this

study and are being pursued as potential future work for this project. It is also worth mentioning that supercritical drying could be employed to remove solvents without disturbing the gel network, however, such procedure will render a highly porous solid rather than the dense surrogate we are seeking for.

The calculated standard deviation for the element of interest Fe may also be affected by the uncorrected measurement data following heat treatment. Of value is the qualitative comparison between the EDS spectra of the two heat treatments and the lack of significant difference between them that still provided insights and correlated to the DSC analysis (Figure 31, Right Image).

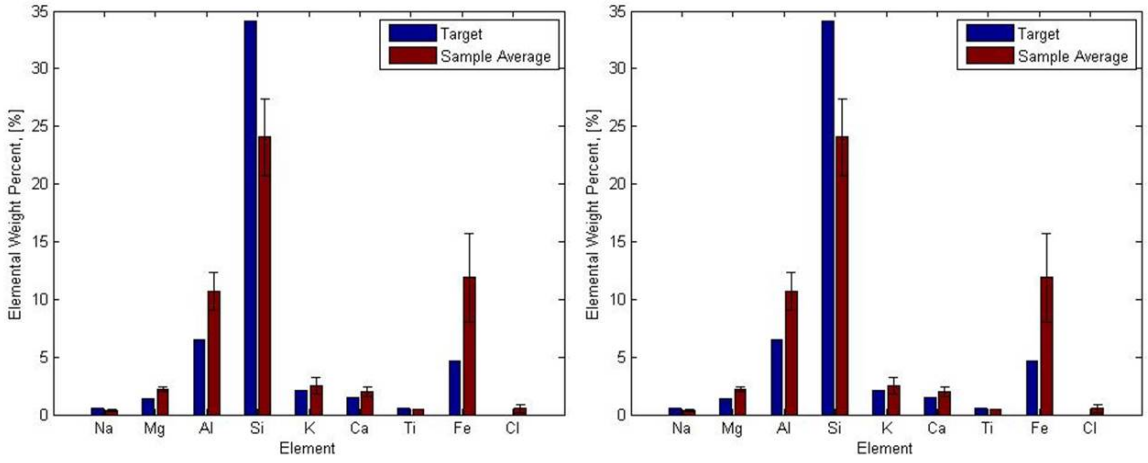

Note: The calculated standard deviation values are shown as line marker overlays on the top end of the Sample Average columns.

Left: Thermal bath basic fabrication, post-heat treatment HT #6.

Right: Thermal bath basic fabrication, post-heat treatment HT #7.

Figure 38. EDS Spectra Data Comparison for Basic Solution with Fe and Ti in Solution, Thermal Bath Fabrication, Post-heat Treatment

XRD analysis of the thermal bath basic fabrication was performed. Post-heat treatment structures were noted including iron titanium oxide, calcium aluminum iron oxide and hematite (Figure 38) [36]. The background shape supporting the existence of an amorphous matrix is still visible even after the post-production heat treatment.

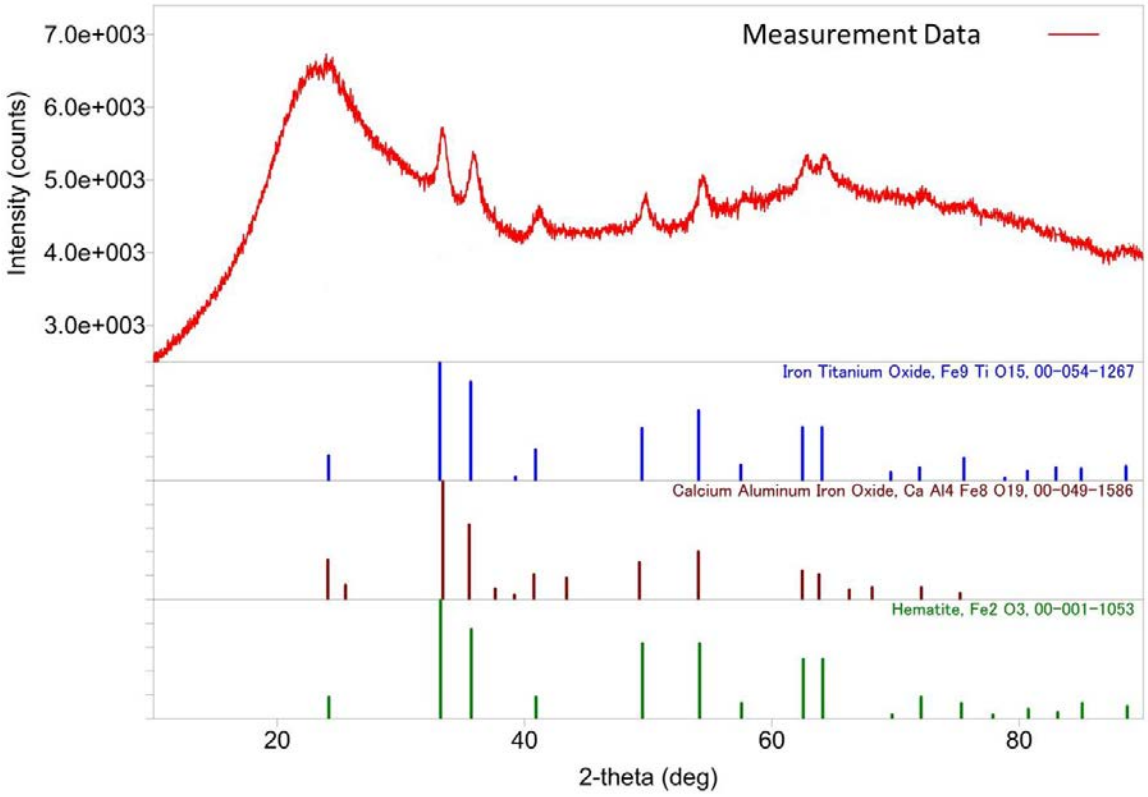

Figure 39. XRD Analysis for Thermal Bath Basic Fabrication with Fe and Ti Added in Solution, Post-furnace HT #7

C. SUMMARY

Adding the elements of interest, Fe and Ti, as oxides was expected to result in phase segregation during the fabrication process but was a necessary step to provide an assessment of the product created for comparison to the product created by adding the elements of interest in solution.

Adding the elements of interest as a salt and an alkoxide allowed dissolution into the solutions A and B prior to their combination and subsequent experiencing of hydrolysis and polymerization while being heated and mixed during production.

The thermal bath setup provided a heat source that allowed for a thermal energy reservoir to be available when endothermic reactions occurred during fabrication which sustained the rate of reactions by minimizing temperature fluctuations. This thermal control is a critical process during the production of sol-gel materials as the drying,

dehydration and densification directly affect the gel formation of the specimen [20], [21], [23], [26]. Changes to these processes direct the form of the product as an aerogel, xerogel or film. The dehydration step was affected using the drying methods listed in Chapter II and the densification step was affected using the heat treatments listed in Table 5.

Improvements were made to the homogeneity of the resultant xerogel through manipulation of fabrication parameters and post-production processing. A consistent drying protocol was identified and used for drying and dehydration. Heat treatment protocols were established for sample densification. Post-production heat treated samples were shown to have consistent averaged results when compared to each other however, the standard deviation among critical precursors, specifically Fe, Al and Si was high and the corresponding sample composition averages were significantly deviated from the target composition.

Of the solution fabrications utilizing a base as the catalyst the most homogeneous and consistent products were produced using the thermal bath basic fabrication method adding Fe as a salt and Ti as an alkoxide.

THIS PAGE INTENTIONALLY LEFT BLANK

IV. RESULTS AND DISCUSSION FOR ACIDIC PH CATALYST APPROACH

A. OVERVIEW

The adaptability of the sol-gel process created trade space for the investigation of parameter variation to guide the optimization of a protocol using the sol-gel process. Incorporating lessons learned from fabrications using the basic pH catalyst and applying characterization methods described in Chapter II for the acidic pH catalyst specimens allowed for the selective elimination of production paths and prioritization of the fabrication processes most likely to produce a homogeneous product using the acidic pH catalyst (Figure 39).

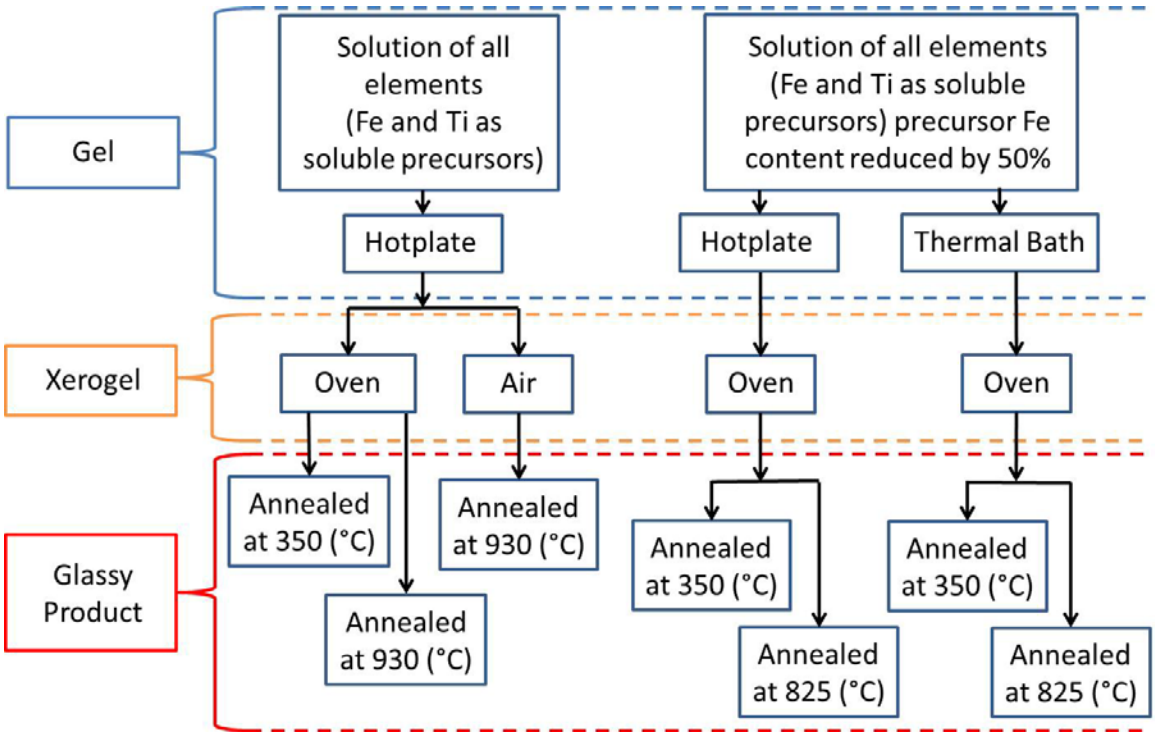

Precursor chemicals for the elements and soluble precursors for Fe and Ti identified in Table 6.

Figure 40. Overview of Acidic pH Catalyst Fabrication Products Using a Solution with All Elements and Fe and Ti Added as Soluble Precursors

As discussed in Chapter I and Chapter II the reactants undergo transitions during both production of the gel and post-production of the xerogel as, a) a sol formed using the selected catalyst, precursors and medium, b) a gel which took form following polymerization of the sol, c) a xerogel from evaporation of the solvents, primarily water and alcohol and d) a glassy product following densification through heat treatment (Figure 20).

Fabrication with Fe and Ti added in solution using an acidic catalyst was performed with the same two forms of thermal input used during the basic solution productions. Thermal input was provided through conduction from the heater plate to the bottom of the beaker or conduction on all sides of the beaker from the thermal bath setup. The thermal bath setup fabrications provided a more uniform temperature profile during production to promote homogeneous nucleation and gelation [20], [21], [26]. This was as expected and in keeping with observations from the productions and characterizations performed for the basic pH catalyst solution fabrications.

As discussed the addition of Fe and Ti as oxides was not anticipated to yield satisfactory homogeneity in the xerogel product. This was verified with the basic solution fabrications and therefore the acid fabrications were performed only with Fe and Ti being added in solution. Experimentation was instead directed toward the investigation and refinement of other production parameters such as temperature control during production, drying time variation, reactant ratio of element of interest Fe and heat treatments. Acidic pH catalyst solution fabrications were conducted multiple times with these protocol parameters used as variables.

Multiple fabrications using variations of the acidic pH catalyst methods were performed and the difference in effects of stricter thermal parameter control was observed. Ultimately a path involving a thermal bath for temperature control was selected for the production protocol with all elements being added as soluble precursors. The next sections of this chapter have been divided in two, both of them used an acidic pH, however, the amount of Fe was optimized and the use of hotplate vs thermal bath was contrasted.

B. STRATEGY TWO: ACIDIC PH CATALYST

1. Acid Solution Hotplate Fabrications with Fe and Ti Added as Soluble Precursors

The constituent chemicals were measured during the fabrications and the standard deviation of these values was calculated to provide a qualitative estimate of ingredient measurement variation among the multiple fabrications (Figure 40).

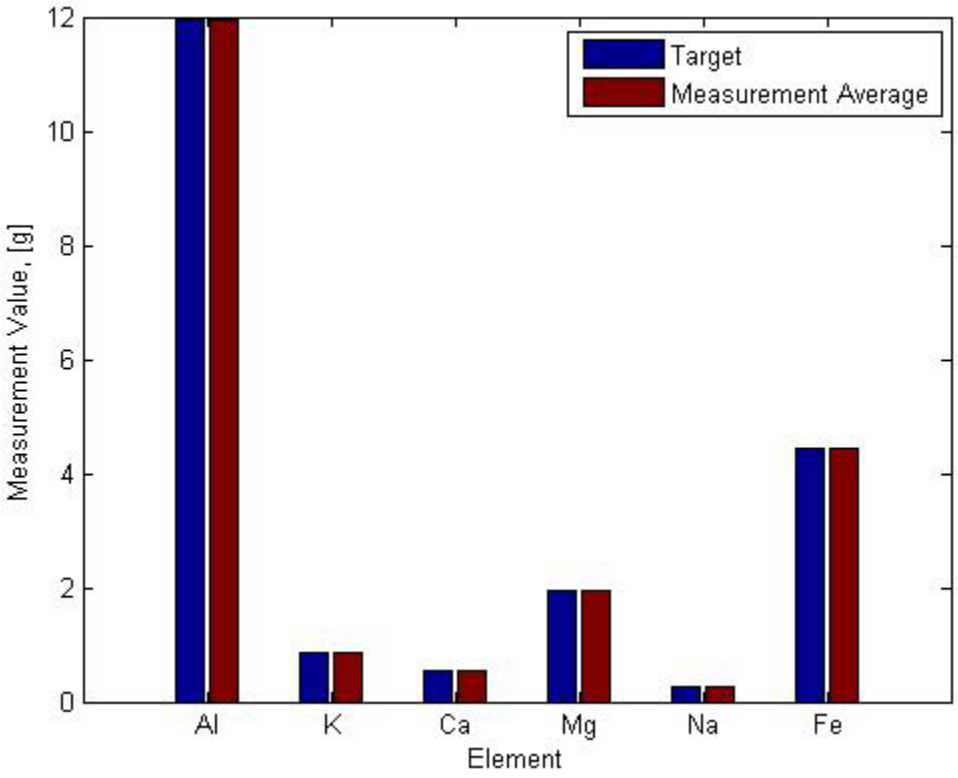

Note: The calculated standard deviation values are so small that the line markers delineating them essentially overlay on the top end of the Measurement Average columns.

Calculated standard deviations were extremely small and blend in with the tops of the Measurement Average columns.

Figure 41. Surrogate Material Precursor Measurement Variation during Production

The product of these hotplate acid solution fabrications was a xerogel formed through solidification of the matrix (Figure 41). During the drying process off-gassing

occurred which allowed for partial collapses of the internal networks and subsequent shrinkage of the product [26]. Even though cracks formed allowing further avenues for off-gassing significant quantities of volatile constituents remained trapped within the porous structure of the xerogel [22].

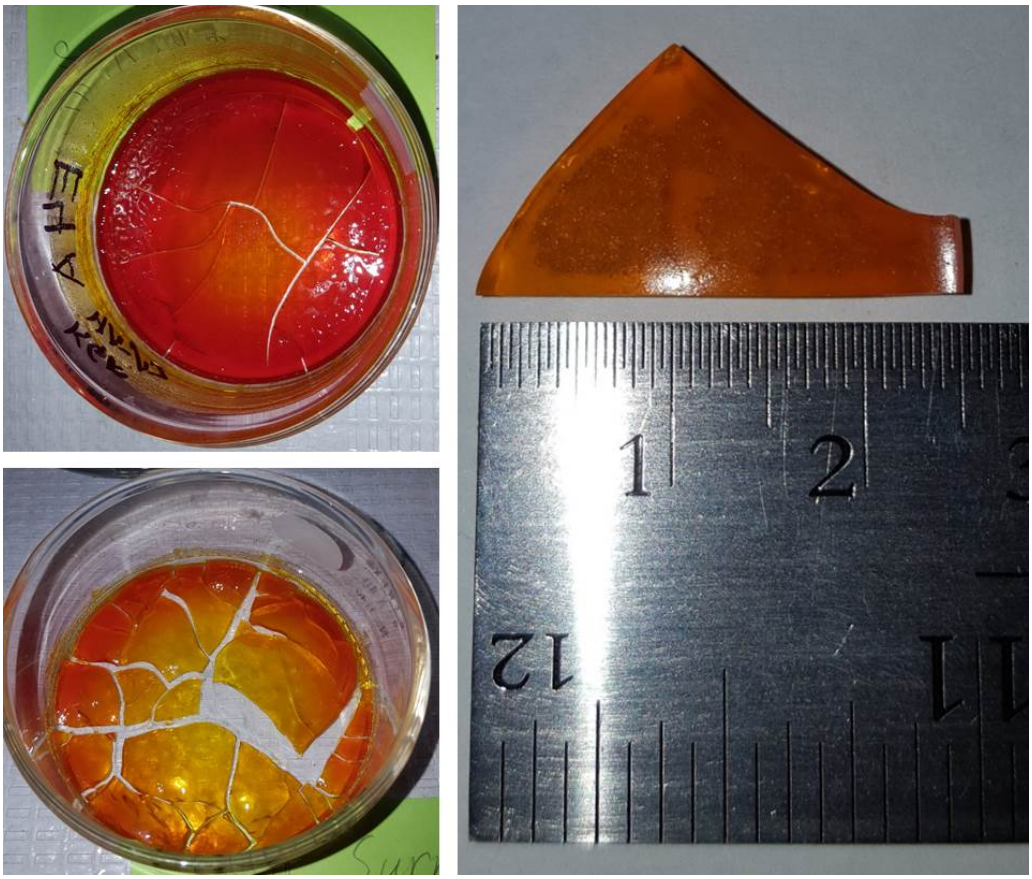

Hotplate acid fabrication xerogel product, oven dried.

Left images (top and bottom): Glass container is 3.1 inches in diameter.

Figure 42. Hotplate Acid Solution Fabrication with Fe and Ti Added as Soluble Precursors, as Fabricated

The oven drying parameter was varied in an effort to assess potential benefits to longer off-gassing of solvents during the fabrication process and to confirm that the oven drying process was not significantly impacting thermogravimetric behavior of the products. These trials primarily affected the removal of EtOH by aiding in the promotion of evaporation during drying due to its relatively low boiling point. The rate of EtOH

removal during drying was not intended to be enough to induce further widespread cracking of the product beyond cracks already forming due to anticipated shrinkage of the product.

The heat-up rate applied during thermogravimetric analysis promoted rapid phase transformations of ethanol and other volatile components from liquid to gas throughout the product leading to widespread cracking of the xerogel network to allow for the gasses to escape (Figure 42). Endothermic activity was present leading up to the boiling point of the EtOH at 78.37 °C.

Rate of change for TG decreases were observed to coincide with the EtOH and H_2O phase changes as expected. There was no significant mass loss observed above 800 °C similar to the basic solution fabrications.

Initial annealing took the hotplate acid solution samples to 930 °C (HT #3 from Table 5) (Figure 43). Mechanical robustness was visually comparable to that of hotplate basic solution samples.

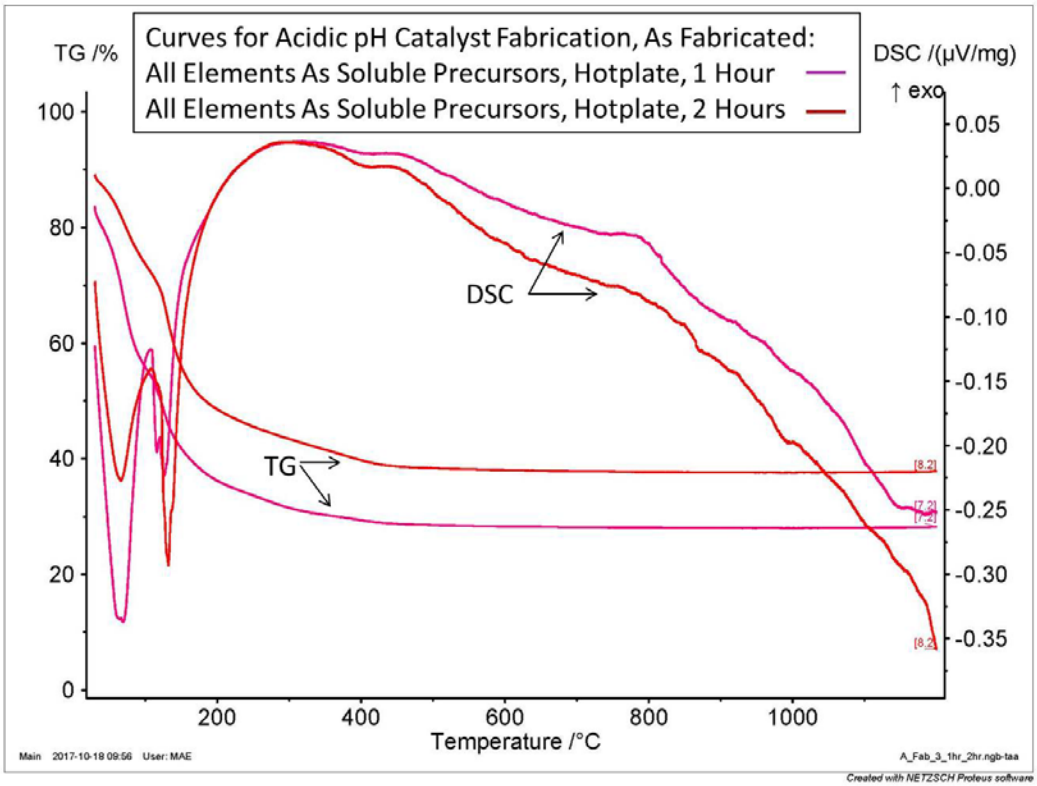

Oven drying time variable modified from 80 minute standard used during production protocol to evaluate thermogravimetric effect of additional off-gassing on product characteristics.

Figure 43. DSC-TGA Data for Hotplate Acid Solution Fabrication with Fe and Ti Added as Soluble Precursors, as Fabricated, Variable Duration of Drying Method

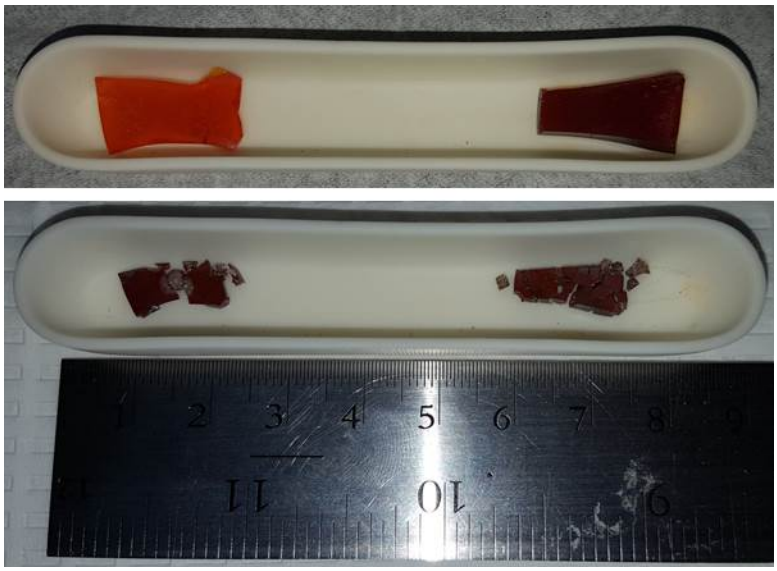

Top: Hotplate fabrication with Fe and Ti added as soluble precursors, as fabricated, left side is acidic pH catalyst solution and right side is basic pH catalyst solution.

Bottom: Hotplate fabrication with Fe and Ti added as soluble precursors, post-heat treatment to 930 °C (HT #3 from Table 5), left side is acidic pH catalyst solution and right side is basic pH catalyst solution.

Ruler for scale.

Figure 44. Hotplate Acid Solution Fabrication Visual Comparison to Hotplate Basic Solution Fabrication with Fe and Ti Added as Soluble Precursors, Pre- and Post-heat Treatment

Heat treatments were conducted with the acid solution xerogels both in their solid – single piece form and in a crushed form (Figure 44). Since the possibility of creating pellets through crushing, heat treating and sintering was introduced during the basic solution fabrication characterizations, the acid solution xerogel was crushed and heat treated to observe possible effects on removal of volatiles while in a powder form. As expected, visual observations following the heat treatment showed that the crushed acid xerogel product could not be effectively sintered while loosely packed into a crucible. Compacting under higher pressure into a pellet form would produce a more likely candidate for sintering that would subsequently produce a solid with enough mechanical robustness to allow processing via LDHP. Further evaluation would be needed if pellets are created to assess the differences between a) heat treating the powder prior to pellet

formation and subsequent sintering and b) forming the pellet and then performing the heat treatment concurrent with sintering.

Hotplate acid solution fabrication product prepared crushed into a powder and heat treated for further analysis and initial assessment of possible effects on removal of volatiles while in a powder form.

Ruler for scale.

Figure 45. Hotplate Acid Solution Fabrication with Fe and Ti Added as Soluble Precursors, Prepared for Heat Treatment as a Solid (top) and as Crushed Powder (bottom)

The hotplate acid solution fabrications produced sols that underwent drying at different stages and thus promoted slight elemental component separation into gels and dried to form a material that was glass like in appearance. Drying time varied between 24 to 48 hours during which time the product was still a sol through which diffusion of heavier particles would be more facilitated by gravity. To assess this potential effect samples were taken from the top and bottom of the product when oriented flat in the position the xerogel dried in. No appreciable differences were noted for the EDS spectra data, which was not skewed toward either side of the sample. SEM imagery showed more physical breakup of one side but this could be attributable to variations in trapped EtOH or H_2O distribution within the porous matrix of the xerogel when placed in vacuum prior to SEM-EDS analysis (Figure 45).

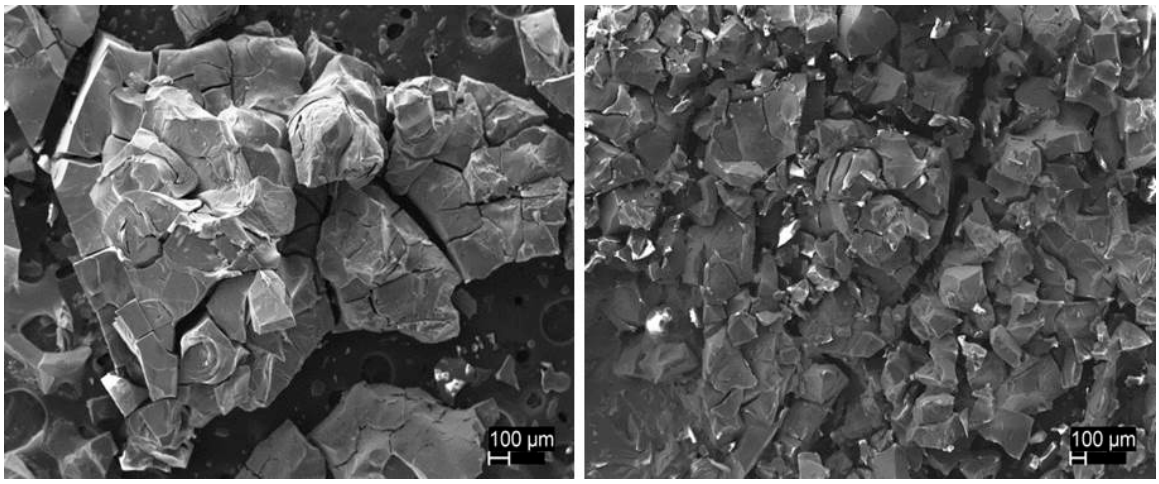

Samples taken from areas on opposite sides of the xerogel glass produced as oriented flat in the position the xerogel dried in for comparison of gravitational effects on diffusion during drying process.

Left: Sample taken from area on top of the xerogel glass.

Right: Sample taken from area on bottom of the xerogel glass.

Figure 46. SEM Image: Hotplate Acid Solution with Fe and Ti Added as Soluble Precursors, as Fabricated

SEM images for specimen were selected for particles of approximately the same size so the same xerogel product could be shown as fabricated, post-heat treatment (HT #6) and post-thermogravimetric analysis (Figure 46). Surface morphology could be

observed to change as the product was exposed to higher temperatures. Crystallization was promoted as the temperature was increased toward 800 °C (Figure 42).

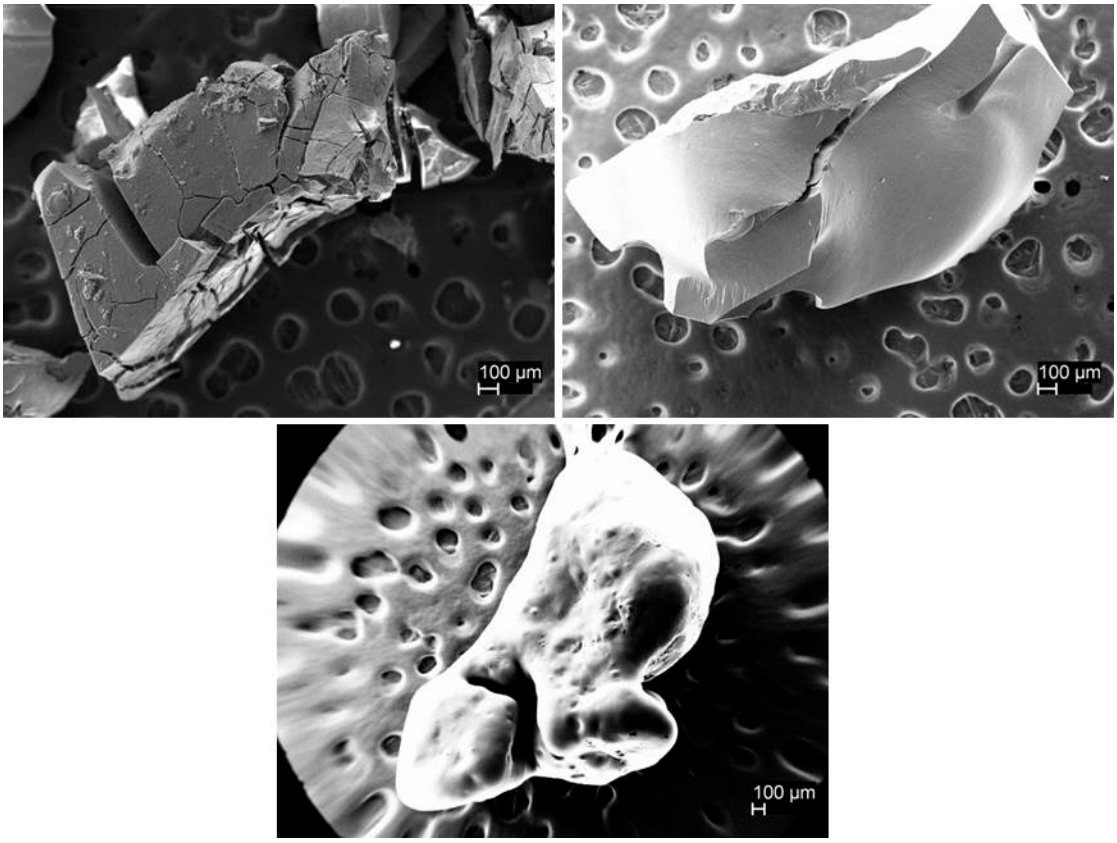

Top left: Hotplate acid solution with Fe and Ti added as soluble precursors, as fabricated.

Top right: Hotplate acid solution with Fe and Ti added as soluble precursors, post-heat treatment HT #6.

Bottom: Hotplate acid solution with Fe and Ti added as soluble precursors, post-thermal analysis.

Figure 47. SEM Image: Hotplate Acid Solution with Fe and Ti Added as Soluble Precursors, as Fabricated, HT #6, Post-thermal Analysis

The higher temperatures achieved during thermogravimetric analysis drove more complete off-gassing of not just EtOH and H_2O but also additional volatiles, such as chlorine which was introduced with the reactant $CaCl_2$ used as a precursor for Ca as well as with the HCl used as the acidic pH catalyst. More collapsing of the xerogel network would be induced by these higher temperatures [22], [26].

EDS spectra was collected and evaluated for comparison of the xerogel product compositions to the target composition and to assess improvements being made to product homogeneity following variation of protocol parameters between fabrications with standard deviation of the population still used as an indicator of homogeneity among the samples analyzed.

For the hotplate acid fabrication, which produced the xerogel through slower solidification the largest standard deviations, calculated standard deviations for the elements of Al, Si and Fe (Figure 47). While many of the other recorded elements demonstrated a more even dispersion of the reactants the Al, Si and Fe were still displacing one another and affecting the homogeneity of the product. This is similar to the results from the hotplate basic solution fabrication. The elemental wt% of K compared to the target composition was improved during the hotplate acid solution fabrications when compared to the basic pH catalyst solution fabrications. The elemental wt% of Al, Si and Fe continued to be noticeably off of the target composition with the largest calculated standard deviations among the samples. Cl continued to appear as a volatile element present that could be reduced and eliminated through adequate post-production heat treatment of the fabricated sample.

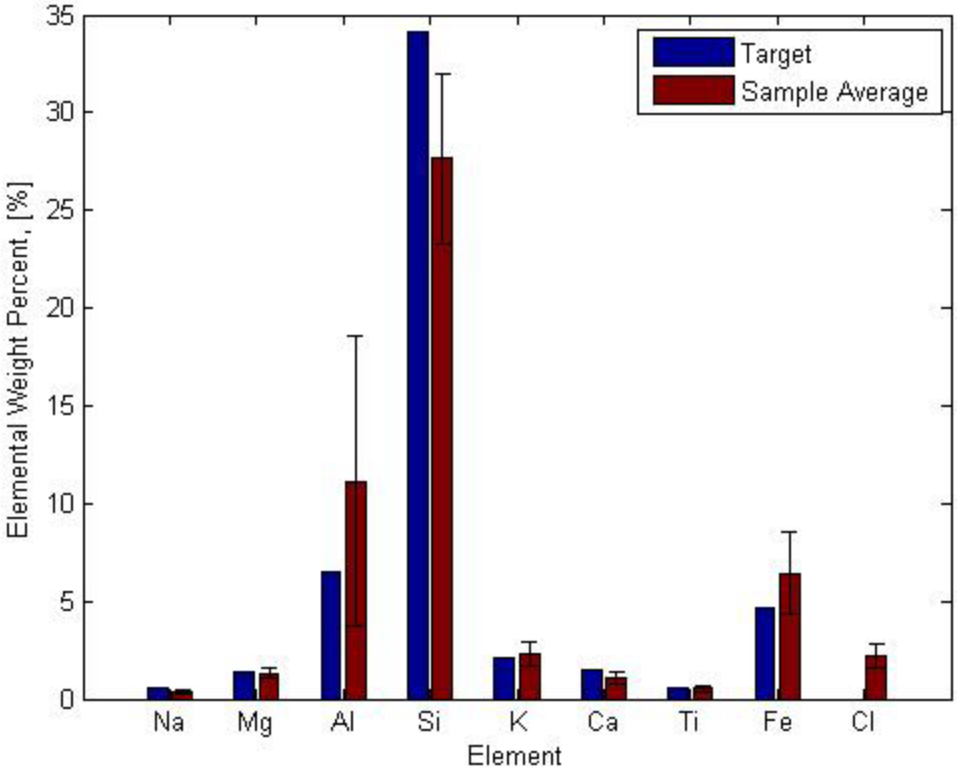

Note: The calculated standard deviation values are shown as line marker overlays on the top end of the Sample Average columns.

EDS spectra data from hotplate acid solution with Fe and Ti added as soluble precursors, as fabricated.

Figure 48. EDS Spectra Data Comparison for Hotplate Acid Solution with Fe and Ti Added as Soluble Precursors, as Fabricated

EDS spectra data supported the conclusion that volatiles, such as Cl, could be reduced and eliminated through heat treatment. EDS mapping was performed to gain a visual representation of the dispersion of the reactant elements starting with the product as fabricated. Fairly uniform dispersion of reactant elements was observable for the xerogel as fabricated with Cl present among them (Figure 48).

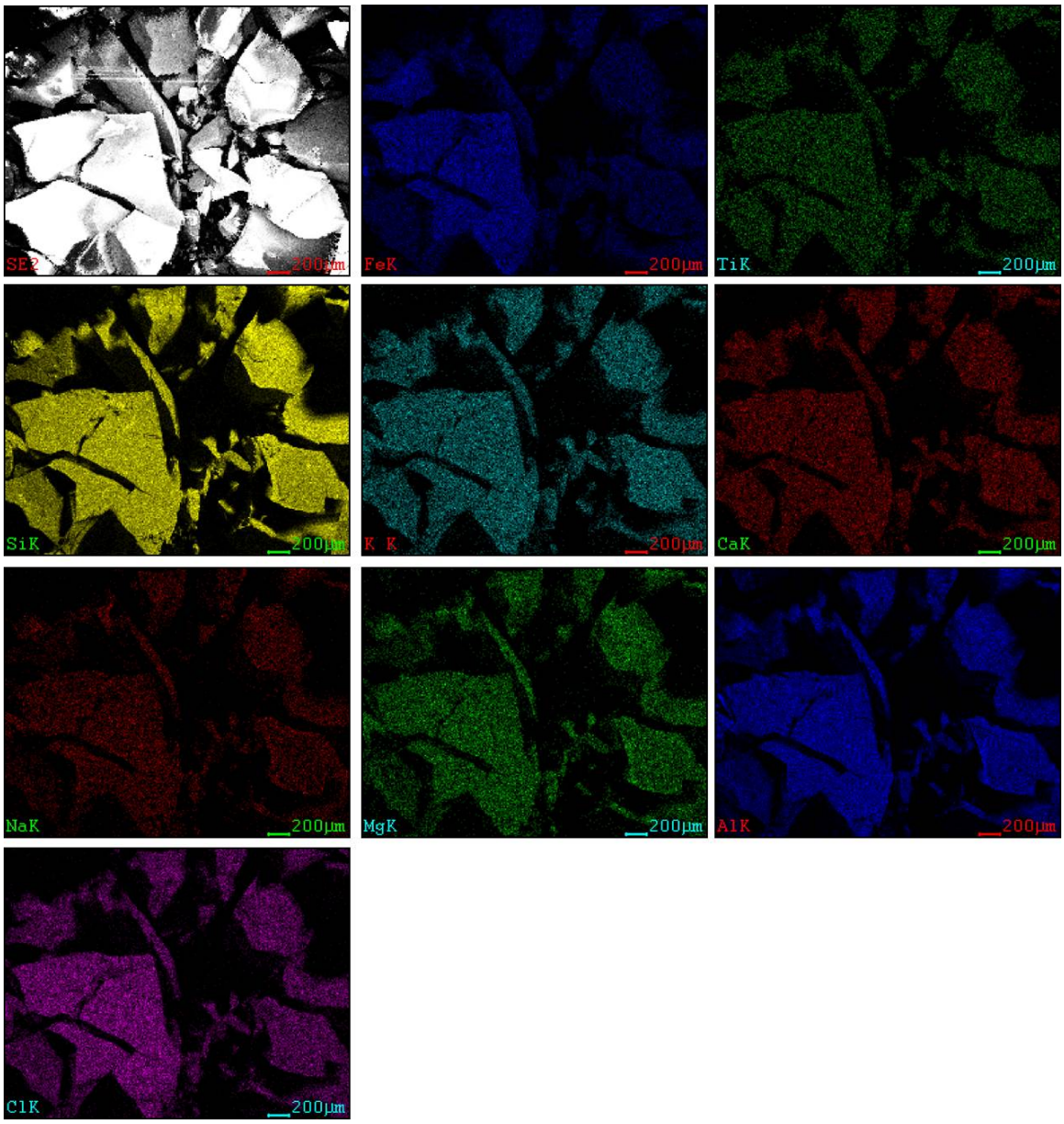

First row (left to right): Secondary electron image of sample area being mapped, map showing Fe distribution, map showing Ti distribution.

Second row (left to right): Map showing Si distribution, map showing K distribution, map showing Ca distribution.

Third row (left to right): Map showing Na distribution, map showing Mg distribution, map showing Al distribution.

Fourth row: Map showing Cl distribution.

Figure 49. EDS Mapping of Hotplate Acid Solution with Fe and Ti Added as Soluble Precursors, as Fabricated

Homogeneity, to the degree sought after for this study, was not fully achieved during post-production of specimens from fabrications using the hotplate. The use of the sol-gel process allowed for definite improvement in homogeneity and element dispersion over the inhomogeneous natural material tektite. EDS mapping from the characterization of natural tektite performed during a previous study showed more gradient in the EDS map colors indicating changes in concentrations for the corresponding elements as seen with Si and other areas with denser oxides present as seen with Si, Fe, Ti and Al (Figure 49 and Figure 50) [12].

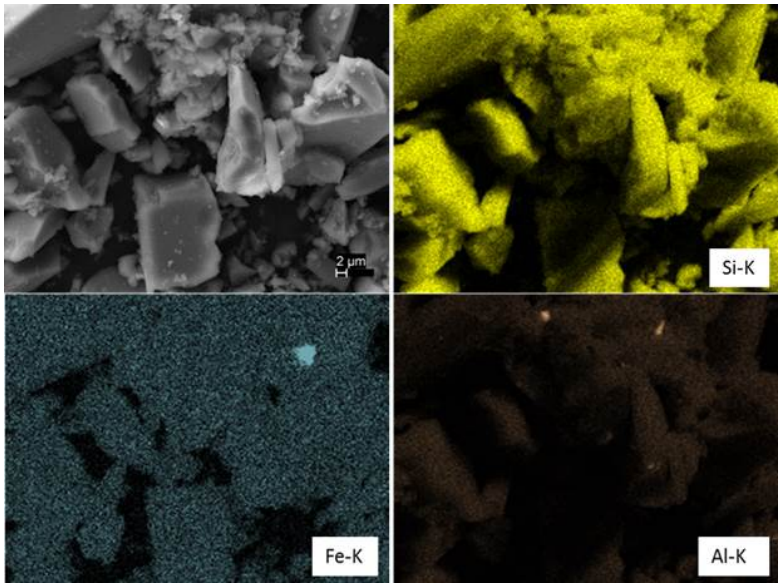

"Secondary Electron image of a crushed tektite sample (top left). SEM-EDS mapping showing Si distribution (top right), Fe-rich oxide particle (bottom left), and Al-rich oxide particles (bottom right). Source: [12].

Figure 50. EDS Mapping Completed during Previous Characterization of Inhomogeneous Natural Material Tektite. Source: [12].

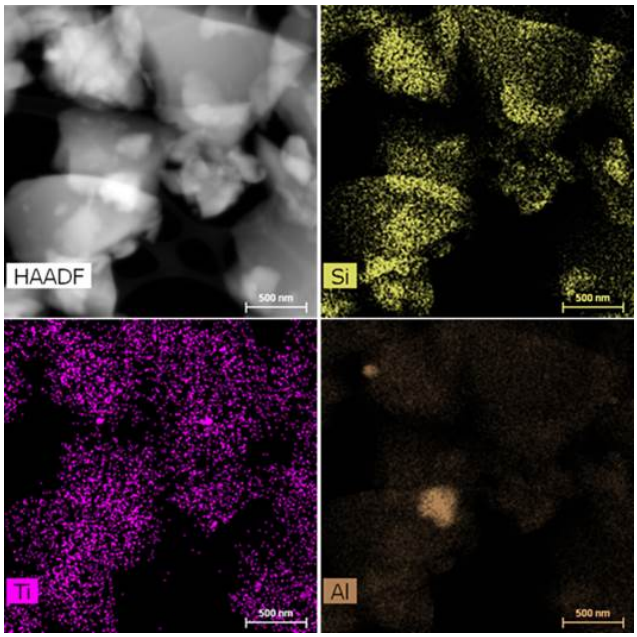

STEM-EDS mapping showing oxide particles rich in Si (top right), Ti (bottom left), and Al (bottom right). Source: [12].

Figure 51. STEM-EDS Mapping Completed during Previous Characterization of Inhomogeneous Natural Material Tektite. Source: [12].

Following heat treatment of the hotplate acid fabrication samples EDS mapping showed similar gradients in color indicating changes in concentrations for the elements and darker spots representing the formation and agglomeration of oxides within the xerogel matrix (Figure 51). Even through heat treatments being applied volatiles, such as Cl, were still present and Cl can be seen to still be fully integrated into the xerogel matrix. This implied that heat treatments were promoting off-gassing of EtOH and H_2O but other volatiles within the porous xerogel matrix were not being removed. While elemental Cl has a low boiling point of -34.04 °C the boiling point to remove the Cl once it is combined with other reactants is significantly higher as shown in [39]. For example NaCl has a boiling point of closer to 1413 °C due to the nature of electrostatic attractive forces between the Na and Cl ions [39].

Evidence of off-gassing of these volatiles was seen in the hotplate acid solution fabrications following thermogravimetric analysis due to the much higher temperatures achieved during the analysis and the small mass used for the analysis. EDS mapping of

post-thermal analysis samples showed some gradients in color concentrations and small areas with oxides being concentrated but Cl was no longer present in sufficiently measurable quantities to be recorded (Figure 52).

As the samples were heat treated and off-gassing was induced the partial collapses of the xerogel network strengthened the network while the sample sizes were reduced [22], [26]. As a result the wt% readings for heat treated samples continued to track farther from the target composition values due to reactants used now being a larger percentage of the remaining mass. As mentioned in the previous chapter an in depth investigation into the effect of volatile burn off and anticipation of effect on elemental composition would require techniques that would yield a more precise composition of all elements present in the fabrication. Such techniques could include atomic absorption spectrometry and inductively coupled plasma atomic emission spectrometry. Through these analyses a correction might be made to the measurement values to account for the burn off bias.

These techniques were not pursued during this study since, as discussed in Chapter III, the SEM EDS analysis was perfectly suited for this endeavor to assess product homogeneity and dispersion of constituent elements. The difference between measurement values for the identified elements and the whole sample was consolidated and assigned to oxygen and was identified as the oxygen by difference method. Any additional volatiles trapped within the surrogate matrix would be accounted for as part of this weight percentage assigned to oxygen.

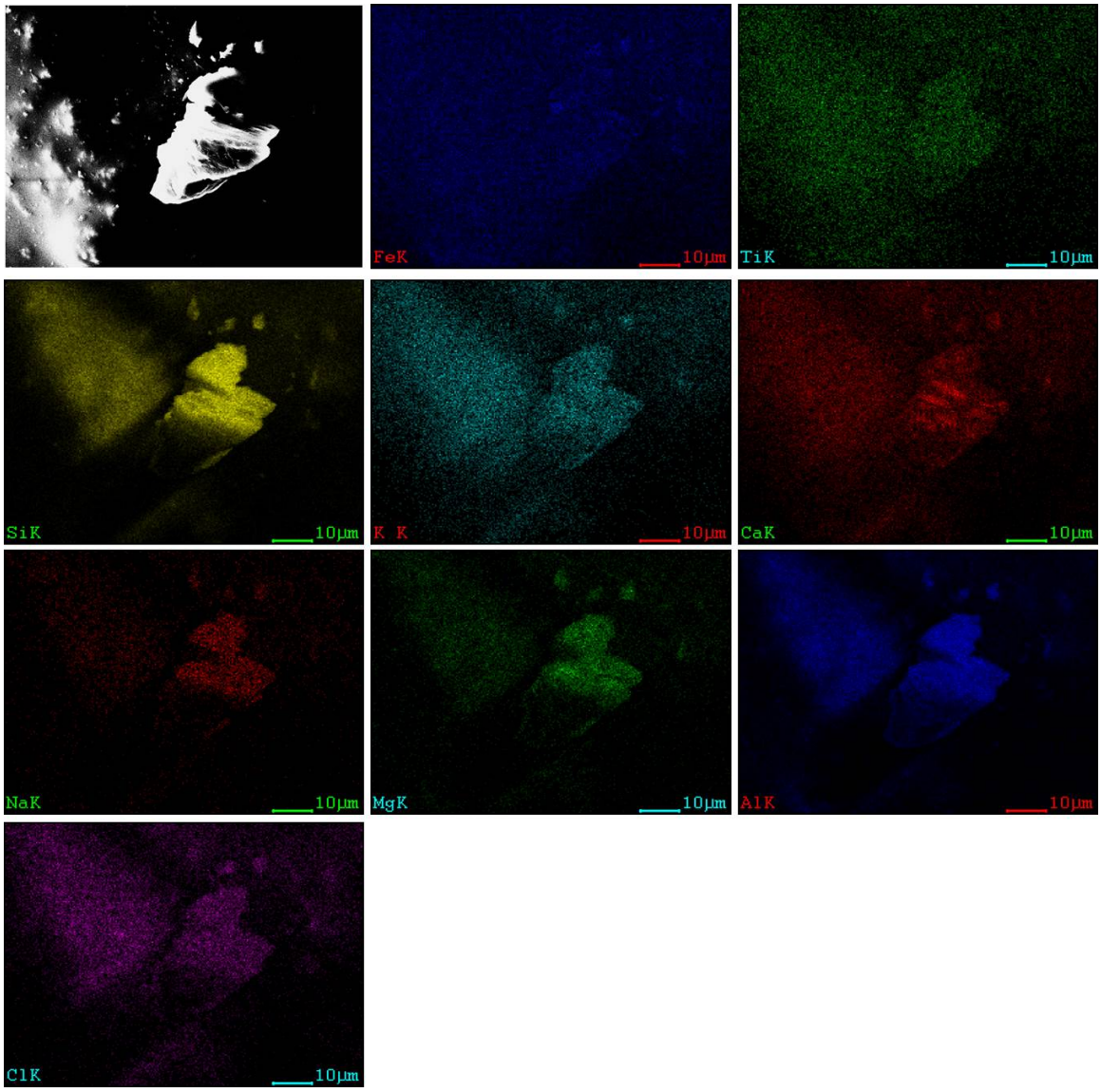

First row (left to right): Secondary electron image of sample area being mapped, map showing Fe distribution, map showing Ti distribution.

Second row (left to right): Map showing Si distribution, map showing K distribution, map showing Ca distribution.

Third row (left to right): Map showing Na distribution, map showing Mg distribution, map showing Al distribution.

Fourth row: Map showing Cl distribution.

Figure 52. EDS Mapping of Hotplate Acid Solution with Fe and Ti Added as Soluble Precursors, Post-heat Treatment (HT #6)

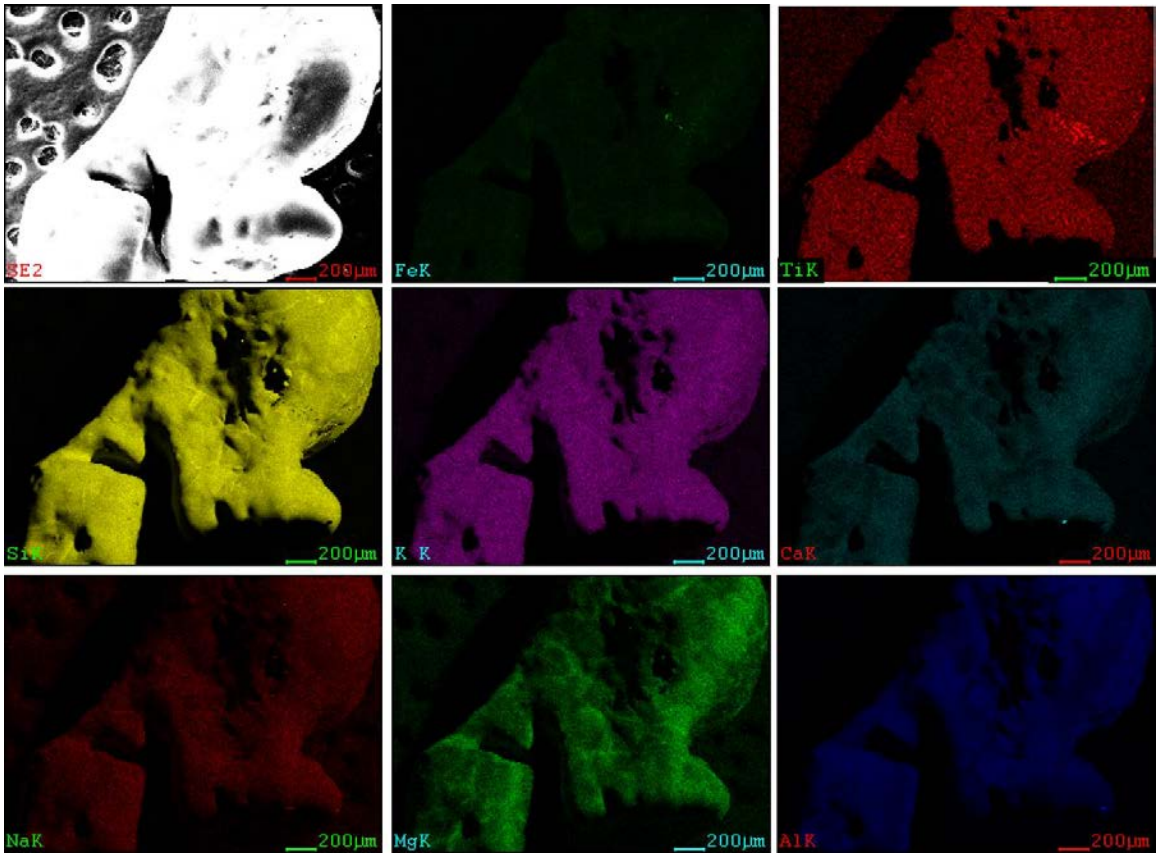

First row (left to right): Secondary electron image of sample area being mapped, map showing Fe distribution, map showing Ti distribution.

Second row (left to right): Map showing Si distribution, map showing K distribution, map showing Ca distribution.

Third row (left to right): Map showing Na distribution, map showing Mg distribution, map showing Al distribution.

Figure 53. EDS Mapping of Hotplate Acid Solution with Fe and Ti Added as Soluble Precursors, Post-thermal Analysis (DSC)

2. Acid Solution Hotplate and Thermal Bath Fabrications with Fe and Ti Added as Soluble Precursors (Precursor Fe Content Reduced by 50%)

The constituent chemicals were measured during the fabrications conducted with the precursor for Fe reduced by 50% and the standard deviation of these values was calculated to provide a qualitative estimate of ingredient measurement variation among the multiple fabrications (Figure 53).

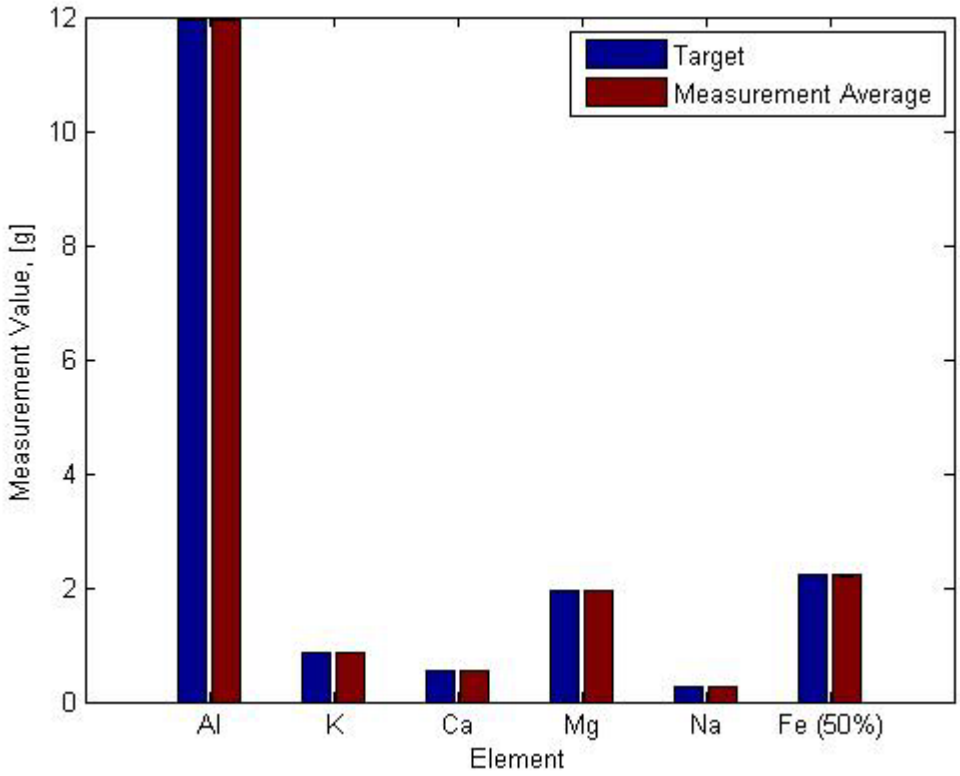

Note: The calculated standard deviation values are so small that the line markers delineating them essentially overlay on the top end of the Measurement Average columns.

Calculated standard deviations were extremely small and blend in with the tops of the Measurement Average columns.

Figure 54. Surrogate Material Precursor Measurement Variation during Production (Precursor Fe Content Reduced by 50%)

A hotplate acid solution fabrication was conducted for the production with the precursor Fe content reduced by 50% since a) reducing the precursor Fe content was a new variable in the production process and this would allow for comparison of effects of the precursor Fe content change with the initial hotplate fabrications and b) a more direct comparison could then be made for the effects of temperature control between the hotplate and thermal bath setups with the precursor Fe content reduced by 50%.

The elemental wt% of Fe compared to the target composition was improved during the hotplate acid solution fabrication with the precursor Fe content reduced by 50% (Figure 54) when compared to the initial hotplate acid solution fabrications (Figure 47). The calculated standard deviation for Fe showed very little improvement. Whereas

the elemental wt% of Al and Si maintained their respective averages and values with regard to the target composition but with marked improvement in the calculated standard deviations among the samples, indicating gains in homogeneity. The elemental wt% of K and Ca continued to be noticeably off of the target composition with calculated standard deviations showing little change. Cl continued to appear as a volatile element present that could be reduced and eliminated through adequate post-production heat treatment of the fabricated samples.

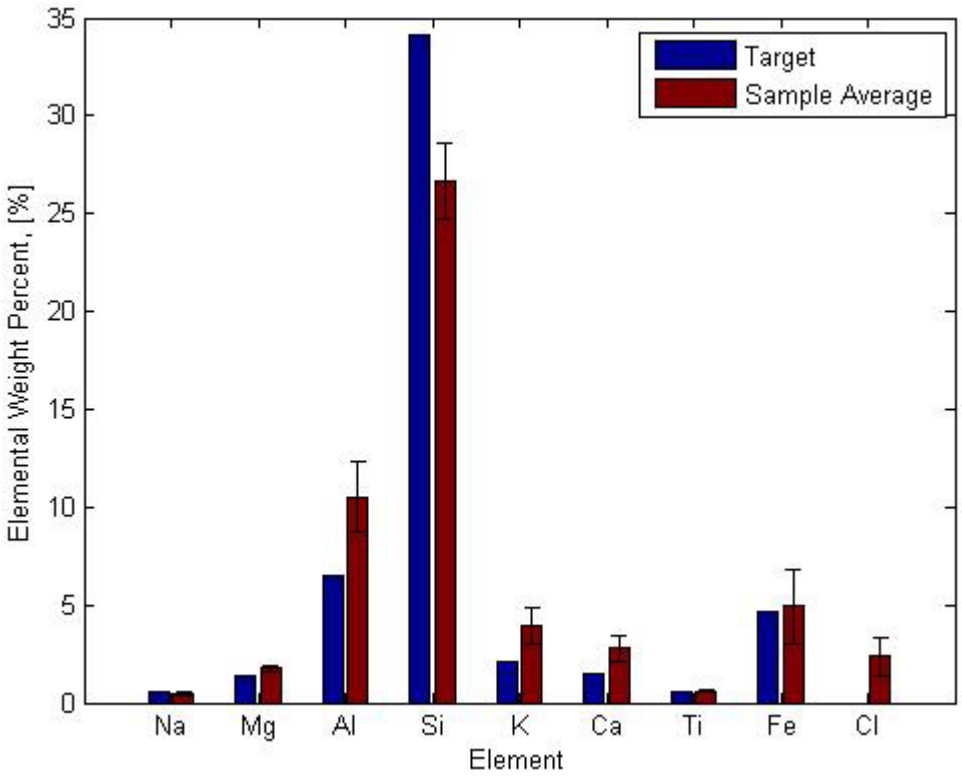

Note: The calculated standard deviation values are shown as line marker overlays on the top end of the Sample Average columns.

EDS spectra data from hotplate acid solution with Fe and Ti added as soluble precursors (Precursor Fe Content Reduced by 50%), as fabricated

Figure 55. EDS Spectra Data Comparison for Hotplate Acid Solution with Fe and Ti Added as Soluble Precursors (Precursor Fe Content Reduced by 50%), as Fabricated

The stricter thermal control introduced to the production process using the thermal bath setup of Chapter II lead to a more uniform sol, which promoted uniform nucleation during production, and the formation of the acid xerogel through homogeneous nucleation during gelation. This homogeneous nucleation effect was observed visually via rapid and uniform gelation of the sol as opposed to the slower solidifications and heterogeneous products observed in the initial fabrications. The increased rate of the reaction was measurable with gelation starting less than 13 minutes after Solutions A and B were combined and gelation occurring in much less than 1 minute, whereas initial fabrications took ~24-48 hours to solidify. This provided better probability that diffusion of heavier particles would not be significant during the drying process since the xerogel matrix had already formed from the sol in a much more rapid fashion than for the hotplate acid solution fabrications. The xerogel product from the thermal bath acid solution fabrications resembled a gel instead of the glassy form from the initial fabrications (Figure 55).

Based on experience gained during the characterization of basic pH catalyst solution fabrications and acidic pH catalyst solution fabrications, achieving product homogeneity was prioritized over maintaining the product as an intact glassy form. Achieving rapid gelation during production was a step in this direction and stirring continued until the viscosity of the gel prevented magnetic stirrer movement [34].

Thermogravimetric analysis was performed on the fabrications formed through rapid gelation to assess potential differences to the fabrications formed through slower solidification of the gel since sol-gel methods can produce wide variations in the properties of the xerogels produced [20], [22], [26].

Thermal bath acid solution fabrication xerogel product formed during last production through gelation and oven dried for 80 minutes. Gelation observed for acid solution fabrications with Fe and Ti added as soluble precursors (precursor Fe content reduced by 50%).

Glass container is 3.1 inches in diameter.

Figure 56. Thermal Bath Acid Solution Fabrication with Fe and Ti Added as Soluble Precursors (Precursor Fe Content Reduced by 50%), as Fabricated

DSC data shows that the event temperatures and types (endothermic or exothermic) are similar for the hotplate acid solution fabrications and the thermal bath acid solution fabrications (Figure 56). Due to rapid gelation, more EtOH and H_2O are trapped within the xerogel matrix for the thermal bath acid solution fabrication. Event temperatures for EtOH and H_2O are consistent among the thermogravimetric analyses for all acid fabrications (Figure 42 and Figure 56). Exothermic events of varying intensity are consistently recorded at ~800 °C and in the range of 1000 °C to 1100 °C (Figure 57). These indicate crystallization is likely to be occurring within the product. TG effects due to off-gassing have been discussed in detail earlier in this chapter.

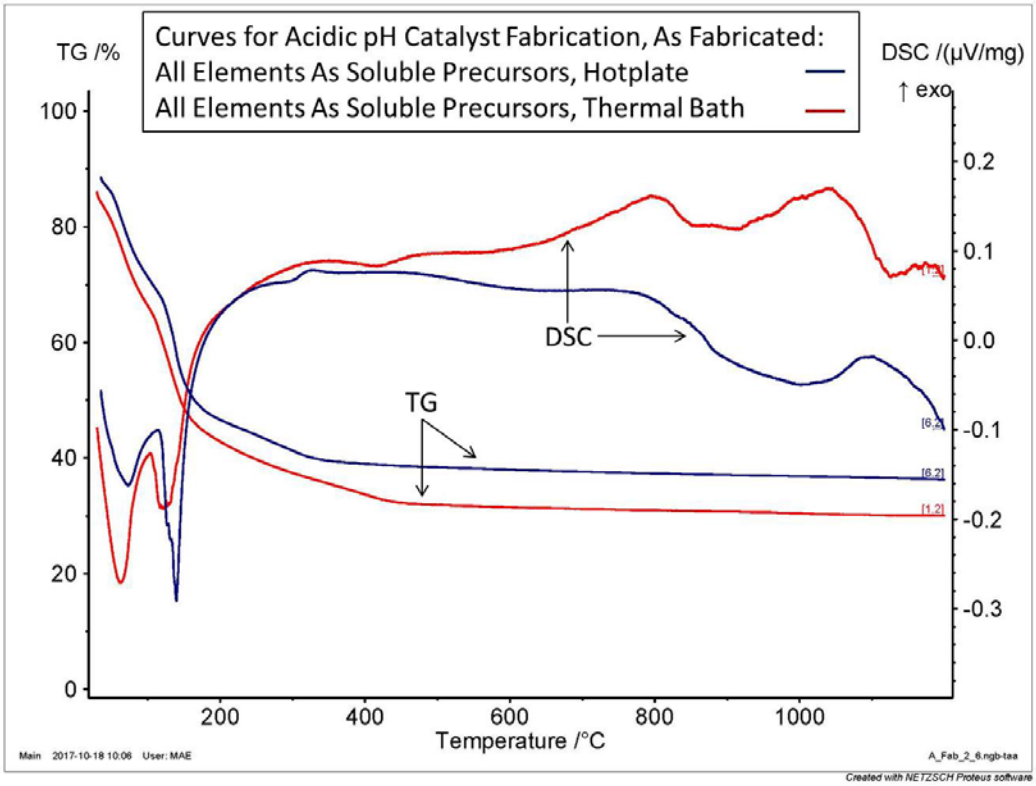

Hotplate acid solution fabrication data from production with initial precursor Fe content.

Thermal bath acid solution fabrication data from production with precursor Fe content reduced by 50%.

Figure 57. DSC-TGA Data for Acid Solution Fabrications with Fe and Ti Added as Soluble Precursors, as Fabricated, Variable Temperature Control during Production

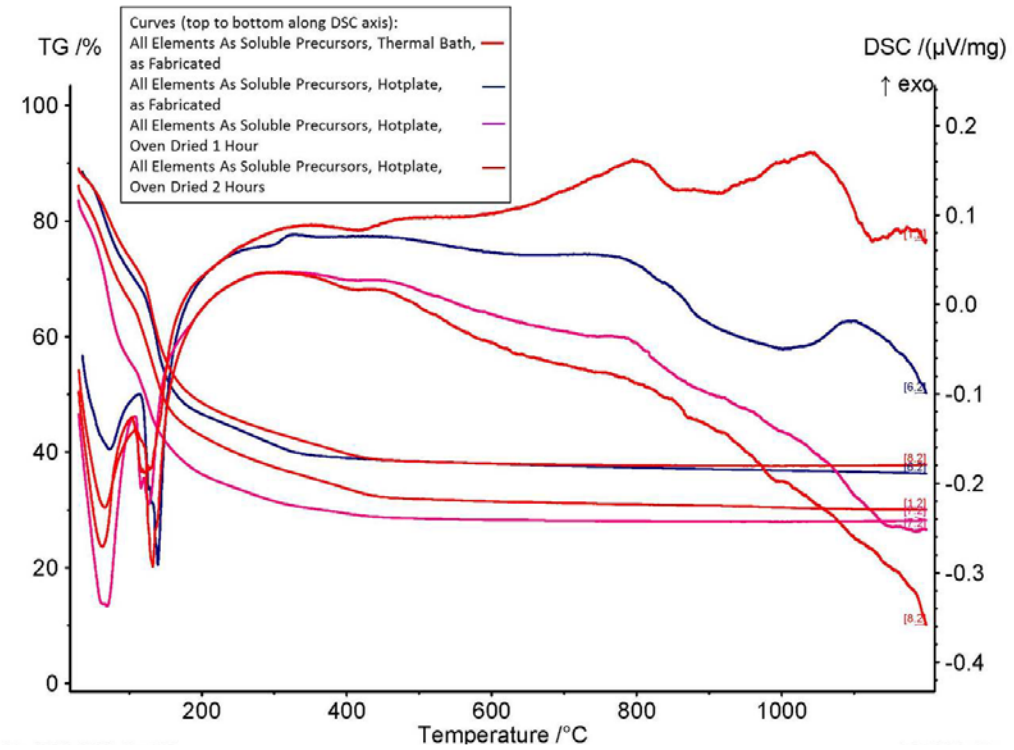

Hotplate acid solution fabrication data from production with initial precursor Fe content.

Thermal bath acid solution fabrication data from production with precursor Fe content reduced by 50%.

Oven drying time variable modified from 80 minute standard used during production protocol to evaluate thermogravimetric effect of additional off-gassing on product characteristics.

Single plot with Figure 42 and Figure 56 data overlaid for qualitative comparison.

Figure 58. DSC-TGA Data for Acid Solution Fabrications with Fe and Ti Added as Soluble Precursors, Comparison of Effects from Variable Drying Method and Temperature Control during Production, Overlaid on Single Plot

Based on DSC data the thermal bath acid fabrications were heat treated to just above the first exothermic peak at ~800 °C (Figure 56) using heat treatment to 825 °C (HT #7 from Table 5) (Figure 58). Mechanical breakup of the sample was observed as expected. SEM-EDS analysis and XRD analysis were used to assess homogeneity and crystallization respectively for comparison to the as fabricated thermal bath acid fabrication xerogel product and fabrication xerogel products heat-treated to 350 °C (HT #6 from Table 5).

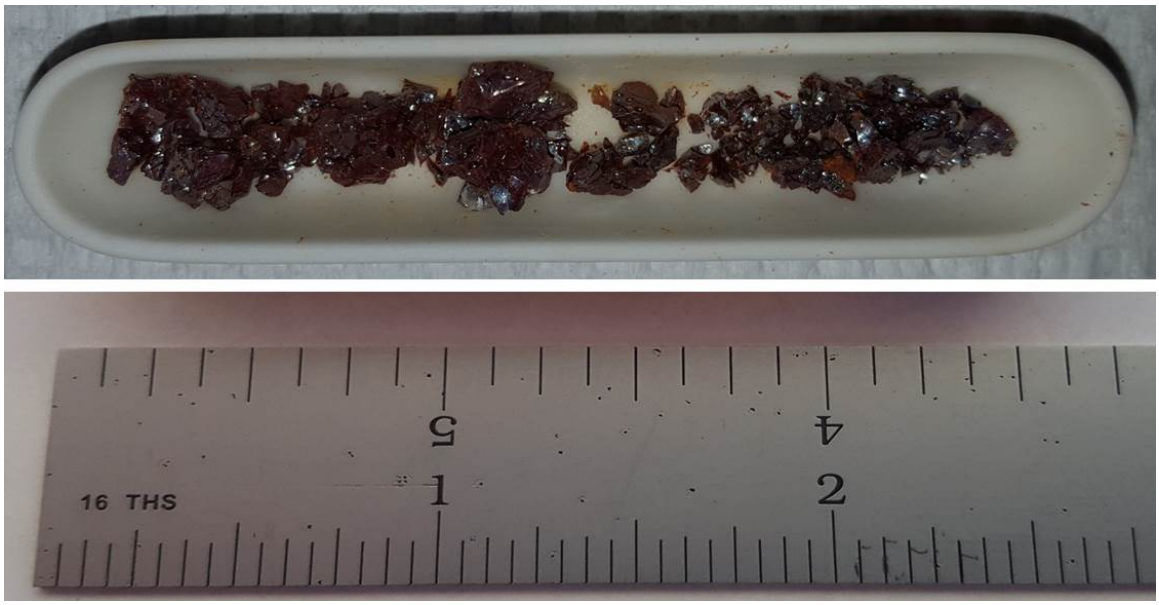

Ruler for scale.

Figure 59. Thermal Bath Acid Solution with Fe and Ti Added as Soluble Precursors (Precursor Fe Content Reduced by 50%), Post-heat Treatment to 825 °C (HT #7 from Table 5)

SEM imagery shows thermal bath acid fabrication xerogel product formed through gelation as fabricated and post-heat treatment to either 350 °C (HT #6 from Table 5) or 825 °C (HT #7 from Table 5) (Figure 59). More porous surface morphology can be observed for the as fabricated sample while smoother surface morphology can be observed for the post-heat treatment samples. HT #7 was performed to a temperature higher than the first crystallization temperatures observed in the DSC data (Figure 42 and Figure 56) and there is a change in the surface morphology following this heat treatment when compared to the sample heat-treated using HT #6.

As expected thermal parameters and temperature play a critical role when using the sol-gel method and can lead to many results from productions using the same reactants as shown by [20]–[23], [26].

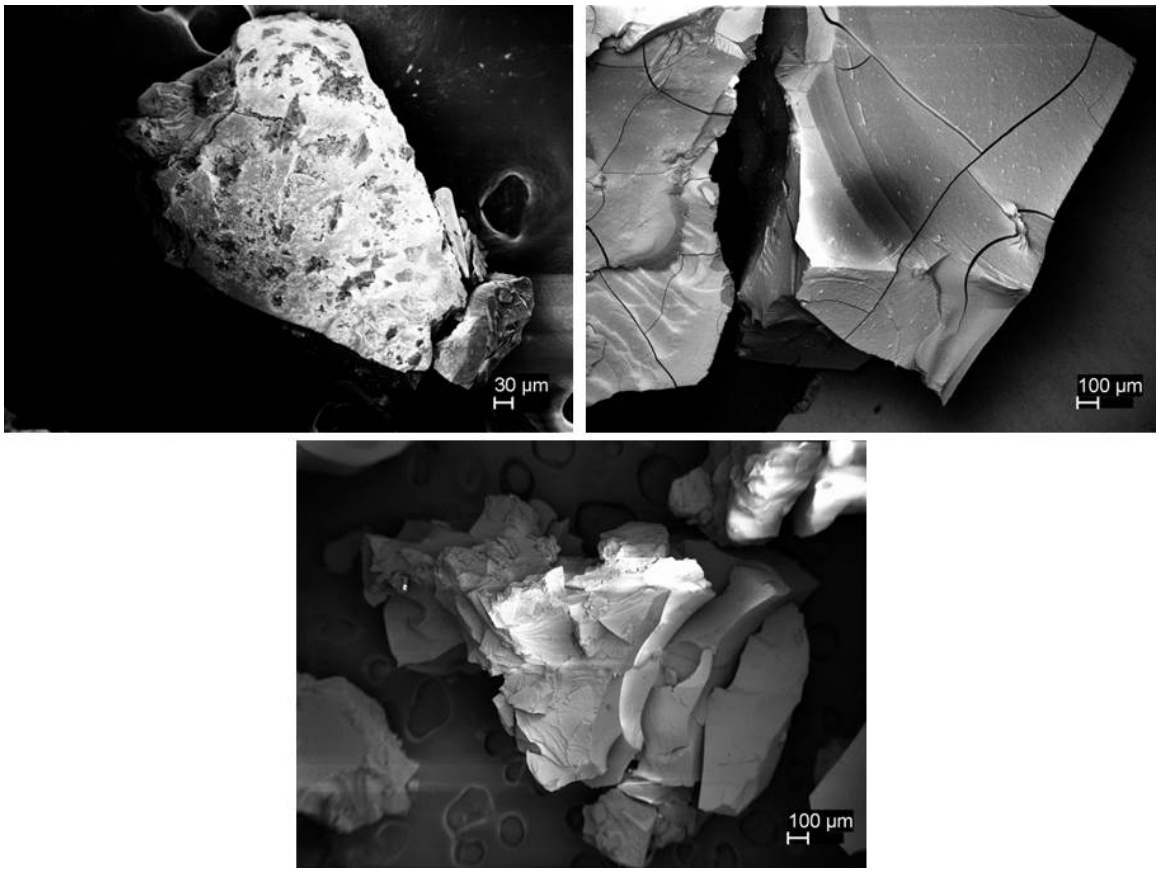

Top left: Thermal bath acid solution fabrication with Fe and Ti added as soluble precursors (precursor Fe content reduced by 50%), as fabricated.

Top right: Thermal bath acid solution fabrication with Fe and Ti added as soluble precursors (precursor Fe content reduced by 50%), post-heat treatment to 350 °C (HT #6 from Table 5).

Bottom: Thermal bath acid solution fabrication with Fe and Ti added as soluble precursors (precursor Fe content reduced by 50%), post-heat treatment to 825 °C (HT #7 from Table 5).

Figure 60. SEM Image: Thermal Bath Acid Solution Fabrication with Fe and Ti Added as Soluble Precursors (Precursor Fe Content Reduced by 50%), as Fabricated, Post-heat Treatment to 350 °C (HT #6 from Table 5), Post-heat Treatment to 825 °C (HT #7 from Table 5)

For the thermal bath acid fabrication, which produced the xerogel through rapid gelation, the standard deviations calculated for the elements of Al, Si and Fe showed great improvement compared to initial hotplate acid fabrications formed through slower solidification (Figure 60). The other recorded elements also demonstrated a more even dispersion of the reactants as all calculated standard deviations were reduced (Table 7).

Table 7. EDS Spectra Standard Deviation (σ) Comparison of Acid Solution Fabrication Xerogel Products Formed through Slow Solidification and Rapid Gelation, as Fabricated

EDS Spectra Standard Deviation (σ) Comparison of Acid Solution Fabrication Xerogel Products Formed Through Slow Solidification and Rapid Gelation, as Fabricated			
	Percent Change for formation through rapid gelation vice slow solidification	Acid Synthesis, Fe and Ti added as soluble precursors, σ	
	Thermal Bath Fabrication	Thermal Bath Fabrication	Initial Hotplate Fabrication
Na	-49.3	0.0524	0.1033
Mg	-63.8	0.0847	0.2337
Al	-87.6	0.9201	7.4195
Si	-76.0	1.0506	4.3760
K	-42.1	0.3398	0.5868
Ca	-50.2	0.1528	0.3071
Ti	-17.0	0.1243	0.1498
Fe	-66.9	0.6904	2.0876
Cl	-73.7	0.1607	0.6115

Al and Si sample averages continued to be the farthest off of the target compositions with Al being closer to its target composition than in initial acid fabrications (Figure 60). Considerable improvement in the dispersion of the reactants improved homogeneity of the product.

While Al and Si sample averages were off from the target compositions, the sample average for the element of interest Fe was improved to be very close to the target composition and with a greatly reduced standard deviation (Figure 60). This is important when the proposed mechanism of LDHP is applied and the elements of interest are preferentially separated. Precise sample composition of these elements would be more critical than for the Si that forms the matrix since the Si would be separated out. Also, if the sample averages are consistently deviated from target composition this could be corrected for over the course of future fabrications. The reduction in variation represented

by the calculated standard deviations in Table 7 is indication that greater homogeneity of the xerogel products was successfully achieved.

Apart from the Al and Si and a slightly higher difference between the sample average and target composition for K the remaining recorded reactants all showed improvements for sample average wt% in comparison to the target composition (Figure 60).

Cl, though evenly dispersed, continued to appear as a volatile element present that could be reduced and eliminated through adequate post-production heat treatment of the fabricated sample.

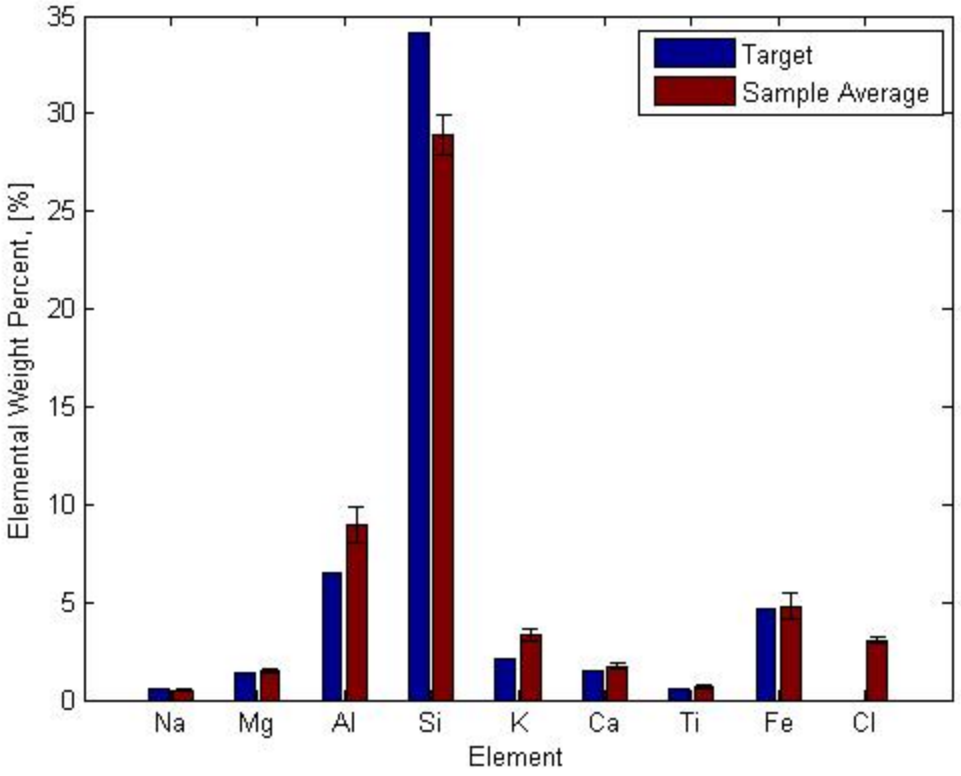

Note: The calculated standard deviation values are shown as line marker overlays on the top end of the Sample Average columns.

EDS spectra data from thermal bath acid solution fabrication with Fe and Ti added as soluble precursors (Precursor Fe Content Reduced by 50%), as fabricated.

Figure 61. EDS Spectra Data Comparison for Thermal Bath Acid Solution with Fe and Ti Added as Soluble Precursors (Precursor Fe Content Reduced by 50%), as Fabricated

EDS mapping was performed to allow for visual representations of the dispersion of the reactants to be observed. Imagery for the thermal bath acid solution fabrication, which produced the xerogel through rapid gelation showed less gradients of colors for each of the elements and a lack of oxide concentrations for the as fabricated samples (Figure 61). This was consistent with the EDS spectra analysis and calculated standard deviations for the as fabricated samples.

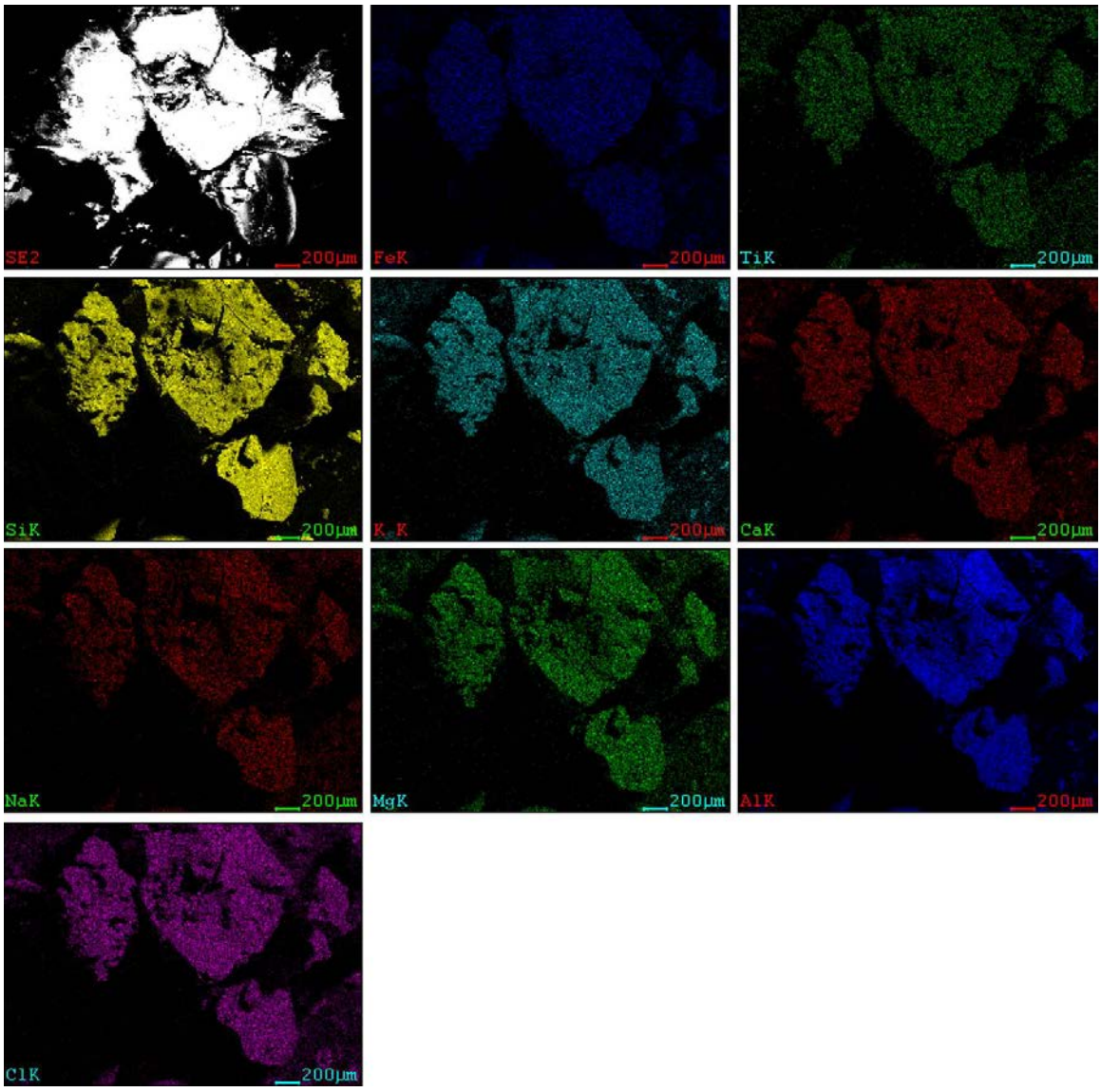

First row (left to right): Secondary electron image of sample area being mapped, map showing Fe distribution, map showing Ti distribution.

Second row (left to right): Map showing Si distribution, map showing K distribution, map showing Ca distribution.

Third row (left to right): Map showing Na distribution, map showing Mg distribution, map showing Al distribution.

Fourth row: Map showing Cl distribution.

Figure 62. EDS Mapping of Thermal Bath Acid Solution Fabrication with Fe and Ti Added as Soluble Precursors (Precursor Fe Content Reduced by 50%), as Fabricated

EDS spectra analysis of post-heat treatment samples showed that measured homogeneity was being adversely affected during the heat treatments (Figure 62). Full quantification of the effects would require more precise determination of the complete xerogel product as discussed previously since the sample is being reduced and reactant wt% will be expected to change a certain amount since, for example, Fe would now be a greater wt% of the heat treated sample even without Fe being added or lost. Volatiles removal and off-gassing during heat treatment to above crystallization temperatures will play a critical role in maintaining the level of homogeneity achieved during production.

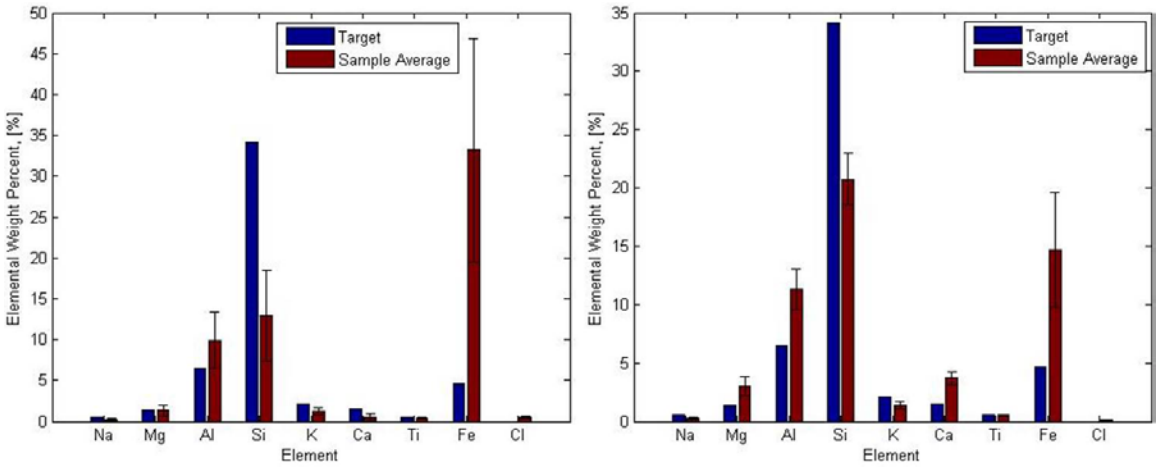

Note: The calculated standard deviation values are shown as line marker overlays on the top end of the Sample Average columns.

Left: Thermal bath acid fabrication, post-heat treatment to 350 °C (HT #6 from Table 5).

Right: Thermal bath acid fabrication, post-heat treatment to 825 °C (HT #7 from Table 5).

Figure 63. EDS Spectra Data Comparison for Thermal Bath Acid Solution Fabrication with Fe and Ti Added as Soluble Precursors (Precursor Fe Content Reduced by 50%), Post-heat Treatment

EDS mapping of the heat treated thermal bath acid fabrication xerogel products is consistent with the EDS spectra analysis and calculated standard deviations of Figure 62. Color gradient in the images is more evident implying greater variations in dispersion of the reactants (Figure 63). As temperature of the heat treatment was increased, the presence of oxide concentrations became observable (Figure 64).

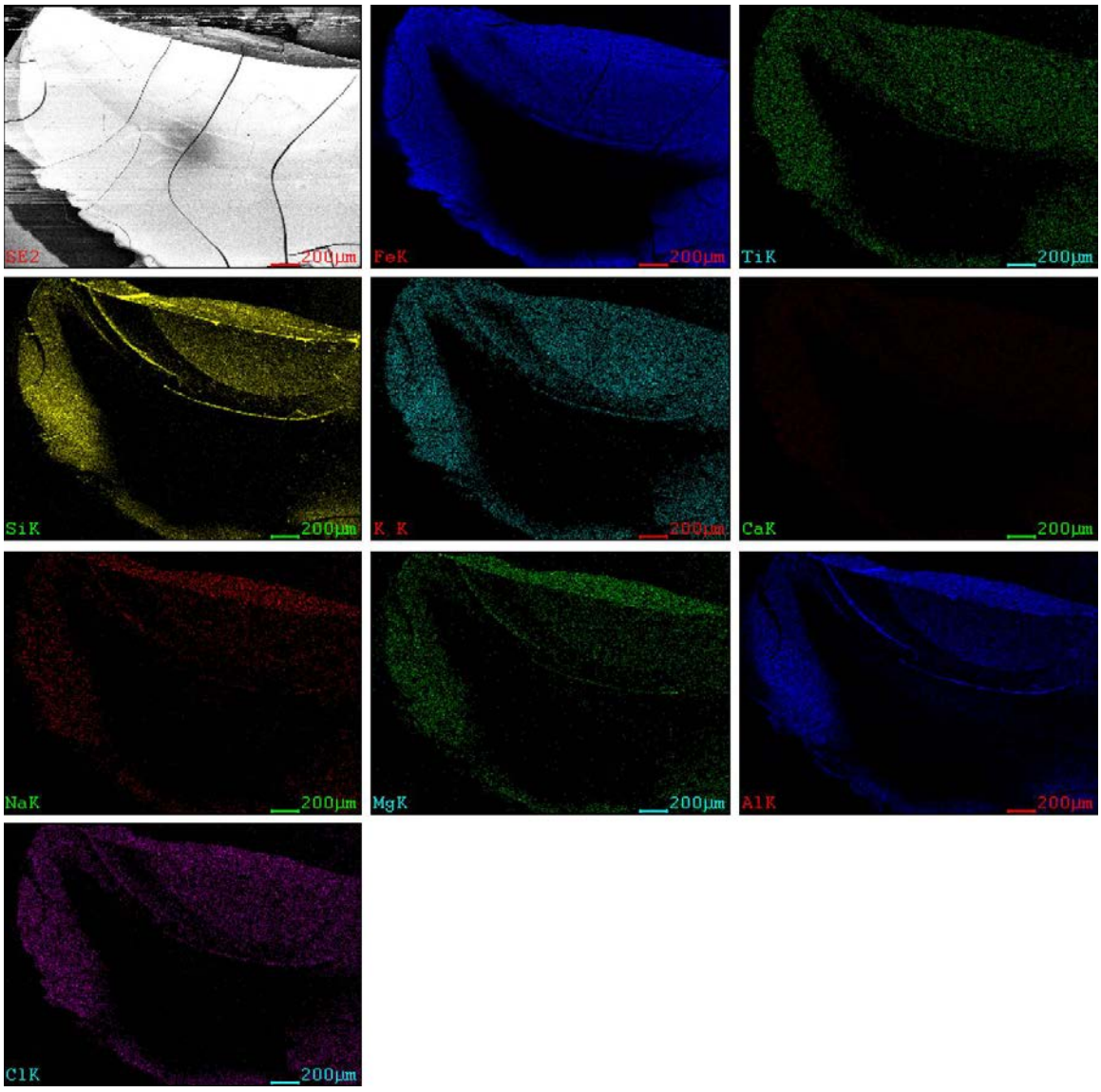

First row (left to right): Secondary electron image of sample area being mapped, map showing Fe distribution, map showing Ti distribution.

Second row (left to right): Map showing Si distribution, map showing K distribution, map showing Ca distribution.

Third row (left to right): Map showing Na distribution, map showing Mg distribution, map showing Al distribution.

Fourth row: Map showing Cl distribution.

Figure 64. EDS Mapping of Thermal Bath Acid Solution Fabrication with Fe and Ti Added as Soluble Precursors (Precursor Fe Content Reduced by 50%), Post-heat Treatment to 350 °C (HT #6 from Table 5)

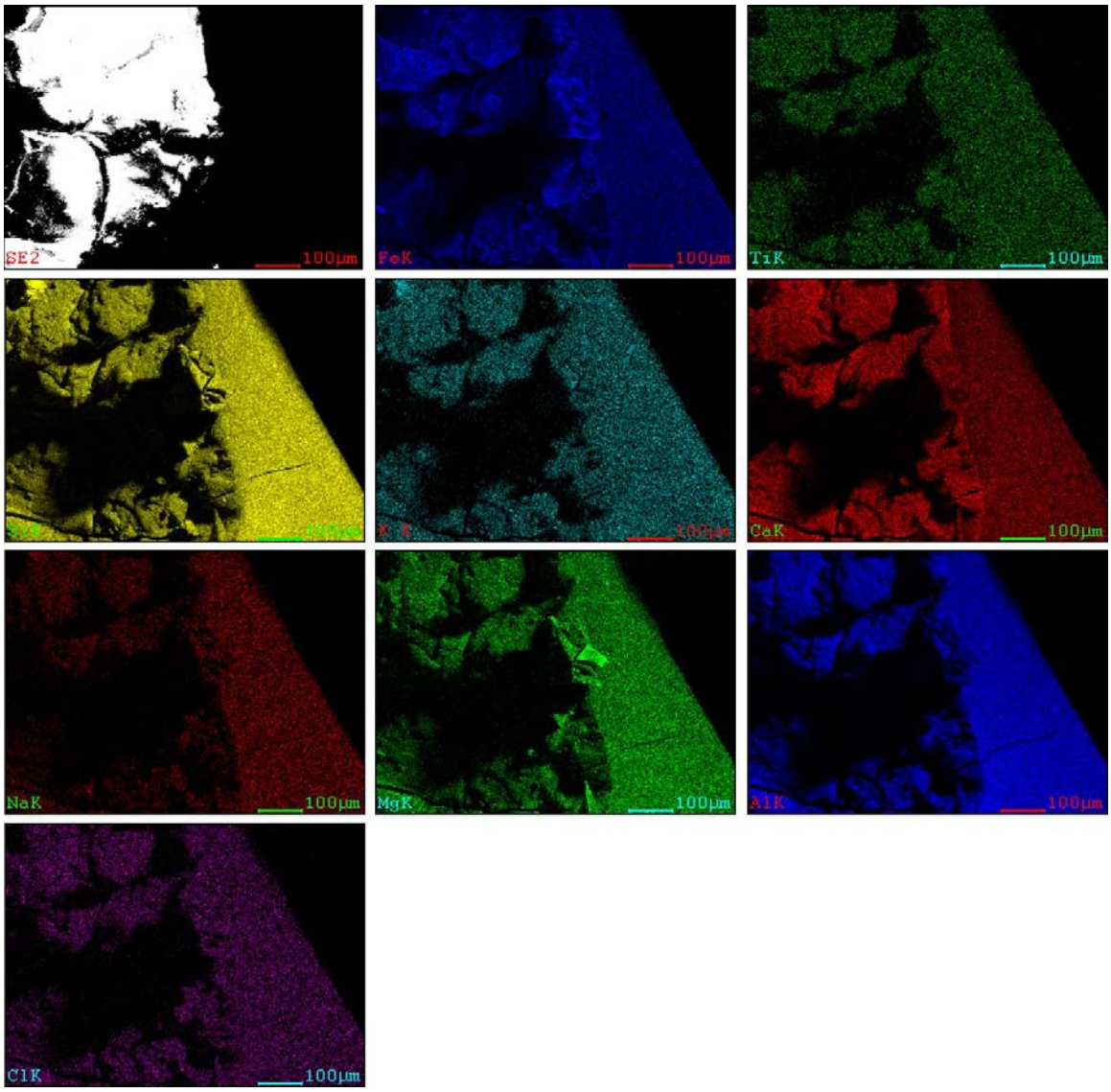

First row (left to right): Secondary electron image of sample area being mapped, map showing Fe distribution, map showing Ti distribution.

Second row (left to right): Map showing Si distribution, map showing K distribution, map showing Ca distribution.

Third row (left to right): Map showing Na distribution, map showing Mg distribution, map showing Al distribution.

Fourth row: Map showing Cl distribution.

Figure 65. EDS Mapping of Thermal Bath Acid Solution Fabrication with Fe and Ti Added as Soluble Precursors (Precursor Fe Content Reduced by 50%), Post-heat Treatment to 825 °C (HT #7 from Table 5)

XRD analysis of both hotplate and thermal bath acid fabrication products in the as fabricated condition showed the expected amorphous characteristics of a silicate matrix (Figure 65). This showed that the xerogels were produced with an amorphous matrix when formed through slower solidification or rapid gelation.

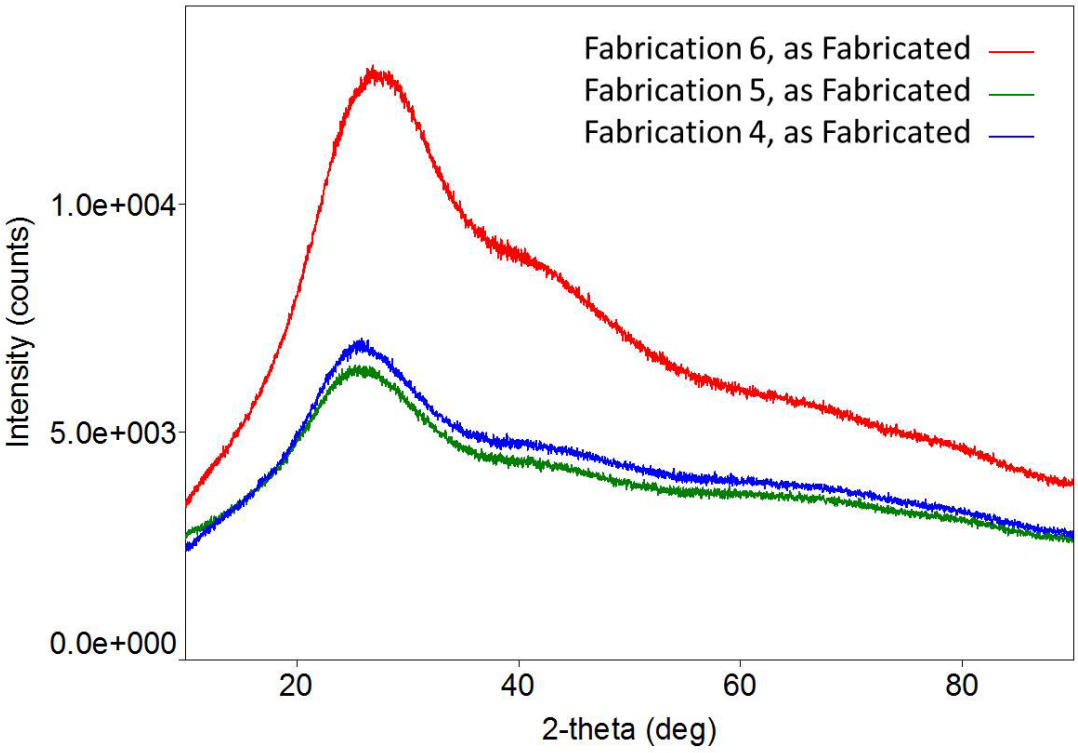

Acid solution fabrication 4 was a hotplate acid solution fabrication with precursor Fe content reduced by 50%.

Acid solution fabrications 5 and 6 were thermal bath acid solution fabrications with precursor Fe content reduced by 50%.

Figure 66. XRD Analysis for Acid Solution Fabrications (from Multiple Fabrications) with Fe and Ti Added as Soluble Precursors (Precursor Fe Content Reduced by 50%), as Fabricated

XRD analyses of the thermal bath acid fabrications were performed. Post-heat treatment structures were noted including iron titanium oxide, calcium aluminum iron oxide and hematite (Figure 66) [36]. As expected the level of crystallization appeared to be greater for the heat treatment to 825 °C (HT #7 from Table 5) which was performed at

a higher temperature as seen by the relative peak sizes for the post-heat treatment to 350 °C (HT #6 from Table 5) and post-heat treatment to 825 °C (HT #7 from Table 5) samples (Figure 66). Similar to the thermal bath basic fabrication the background shape supporting the existence of an amorphous matrix is still visible even after the post-production heat treatment.

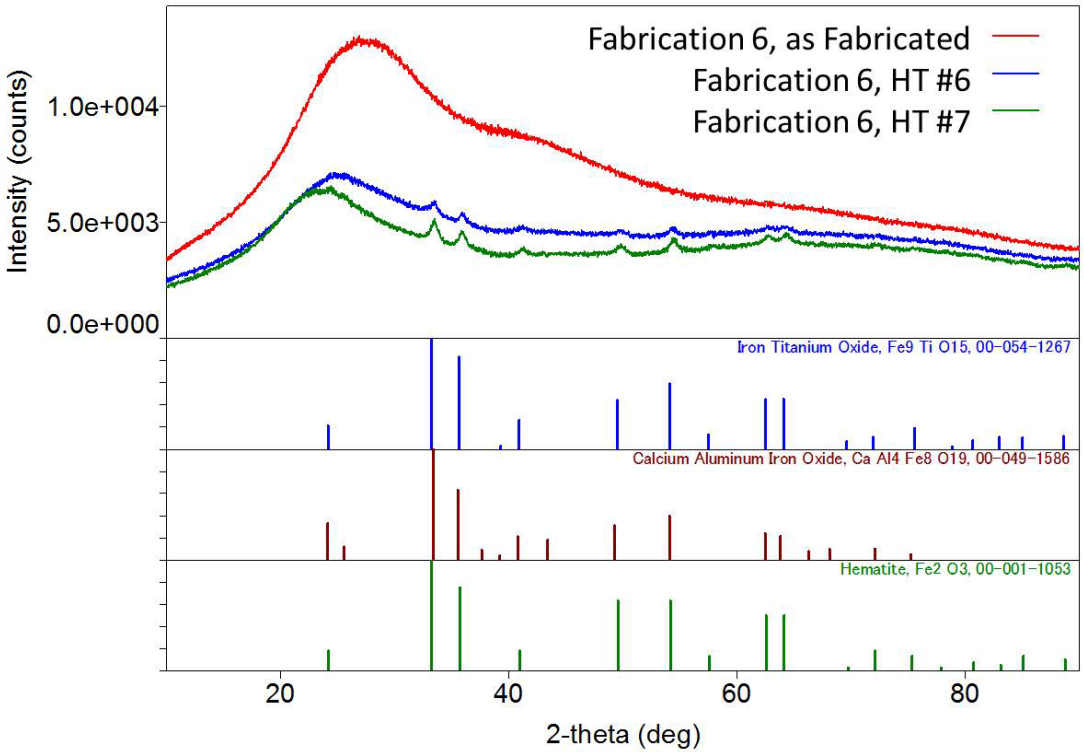

Acid solution fabrication 6 was a thermal bath acid solution fabrication with precursor Fe content reduced by 50%.

Figure 67. XRD Analysis for Thermal Bath Acid Solution Fabrication (from Same Fabrication) with Fe and Ti Added as Soluble Precursors (Precursor Fe Content Reduced by 50%), as Fabricated, Post-heat Treatment to 350 °C (HT #6 from Table 5), Post-heat Treatment to 825 °C (HT #7 from Table 5)

Consistency was noted between the thermal bath acid fabrication xerogel products from separate fabrication runs that had undergone heat treatment to 825 °C (HT #7 from Table 5) with respect to both peak locations and relative intensities (Figure 67).

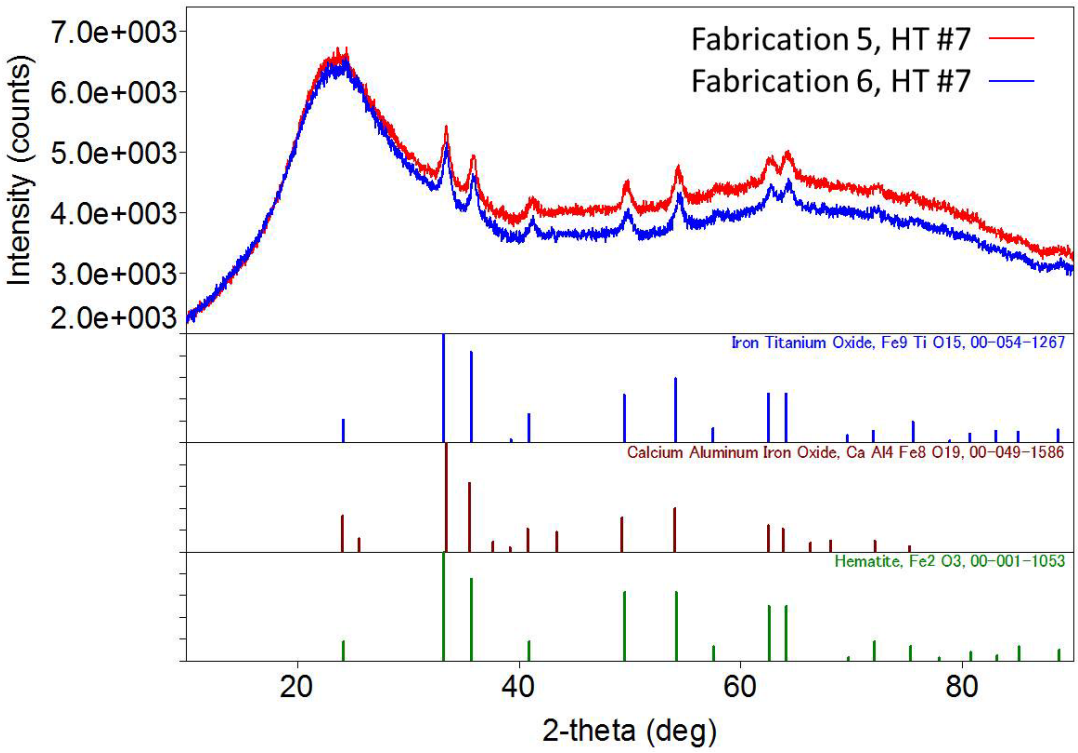

Acid solution fabrications 5 and 6 were thermal bath acid solution fabrications with precursor Fe content reduced by 50%.

Figure 68. XRD Analysis for Thermal Bath Acid Solution Fabrications (from Multiple Fabrications) with Fe and Ti Added as Soluble Precursors (Precursor Fe Content Reduced by 50%), Post-heat Treatment to 825 °C (HT #7 from Table 5)

C. SUMMARY

Adding the elements of interest, Fe and Ti, as a salt and an alkoxide respectively allowed dissolution into the solutions A and B prior to their combination and subsequent experiencing of hydrolysis and polymerization while being heated and mixed during production.

The thermal bath setup provided a heat source that allowed a thermal energy reservoir to be available when endothermic reactions occurred during fabrication, which sustained the rate of reactions by minimizing temperature fluctuations. This thermal control is a critical process during the production of sol-gel materials as the drying, dehydration and densification directly affect the formation of the specimen through

slower solidification or rapid gelation [20]–[23], [26]. The dehydration step was affected using the drying methods listed in Chapter II and the densification step was affected using the heat treatments listed in Table 5.

Improvements in homogeneity and composition were observable for the acid solution fabrications with the most consistent improvement being for the fabrications that produced a xerogel through rapid gelation. Calculated standard deviations for multiple acid solution fabrications (hotplate fabrication with initial precursor Fe content, hotplate fabrication with precursor Fe content reduced by 50% and thermal bath fabrications with precursor Fe content reduced by 50%) were compared to the standard deviations calculated for the most homogeneous basic solution fabrication (thermal bath basic fabrication) (Table 8). The elements of interest Fe and Ti showed increased standard deviations when compared to the thermal bath basic solution fabrication but notably the dispersion of Fe steadily improved, as seen by the calculated percent change reduction from 228.4% for hotplate acid fabrication with initial precursor Fe content xerogel samples to 8.6% for thermal bath acid solution fabrication with precursor Fe content reduced by 50% xerogel samples (Table 8). The calculated percent change related to the Ti dispersion was more prone to variation due to the quantity of the reactant present but did show a very general, if not consistent, improvement. For all other recorded reactants there was considerable improvement in dispersion as seen by the calculated percent changes with these changes being consistently improved for the xerogel products formed through rapid gelation, thermal bath acid solution fabrications.

While other drying protocols were investigated, the 80 minute drying protocol was selected and maintained as the standard for drying. Heat treatment protocols were established for sample dehydration. Post-production heat treated sample averages were not consistent when compared with each other. The calculated standard deviations for critical precursors, specifically Fe, Al and Si was high and the corresponding sample composition averages were significantly deviated from the target composition. The action of volatiles, off-gassing and crystallization during heat treatment was being observed to skew the homogeneity achieved when the xerogel samples were formed.

This homogeneity of the resultant xerogel through manipulation of fabrication parameters and post-production processing indicates that further refinement is possible to continue improving both homogeneity among the xerogel products and the sample wt% deviations from the target composition.

Of the solution fabrications utilizing an acid as the catalyst the most homogeneous and consistent products were produced using the thermal bath acid fabrication method adding Fe as a salt and Ti as an alkoxide which resulted in xerogel formation through rapid gelation.

Table 8. Comparison of EDS Spectra Analysis Calculated Standard Deviation (σ) for Acid Solution Fabrications versus Thermal Bath Basic Solution Fabrication, with Fe and Ti Added as Soluble Precursors

EDS Analysis Standard Deviation (σ) Comparison, as Fabricated									
Thermal Bath Basic Synthesis, Fe and Ti Added as Soluble Precursors, σ		Percent Change from Thermal Bath Basic Synthesis to Acid Syntheses				Acid Syntheses, Fe and Ti Added as Soluble Precursors, σ			
		Thermal bath		Hotplate		Thermal bath		Hotplate	
		Fe Content Reduced by 50%			Initial Fe	Fe Content Reduced by 50%			Initial Fe
Na	0.083	-37.1	-26.5	18.3	23.9	0.052	0.061	0.099	0.103
Mg	0.296	-71.4	-60.2	-39.9	-21.0	0.085	0.118	0.178	0.234
Al	2.840	-67.6	-71.5	-37.4	161.3	0.920	0.809	1.778	7.420
Si	2.675	-60.7	-38.5	-28.5	63.6	1.051	1.645	1.913	4.376
K	0.914	-62.8	-68.5	2.3	-35.8	0.340	0.288	0.935	0.587
Ca	0.282	-45.7	-11.2	146.8	9.1	0.153	0.250	0.695	0.307
Ti	0.079	57.9	-20.9	-60.2	90.2	0.124	0.062	0.031	0.150
Fe	0.636	8.6	20.1	192.3	228.4	0.690	0.763	1.858	2.088
Cl	0.296	-45.7	-25.8	237.9	106.6	0.161	0.220	1.000	0.611

V. CONCLUSION

The objective of this study, to create a surrogate material that elementally resembled the average composition of tektite but that presented a homogeneous distribution of phases, was achieved successfully through the application and adaptation of the principles of sol-gel processing.

Hypotheses guiding this research have been supportive and correlative of the results. The hypothesis that a process such as the sol-gel method, combined with the right drying techniques and the correct combination of reactants, could create a homogeneous xerogel that, once annealed, will result in a homogeneous body with the appropriate chemical composition has proved true through fabrication and shows great potential for being successfully implemented through post-production processing, such as heat-treatments. Soluble precursor chemicals, which resulted in ionized species during production, distributed more uniformly within the amorphous silicate matrix of the fabricated product. The execution of drying, dehydration and densification steps does affect the product homogeneity with thermal parameter control during production having the greatest impact.

During this study, new materials were developed. Sol-gel formulations are being widely used in various industries, however, to the best of our knowledge, the formulations for which it is used are simpler, containing only 3-4 cations as a maximum and do not achieve the level of complexity applied here. The tektite surrogates fabricated in the frame of this thesis contained Na, Mg, Al, Si, K, Ca, Ti and Fe in proportions very close to those found in the natural occurrences of the mineral. Thus, we achieved not only the goal of generation a homogeneous distribution of the elements, we also proved that the protocols used are an appropriate route to generate them. This resulted in the creation, during this study, of optimized protocols to form the sol, gel and eliminate volatiles during the drying and densifying steps while being annealed for the particular precursors and stoichiometric proportions of interest.

Of all the solution fabrications (acidic pH catalyst and basic pH catalyst) the most homogeneous and consistent products were produced using the thermal bath acidic pH catalyst fabrication method adding Fe as a salt and Ti as an alkoxide which resulted in xerogel formation through rapid gelation. Maintain vigorous stirring and thermal input during production from mixture of the solvents, precursors, catalyst and medium through gel formation to ensure the most effective dispersion of elements. The thermal bath basic pH catalyst formulation exhibited potential for continued refinement and would introduce less Cl as a volatile during fabrication. The use of soluble precursors for Fe and Ti provided more uniform dispersion and with advanced thermal regulation during production rapid gelation was induced which creates the potential for including Fe, Ti or other elements as oxides in future fabrications. These oxides would not be homogenous within the gel network but could serve to represent uniformly distributed inclusions.

Gel formation during the thermal bath fabrications represented wide spread homogeneous nucleation during production vice slower solidification during production. This difference was directly affected by the thermal parameters during production. The energy reservoir provided by the sand of the thermal bath and resulting temperature profile through the gel enhanced the reaction rates leading to gelation.

Xerogel formation through drying and dehydration produced a homogeneous phase distribution. Mechanical robustness and maintenance of the homogeneous phase distribution through densification and the annealing process requires further refinement. Volatiles removal and off-gassing during heat treatment to above crystallization temperatures will play a critical role in post-production processing.

Xerogel product composition can be adjusted to more closely match target composition through calculated experimentation as shown when the Fe reactant content of the last three acid solution fabrications was reduced by 50%, which produced a xerogel through rapid gelation with close to the target composition wt% in its fabricated state. Of note the acid solution fabrication with the Fe reactant content that was reduced by 50% but formed through slower solidification did not experience this improvement in composition wt%s.

Fabrication of surrogate materials aimed to support validation of nuclear forensic techniques, such as LDHP, through sol-gel methods is a viable avenue with potential for achieving the desired objectives of homogeneity and control of product composition.

Applying the sol-gel synthesis method to support the field of nuclear forensics is also in keeping with the spirit of exploration into the uses and benefits of the sol-gel methodology as shown by [22], [24], [25], [40].

THIS PAGE INTENTIONALLY LEFT BLANK

VI. FUTURE WORK

The results of this study support production of surrogate materials using sol-gel methods as a viable means to fabricate homogeneous surrogate materials to aid in the validation of the LDHP technique.

SEM EDS analysis was perfectly suited for this study to assess product homogeneity, dispersion of constituent elements since different sections of a given specimen could be evaluated, and EDS mapping could be performed. While a more accurate accounting of volatiles may prove useful due to their observed effects on post-production characteristics of the xerogel products, the mass spectrometry techniques required would result in both consuming of the specimen tested through sample dissolution and a mere composition of the sample as a whole, not the dispersion of elements present. Due to these considerations regarding mass spectrometry and the nature of this study, the SEM EDS analysis was the perfect choice for this endeavor.

Due to volatile burn off of Cl and other reactants not fully quantified during analyses it would be beneficial that corrections to heat treated samples be performed to account for volatiles trapped within the porous networks of the xerogel products. This could be accomplished by utilizing characterization techniques that would more precisely measure the composition of all elements present in the xerogel products. Atomic absorption spectrometry and inductively coupled plasma atomic emission spectrometry are examples of such techniques.

Post-production processing to form a homogeneous xerogel into a form that can be more effectively used to validate the LDHP technique could be accomplished in a variety of ways. One method to investigate is sintering a crushed version of the xerogel product that has been compacted into pellets, or another shape, to provide a suitable sample form for LDHP as mentioned earlier [37]. Another method could be melting of the xerogel into a glass using the ceramic method [41]. Further characterization would then be needed to verify the composition of the sintered or melted xerogels was not significantly altered using methods as mentioned earlier [42].

Different elements of interest can be added to the list of reactants to allow for validation of the LDHP technique using various input samples and not just the surrogate based on tektite. No radioactive elements or isotopes would be recommended at this time but could be investigated at a later time at a facility other than Naval Postgraduate School.

Xerogel matrices have been shown to have biocompatibility and can be functionalized with organic and inorganic groups [25]. Some future studies could possibly be directed towards the investigation of stochastic effects [1], [4]. This would be applicable to nuclear related activities on Earth as well as prolonged exposure from the space environment during manned missions.

APPENDIX A. BASIC SOLUTION SYNTHESIS MATLAB CODE

```
%%Elemental Composition calculations for Tektite fabrication using
surrogate materials
%LCDR Ken Foos
%In support of surrogate material fabrication for LDHP Thesis Work
%%
%%Elements and corresponding Molecular Weights (MW's)
Si = 28.0855; %[g/mol]
Al = 26.981536; %[g/mol]
K = 39.0983; %[g/mol]
Ca = 40.078; %[g/mol]
Mg = 24.3050; %[g/mol]
Na = 22.989770; %[g/mol]
Fe = 55.845; %[g/mol]
Ti = 47.867; %[g/mol]
O = 15.9994; %[g/mol]
C = 12.0107; %[g/mol]
H = 1.00794; %[g/mol]
Cl = 35.453; %[g/mol]
Br = 79.904; %[g/mol]
N = 14.0067; %[g/mol]
%Values taken from the Sargent-Welch Periodic Table,
%Copyright 2004 VWR International
%%
%Elemental Calculations for the grams needed of each element to achieve
%desired output quantity of Tektite based on Weight Percent data
determined
%through material characterization
product = 18.558; %Desired output quantity of Tektite [g]
fprintf('\nTarget quantity of Tektite is %2.4f [g]\n', product)
%Input Weight Percents (Wt%'s)
%From Table 4 of Reference:
%A. Camargo, “Characterization of Particles Created by Laser-Driven
%Hydrothermal Processing,” M.S. Thesis, Dept. of Mechanical and
Aerospace
%Engineering, NPS, Monterey, CA, USA, 2016.
WtPct_SiO2 = 0.7304;
WtPct_Al2O3 = 0.1234;
WtPct_K2O = 0.0254;
WtPct_CaO = 0.0205;
WtPct_MgO = 0.0234;
WtPct_Na2O = 0.0076;
WtPct_FeO = 0.0598;
WtPct_TiO2 = 0.0090;

%Silicon (Si)
Si_Desired = WtPct_SiO2*product; %[g]
SiO2_MW = Si+(2*O); %[g/mol]
Pct_Si_SiO2 = Si/SiO2_MW; %[percent of SiO2 weight from Si in decimal
form]
Si_needed = Pct_Si_SiO2*Si_Desired; %amount of Si needed for the
desired product size [g]
```

```
fprintf('\nAmount of SiO2 desired is %2.4f [g]', Si_Desired)
fprintf('\nSiO2 Molecular Weight is %3.4f [g/mol]', SiO2_MW)
fprintf('\nPercent of SiO2 weight from Si in decimal form is %1.4f',
Pct_Si_SiO2)
fprintf('\nAmount of Si needed for the desired product size is %1.4f
[g]\n', Si_needed)

%Aluminum (Al)
Al_Desired = WtPct_Al2O3*product; %[g/mol]
Al2O3_MW = (2*Al)+(3*O); %[g/mol]
Pct_Al_Al2O3 = (2*Al)/Al2O3_MW; %[percent of Al2O3 weight from Al in
decimal form]
Al_needed = Pct_Al_Al2O3*Al_Desired; %amount of Al needed for the
desired product size [g]
fprintf('\nAmount of Al2O3 desired is %2.4f [g]', Al_Desired)
fprintf('\nAl2O3 Molecular Weight is %3.4f [g/mol]', Al2O3_MW)
fprintf('\nPercent of Al2O3 weight from Al in decimal form is %1.4f',
Pct_Al_Al2O3)
fprintf('\nAmount of Al needed for the desired product size is %1.4f
[g]\n', Al_needed)

%Potassium (K)
K_Desired = WtPct_K2O*product; %[g/mol]
K2O_MW = (2*K)+(O); %[g/mol]
Pct_K_K2O = (2*K)/K2O_MW; %[percent of K2O weight from K in decimal
form]
K_needed = Pct_K_K2O*K_Desired; %amount of K needed for the desired
product size [g]
fprintf('\nAmount of K2O desired is %2.4f [g]', K_Desired)
fprintf('\nK2O Molecular Weight is %3.4f [g/mol]', K2O_MW)
fprintf('\nPercent of K2O weight from K in decimal form is %1.4f',
Pct_K_K2O)
fprintf('\nAmount of K needed for the desired product size is %1.4f
[g]\n', K_needed)

%Calcium (Ca)
Ca_Desired = WtPct_CaO*product; %[g/mol]
CaO_MW = (Ca)+(O); %[g/mol]
Pct_Ca_CaO = (Ca)/CaO_MW; %[percent of CaO weight from Ca in decimal
form]
Ca_needed = Pct_Ca_CaO*Ca_Desired; %amount of Ca needed for the desired
product size [g]
fprintf('\nAmount of CaO desired is %2.4f [g]', Ca_Desired)
fprintf('\nCaO Molecular Weight is %3.4f [g/mol]', CaO_MW)
fprintf('\nPercent of CaO weight from Ca in decimal form is %1.4f',
Pct_Ca_CaO)
fprintf('\nAmount of Ca needed for the desired product size is %1.4f
[g]\n', Ca_needed)

%Magnesium (Mg)
Mg_Desired = WtPct_MgO*product; %[g/mol]
MgO_MW = (Mg)+(O); %[g/mol]
Pct_Mg_MgO = (Mg)/MgO_MW; %[percent of MgO weight from Mg in decimal
form]
```

```
Mg_needed = Pct_Mg_MgO*Mg_Desired; %amount of Mg needed for the desired
product size [g]
fprintf('\nAmount of MgO desired is %2.4f [g]', Mg_Desired)
fprintf('\nMgO Molecular Weight is %3.4f [g/mol]', MgO_MW)
fprintf('\nPercent of MgO weight from Mg in decimal form is %1.4f',
Pct_Mg_MgO)
fprintf('\nAmount of Mg needed for the desired product size is %1.4f
[g]\n', Mg_needed)

%Sodium (Na)
Na_Desired = WtPct_Na2O*product; %[g/mol]
Na2O_MW = (2*Na)+(O); %[g/mol]
Pct_Na_Na2O = (2*Na)/Na2O_MW; %[percent of Na2O weight from Na in
decimal form]
Na_needed = Pct_Na_Na2O*Na_Desired; %amount of Na needed for the
desired product size [g]
fprintf('\nAmount of Na2O desired is %2.4f [g]', Na_Desired)
fprintf('\nNa2O Molecular Weight is %3.4f [g/mol]', Na2O_MW)
fprintf('\nPercent of Na2O weight from Na in decimal form is %1.4f',
Pct_Na_Na2O)
fprintf('\nAmount of Na needed for the desired product size is %1.4f
[g]\n', Na_needed)

%Titanium (Ti)
Ti_Desired = WtPct_TiO2*product; %[g/mol]
TiO2_MW = (Ti)+(2*O); %[g/mol]
Pct_Ti_TiO2 = (Ti)/TiO2_MW; %[percent of TiO2 weight from Ti in decimal
form]
Ti_needed = Pct_Ti_TiO2*Ti_Desired; %amount of Ti needed for the
desired product size [g]
fprintf('\nAmount of TiO2 desired is %2.4f [g]', Ti_Desired)
fprintf('\nTiO2 Molecular Weight is %3.4f [g/mol]', TiO2_MW)
fprintf('\nPercent of TiO2 weight from Ti in decimal form is %1.4f',
Pct_Ti_TiO2)
fprintf('\nAmount of Ti needed for the desired product size is %1.4f
[g]\n', Ti_needed)

%Iron (Fe)
Fe_Desired = WtPct_FeO*product; %[g/mol]
FeO_MW = (Fe)+(O); %[g/mol]
Pct_Fe_FeO = (Fe)/FeO_MW; %[percent of FeO weight from Fe in decimal
form]
Fe_needed = Pct_Fe_FeO*Fe_Desired; %amount of Fe needed for the desired
product size [g]
fprintf('\nAmount of FeO desired is %2.4f [g]', Fe_Desired)
fprintf('\nFeO Molecular Weight is %3.4f [g/mol]', FeO_MW)
fprintf('\nPercent of FeO weight from Fe in decimal form is %1.4f',
Pct_Fe_FeO)
fprintf('\nAmount of Fe needed for the desired product size is %1.4f
[g]\n', Fe_needed)
%%
%Calculated Elemental Composition of Tektite
Si_Pct = (Si_needed/product)*100; %[Percent]
Al_Pct = (Al_needed/product)*100; %[Percent]
K_Pct = (K_needed/product)*100; %[Percent]
```

```
Ca_Pct = (Ca_needed/product)*100; %[Percent]
Mg_Pct = (Mg_needed/product)*100; %[Percent]
Na_Pct = (Na_needed/product)*100; %[Percent]
Fe_Pct = (Fe_needed/product)*100; %[Percent]
Ti_Pct = (Ti_needed/product)*100; %[Percent]
O_Pct = 100-Si_Pct-Al_Pct-K_Pct-Ca_Pct-Mg_Pct-Na_Pct-Fe_Pct-Ti_Pct;
%[Percent] Less than or equal to this percent for Oxygen as there can
also be many minor constituants within the Tektite.
fprintf('\nCalculated Elemental Composition of Tektite as
Percentages\n')
fprintf('\nElement          Percent')
fprintf('\nSilicon          %2.4f', Si_Pct)
fprintf('\nAluminum         %2.4f', Al_Pct)
fprintf('\nPotassium        %2.4f', K_Pct)
fprintf('\nCalcium          %2.4f', Ca_Pct)
fprintf('\nMagnesium        %2.4f', Mg_Pct)
fprintf('\nSodium           %2.4f', Na_Pct)
fprintf('\nIron             %2.4f', Fe_Pct)
fprintf('\nTitanium         %2.4f', Ti_Pct)
fprintf('\nOxygen         <=%2.4f\n', O_Pct)
%%
%Basic Solution Fabrication (with Fe and Ti added in solution)
%Calculations for the amount needed of each surrogate material needed
to achieve
%desired output quantity with proportional elemental composition of
Tektite
fprintf('\nBasic Solution Fabrication (with Fe and Ti added in
solution)\n')

%SiO2 surrogate material C8 H20 O4 Si [TEOS]
S_Si_MW = (8*C)+(20*H)+(4*O)+Si; %[g/mol]
Pct_Si_S_Si = Si/S_Si_MW; %[percent of Si surrogate weight from Si in
decimal form]
S_Si_needed = Si_needed/Pct_Si_S_Si; %amount of Si surrogate needed for
the desired product size [g]
%Using 50 [ml] for basic solution fabrication
p_TEOS = (S_Si_needed/S_Si_MW)*(S_Si_MW/1000)*(1e6/50); %TEOS density
[kg/m^3]
%(1/1000)[kg/g]*(1e6/1)[ml/m^3]*(1/density)[m^3/kg]
BW_S_Si_needed = (1/1000)*((1e6)/1)*(1/p_TEOS)*S_Si_needed; %amount of
Si surrogate needed for the desired product size [ml]
fprintf('\nSiO2 surrogate material is Tetraethyl Orthosilicate [TEOS]')
fprintf('\nAmount of Si needed for the desired product size is %1.4f
[g]', Si_needed)
fprintf('\nTEOS Molecular Weight is %3.4f [g/mol]', S_Si_MW)
fprintf('\nPercent of TEOS weight from Si in decimal form is %1.4f',
Pct_Si_S_Si)
fprintf('\nBased on the Basic Solution formula using 50 [ml] of TEOS:')
fprintf('\nAmount of TEOS needed for the desired product size is %2.4f
[g]', S_Si_needed)
fprintf('\nTEOS density is %3.4f [kg/m^3]', p_TEOS)
fprintf('\nAmount of TEOS needed for the desired product size is %2.4f
[ml]\n', BW_S_Si_needed)

%Al2O3 surrogate material C9 H21 O3 Al [Aluminum Isopropoxide]
```

```
S_Al_MW = (9*C)+(21*H)+(3*O)+Al; %[g/mol]
Pct_Al_S_Al = Al/S_Al_MW; %[percent of Al surrogate weight from Al in
decimal form]
BW_S_Al_needed = Al_needed/Pct_Al_S_Al; %amount of Al surrogate needed
for the desired product size [g]
fprintf('\nAl2O3 surrogate material is Aluminum Isopropoxide')
fprintf('\nAmount of Al needed for the desired product size is %1.4f
[g]', Al_needed)
fprintf('\nAluminum Isopropoxide Molecular Weight is %3.4f [g/mol]',
S_Al_MW)
fprintf('\nPercent of Aluminum Isopropoxide weight from Al in decimal
form is %1.4f', Pct_Al_S_Al)
fprintf('\nAmount of Aluminum Isopropoxide needed for the desired
product size is %2.4f [g]\n', BW_S_Al_needed)

%K2O surrogate material H K O [Potassium Hydroxide]
S_K_MW = H+K+O; %[g/mol]
Pct_K_S_K = K/S_K_MW; %[percent of K surrogate weight from K in decimal
form]
BW_S_K_needed = K_needed/Pct_K_S_K; %amount of K surrogate needed for
the desired product size [g]
fprintf('\nK2O surrogate material is Potassium Hydroxide')
fprintf('\nAmount of K needed for the desired product size is %1.4f
[g]', K_needed)
fprintf('\nPotassium Hydroxide Molecular Weight is %3.4f [g/mol]',
S_K_MW)
fprintf('\nPercent of Potassium Hydroxide weight from K in decimal form
is %1.4f', Pct_K_S_K)
fprintf('\nAmount of Potassium Hydroxide needed for the desired product
size is %2.4f [g]\n', BW_S_K_needed)

%CaO surrogate material Ca Cl2 [Calcium Chloride]
S_Ca_MW = Ca+(2*Cl); %[g/mol]
Pct_Ca_S_Ca = Ca/S_Ca_MW; %[percent of Ca surrogate weight from Ca in
decimal form]
BW_S_Ca_needed = Ca_needed/Pct_Ca_S_Ca; %amount of Ca surrogate needed
for the desired product size [g]
fprintf('\nCaO surrogate material is Calcium Chloride')
fprintf('\nAmount of Ca needed for the desired product size is %1.4f
[g]', Ca_needed)
fprintf('\nCalcium Chloride Molecular Weight is %3.4f [g/mol]',
S_Ca_MW)
fprintf('\nPercent of Calcium Chloride weight from Ca in decimal form
is %1.4f', Pct_Ca_S_Ca)
fprintf('\nAmount of Calcium Chloride needed for the desired product
size is %2.4f [g]\n', BW_S_Ca_needed)

%MgO surrogate material H2 Mg O2 [Magnesium Hydroxide]
S_Mg_MW = (2*H)+(2*O)+Mg; %[g/mol]
Pct_Mg_S_Mg = Mg/S_Mg_MW; %[percent of Mg surrogate weight from Mg in
decimal form]
BW_S_Mg_needed = Mg_needed/Pct_Mg_S_Mg; %amount of Mg surrogate needed
for the desired product size [g]
fprintf('\nMgO surrogate material is Magnesium Hydroxide')
```

```
fprintf('\nAmount of Mg needed for the desired product size is %1.4f
[g]', Mg_needed)
fprintf('\nMagnesium Hydroxide Molecular Weight is %3.4f [g/mol]',
S_Mg_MW)
fprintf('\nPercent of Magnesium Hydroxide weight from Mg in decimal
form is %1.4f', Pct_Mg_S_Mg)
fprintf('\nAmount of Magnesium Hydroxide needed for the desired product
size is %2.4f [g]\n', BW_S_Mg_needed)

%Na2O surrogate material H Na O [Sodium Hydroxide]
S_Na_MW = H+O+Na; %[g/mol]
Pct_Na_S_Na = Na/S_Na_MW; %[percent of Na surrogate weight from Na in
decimal form]
BW_S_Na_needed = Na_needed/Pct_Na_S_Na; %amount of Na surrogate needed
for the desired product size [g]
fprintf('\nNa2O surrogate material is Sodium Hydroxide')
fprintf('\nAmount of Na needed for the desired product size is %1.4f
[g]', Na_needed)
fprintf('\nSodium Hydroxide Molecular Weight is %3.4f [g/mol]',
S_Na_MW)
fprintf('\nPercent of Sodium Hydroxide weight from Na in decimal form
is %1.4f', Pct_Na_S_Na)
fprintf('\nAmount of Sodium Hydroxide needed for the desired product
size is %2.4f [g]\n', BW_S_Na_needed)

%FeO surrogate material Fe N3 O9 9*(H2O) [Iron (III) Nitrate
Nonahydrate]
S_Fe_MW = Fe+(3*N)+(18*O)+(18*H); %[g/mol]
Pct_Fe_S_Fe = Fe/S_Fe_MW; %[percent of Fe surrogate weight from Fe in
decimal form]
BW_S_Fe_needed = Fe_needed/Pct_Fe_S_Fe; %amount of Fe surrogate needed
for the desired product size [g]
fprintf('\nFeO surrogate material is Iron (III) Nitrate Nonahydrate')
fprintf('\nAmount of Fe needed for the desired product size is %1.4f
[g]', Fe_needed)
fprintf('\nIron (III) Nitrate Nonahydrate Molecular Weight is %3.4f
[g/mol]', S_Fe_MW)
fprintf('\nPercent of Iron (III) Nitrate Nonahydrate weight from Fe in
decimal form is %1.4f', Pct_Fe_S_Fe)
fprintf('\nAmount of Iron (III) Nitrate Nonahydrate needed for the
desired product size is %2.4f [g]\n', BW_S_Fe_needed)

%TiO2 surrogate material C12 H28 O4 Ti [Titanium Isopropoxide]
S_Ti_MW = (12*C)+(28*H)+(4*O)+Ti; %[g/mol]
Pct_Ti_S_Ti = Ti/S_Ti_MW; %[percent of Ti surrogate weight from Ti in
decimal form]
S_Ti_needed = Ti_needed/Pct_Ti_S_Ti; %amount of Ti surrogate needed for
the desired product size [g]
p_TiIso = 937; %TiIso density [kg/m^3]
BW_S_Ti_needed = (1/1000)*((1e6)/1)*(1/p_TiIso)*S_Ti_needed; %amount of
Ti surrogate needed for the desired product size [ml]
fprintf('\nTiO2 surrogate material is Titanium Isopropoxide')
fprintf('\nAmount of Ti needed for the desired product size is %1.4f
[g]', Ti_needed)
```

```
fprintf('\nTitanium Isopropoxide Molecular Weight is %3.4f [g/mol]',
S_Ti_MW)
fprintf('\nPercent of Titanium Isopropoxide weight from Ti in decimal
form is %1.4f', Pct_Ti_S_Ti)
fprintf('\nAmount of Titanium Isopropoxide needed for the desired
product size is %2.4f [g]', S_Ti_needed)
fprintf('\nTitanium Isopropoxide density is %3.4f [kg/m^3]', p_TiIso)
fprintf('\nAmount of Titanium Isopropoxide needed for the desired
product size is %2.4f [ml]\n', BW_S_Ti_needed)
%%
%Basic Solution Fabrication (with Fe and Ti added as oxides later in
the process)
%Calculations for the amount needed of each surrogate material to
achieve
%desired output quantity with proportional elemental composition of
Tektite
fprintf('\nBasic Solution Fabrication (with Fe and Ti added as oxides
later in the process)\n')

%SiO2 surrogate material C8 H20 O4 Si [TEOS]
S_Si_MW = (8*C)+(20*H)+(4*O)+Si; %[g/mol]
Pct_Si_S_Si = Si/S_Si_MW; %[percent of Si surrogate weight from Si in
decimal form]
S_Si_needed = Si_needed/Pct_Si_S_Si; %amount of Si surrogate needed for
the desired product size [g]
%Using 50 [ml] for basic solution fabrication
p_TEOS = (S_Si_needed/S_Si_MW)*(S_Si_MW/1000)*(1e6/50); %TEOS density
[kg/m^3]
%(1/1000)[kg/g]*(1e6/1)[ml/m^3]*(1/density)[m^3/kg]
Bwo_S_Si_needed = (1/1000)*((1e6)/1)*(1/p_TEOS)*S_Si_needed; %amount of
Si surrogate needed for the desired product size [ml]
fprintf('\nSiO2 surrogate material is Tetraethyl Orthosilicate [TEOS]')
fprintf('\nAmount of Si needed for the desired product size is %1.4f
[g]', Si_needed)
fprintf('\nTEOS Molecular Weight is %3.4f [g/mol]', S_Si_MW)
fprintf('\nPercent of TEOS weight from Si in decimal form is %1.4f',
Pct_Si_S_Si)
fprintf('\nBased on the Basic Solution formula using 50 [ml] of TEOS:')
fprintf('\nAmount of TEOS needed for the desired product size is %2.4f
[g]', S_Si_needed)
fprintf('\nTEOS density is %3.4f [kg/m^3]', p_TEOS)
fprintf('\nAmount of TEOS needed for the desired product size is %2.4f
[ml]\n', Bwo_S_Si_needed)

%Al2O3 surrogate material C9 H21 O3 Al [Aluminum Isopropoxide]
S_Al_MW = (9*C)+(21*H)+(3*O)+Al; %[g/mol]
Pct_Al_S_Al = Al/S_Al_MW; %[percent of Al surrogate weight from Al in
decimal form]
Bwo_S_Al_needed = Al_needed/Pct_Al_S_Al; %amount of Al surrogate needed
for the desired product size [g]
fprintf('\nAl2O3 surrogate material is Aluminum Isopropoxide')
fprintf('\nAmount of Al needed for the desired product size is %1.4f
[g]', Al_needed)
fprintf('\nAluminum Isopropoxide Molecular Weight is %3.4f [g/mol]',
S_Al_MW)
```

```
fprintf('\nPercent of Aluminum Isopropoxide weight from Al in decimal
form is %1.4f', Pct_Al_S_Al)
fprintf('\nAmount of Aluminum Isopropoxide needed for the desired
product size is %2.4f [g]\n', Bwo_S_Al_needed)

%K2O surrogate material H K O [Potassium Hydroxide]
S_K_MW = H+K+O; %[g/mol]
Pct_K_S_K = K/S_K_MW; %[percent of K surrogate weight from K in decimal
form]
Bwo_S_K_needed = K_needed/Pct_K_S_K; %amount of K surrogate needed for
the desired product size [g]
fprintf('\nK2O surrogate material is Potassium Hydroxide')
fprintf('\nAmount of K needed for the desired product size is %1.4f
[g]', K_needed)
fprintf('\nPotassium Hydroxide Molecular Weight is %3.4f [g/mol]',
S_K_MW)
fprintf('\nPercent of Potassium Hydroxide weight from K in decimal form
is %1.4f', Pct_K_S_K)
fprintf('\nAmount of Potassium Hydroxide needed for the desired product
size is %2.4f [g]\n', Bwo_S_K_needed)

%CaO surrogate material Ca Cl2 [Calcium Chloride]
S_Ca_MW = Ca+(2*Cl); %[g/mol]
Pct_Ca_S_Ca = Ca/S_Ca_MW; %[percent of Ca surrogate weight from Ca in
decimal form]
Bwo_S_Ca_needed = Ca_needed/Pct_Ca_S_Ca; %amount of Ca surrogate needed
for the desired product size [g]
fprintf('\nCaO surrogate material is Calcium Chloride')
fprintf('\nAmount of Ca needed for the desired product size is %1.4f
[g]', Ca_needed)
fprintf('\nCalcium Chloride Molecular Weight is %3.4f [g/mol]',
S_Ca_MW)
fprintf('\nPercent of Calcium Chloride weight from Ca in decimal form
is %1.4f', Pct_Ca_S_Ca)
fprintf('\nAmount of Calcium Chloride needed for the desired product
size is %2.4f [g]\n', Bwo_S_Ca_needed)

%MgO surrogate material H2 Mg O2 [Magnesium Hydroxide]
S_Mg_MW = (2*H)+(2*O)+Mg; %[g/mol]
Pct_Mg_S_Mg = Mg/S_Mg_MW; %[percent of Mg surrogate weight from Mg in
decimal form]
Bwo_S_Mg_needed = Mg_needed/Pct_Mg_S_Mg; %amount of Mg surrogate needed
for the desired product size [g]
fprintf('\nMgO surrogate material is Magnesium Hydroxide')
fprintf('\nAmount of Mg needed for the desired product size is %1.4f
[g]', Mg_needed)
fprintf('\nMagnesium Hydroxide Molecular Weight is %3.4f [g/mol]',
S_Mg_MW)
fprintf('\nPercent of Magnesium Hydroxide weight from Mg in decimal
form is %1.4f', Pct_Mg_S_Mg)
fprintf('\nAmount of Magnesium Hydroxide needed for the desired product
size is %2.4f [g]\n', Bwo_S_Mg_needed)

%Na2O surrogate material H Na O [Sodium Hydroxide]
S_Na_MW = H+O+Na; %[g/mol]
```

```
Pct_Na_S_Na = Na/S_Na_MW; %[percent of Na surrogate weight from Na in
decimal form]
Bwo_S_Na_needed = Na_needed/Pct_Na_S_Na; %amount of Na surrogate needed
for the desired product size [g]
fprintf('\nNa2O surrogate material is Sodium Hydroxide')
fprintf('\nAmount of Na needed for the desired product size is %1.4f
[g]', Na_needed)
fprintf('\nSodium Hydroxide Molecular Weight is %3.4f [g/mol]',
S_Na_MW)
fprintf('\nPercent of Sodium Hydroxide weight from Na in decimal form
is %1.4f', Pct_Na_S_Na)
fprintf('\nAmount of Sodium Hydroxide needed for the desired product
size is %2.4f [g]\n', Bwo_S_Na_needed)

%FeO surrogate material Fe O [Iron Oxide]
Half_Fe_needed = Fe_needed/2;
S_Fe_MW = 231.53; %[g/mol]
Pct_Fe_S_Fe = Fe/S_Fe_MW; %[percent of Fe surrogate weight from Fe in
decimal form]
Bwo_S_Fe_needed = Half_Fe_needed/Pct_Fe_S_Fe; %amount of Fe surrogate
needed for the desired product size [g]
fprintf('\nFeO surrogate material is Iron Oxide')
fprintf('\nSince the oxides will be added to half the volume of the
Basic Solution Formula the needed amount was reduced by half.')
fprintf('\nAmount of Fe needed for the desired product size is %1.4f
[g]', Half_Fe_needed)
fprintf('\nIron Oxide Molecular Weight is %3.4f [g/mol]', S_Fe_MW)
fprintf('\nPercent of Iron Oxide weight from Fe in decimal form is
%1.4f', Pct_Fe_S_Fe)
fprintf('\nAmount of Iron Oxide needed for the desired product size is
%2.4f [g]\n', Bwo_S_Fe_needed)

%TiO2 surrogate material Ti O2 [Titanium Oxide Rutile]
Half_Ti_needed = Ti_needed/2;
S_Ti_MW = (2*O)+Ti; %[g/mol]
Pct_Ti_S_Ti = Ti/S_Ti_MW; %[percent of Ti surrogate weight from Ti in
decimal form]
Bwo_S_Ti_needed = Half_Ti_needed/Pct_Ti_S_Ti; %amount of Ti surrogate
needed for the desired product size [g]
fprintf('\nTiO2 surrogate material is Titanium Oxide Rutile')
fprintf('\nSince the oxides will be added to half the volume of the
Basic Solution Formula the needed amount was reduced by half.')
fprintf('\nAmount of Ti needed for the desired product size is %1.4f
[g]', Half_Ti_needed)
fprintf('\nTitanium Oxide Rutile Molecular Weight is %3.4f [g/mol]',
S_Ti_MW)
fprintf('\nPercent of Titanium Oxide Rutile weight from Ti in decimal
form is %1.4f', Pct_Ti_S_Ti)
fprintf('\nAmount of Titanium Oxide Rutile needed for the desired
product size is %2.4f [g]', Bwo_S_Ti_needed)
```

THIS PAGE INTENTIONALLY LEFT BLANK

APPENDIX B. ACID SOLUTION SYNTHESIS MATLAB CODE

```
%%Elemental Composition calculations for Tektite fabrication using surrogate materials
%LCDR Ken Foos
%In support of surrogate material fabrication for LDHP Thesis Work
%Acid Solution Synthesis
%%
%%Elements and corresponding Molecular Weights (MW's)
Si = 28.0855; %[g/mol]
Al = 26.981536; %[g/mol]
K = 39.0983; %[g/mol]
Ca = 40.078; %[g/mol]
Mg = 24.3050; %[g/mol]
Na = 22.989770; %[g/mol]
Fe = 55.845; %[g/mol]
Ti = 47.867; %[g/mol]
O = 15.9994; %[g/mol]
C = 12.0107; %[g/mol]
H = 1.00794; %[g/mol]
Cl = 35.453; %[g/mol]
Br = 79.904; %[g/mol]
N = 14.0067; %[g/mol]
%Values taken from the Sargent-Welch Periodic Table,
%Copyright 2004 VWR International
%%
%Elemental Calculations for the grams needed of each element to achieve
%desired output quantity of Tektite based on Weight Percent data determined
%through material characterization
product = 13.1517; %Desired output quantity of Tektite [g]
fprintf('\nTarget quantity of Tektite is %2.4f [g]\n', product)
%Input Weight Percents (Wt%'s)
%From Table 4 of Reference:
%A. Camargo, “Characterization of Particles Created by Laser-Driven
%Hydrothermal Processing,” M.S. Thesis, Dept. of Mechanical and Aerospace
%Engineering, NPS, Monterey, CA, USA, 2016.
WtPct_SiO2 = 0.7304;
WtPct_Al2O3 = 0.1234;
WtPct_K2O = 0.0254;
WtPct_CaO = 0.0205;
WtPct_MgO = 0.0234;
WtPct_Na2O = 0.0076;
WtPct_FeO = 0.0598;
WtPct_TiO2 = 0.0090;
```

```
%Silicon (Si)
Si_Desired = WtPct_SiO2*product; %[g]
SiO2_MW = Si+(2*O); %[g/mol]
Pct_Si_SiO2 = Si/SiO2_MW; %[percent of SiO2 weight from Si in decimal form]
Si_needed = Pct_Si_SiO2*Si_Desired; %amount of Si needed for the desired product
size [g]
fprintf('\nAmount of SiO2 desired is %2.4f [g]', Si_Desired)
fprintf('\nSiO2 Molecular Weight is %3.4f [g/mol]', SiO2_MW)
fprintf('\nPercent of SiO2 weight from Si in decimal form is %1.4f', Pct_Si_SiO2)
fprintf('\nAmount of Si needed for the desired product size is %1.4f [g]\n', Si_needed)

%Aluminum (Al)
Al_Desired = WtPct_Al2O3*product; %[g/mol]
Al2O3_MW = (2*Al)+(3*O); %[g/mol]
Pct_Al_Al2O3 = (2*Al)/Al2O3_MW; %[percent of Al2O3 weight from Al in decimal
form]
Al_needed = Pct_Al_Al2O3*Al_Desired; %amount of Al needed for the desired product
size [g]
fprintf('\nAmount of Al2O3 desired is %2.4f [g]', Al_Desired)
fprintf('\nAl2O3 Molecular Weight is %3.4f [g/mol]', Al2O3_MW)
fprintf('\nPercent of Al2O3 weight from Al in decimal form is %1.4f', Pct_Al_Al2O3)
fprintf('\nAmount of Al needed for the desired product size is %1.4f [g]\n', Al_needed)

%Potassium (K)
K_Desired = WtPct_K2O*product; %[g/mol]
K2O_MW = (2*K)+(O); %[g/mol]
Pct_K_K2O = (2*K)/K2O_MW; %[percent of K2O weight from K in decimal form]
K_needed = Pct_K_K2O*K_Desired; %amount of K needed for the desired product size
[g]
fprintf('\nAmount of K2O desired is %2.4f [g]', K_Desired)
fprintf('\nK2O Molecular Weight is %3.4f [g/mol]', K2O_MW)
fprintf('\nPercent of K2O weight from K in decimal form is %1.4f', Pct_K_K2O)
fprintf('\nAmount of K needed for the desired product size is %1.4f [g]\n', K_needed)

%Calcium (Ca)
Ca_Desired = WtPct_CaO*product; %[g/mol]
CaO_MW = (Ca)+(O); %[g/mol]
Pct_Ca_CaO = (Ca)/CaO_MW; %[percent of CaO weight from Ca in decimal form]
Ca_needed = Pct_Ca_CaO*Ca_Desired; %amount of Ca needed for the desired product
size [g]
fprintf('\nAmount of CaO desired is %2.4f [g]', Ca_Desired)
fprintf('\nCaO Molecular Weight is %3.4f [g/mol]', CaO_MW)
fprintf('\nPercent of CaO weight from Ca in decimal form is %1.4f', Pct_Ca_CaO)
fprintf('\nAmount of Ca needed for the desired product size is %1.4f [g]\n', Ca_needed)
```

```
%Magnesium (Mg)
Mg_Desired = WtPct_MgO*product; %[g/mol]
MgO_MW = (Mg)+(O); %[g/mol]
Pct_Mg_MgO = (Mg)/MgO_MW; %[percent of MgO weight from Mg in decimal form]
Mg_needed = Pct_Mg_MgO*Mg_Desired; %amount of Mg needed for the desired
product size [g]
fprintf('\nAmount of MgO desired is %2.4f [g]', Mg_Desired)
fprintf('\nMgO Molecular Weight is %3.4f [g/mol]', MgO_MW)
fprintf('\nPercent of MgO weight from Mg in decimal form is %1.4f', Pct_Mg_MgO)
fprintf('\nAmount of Mg needed for the desired product size is %1.4f [g]\n', Mg_needed)

%Sodium (Na)
Na_Desired = WtPct_Na2O*product; %[g/mol]
Na2O_MW = (2*Na)+(O); %[g/mol]
Pct_Na_Na2O = (2*Na)/Na2O_MW; %[percent of Na2O weight from Na in decimal
form]
Na_needed = Pct_Na_Na2O*Na_Desired; %amount of Na needed for the desired product
size [g]
fprintf('\nAmount of Na2O desired is %2.4f [g]', Na_Desired)
fprintf('\nNa2O Molecular Weight is %3.4f [g/mol]', Na2O_MW)
fprintf('\nPercent of Na2O weight from Na in decimal form is %1.4f', Pct_Na_Na2O)
fprintf('\nAmount of Na needed for the desired product size is %1.4f [g]\n', Na_needed)

%Titanium (Ti)
Ti_Desired = WtPct_TiO2*product; %[g/mol]
TiO2_MW = (Ti)+(2*O); %[g/mol]
Pct_Ti_TiO2 = (Ti)/TiO2_MW; %[percent of TiO2 weight from Ti in decimal form]
Ti_needed = Pct_Ti_TiO2*Ti_Desired; %amount of Ti needed for the desired product
size [g]
fprintf('\nAmount of TiO2 desired is %2.4f [g]', Ti_Desired)
fprintf('\nTiO2 Molecular Weight is %3.4f [g/mol]', TiO2_MW)
fprintf('\nPercent of TiO2 weight from Ti in decimal form is %1.4f', Pct_Ti_TiO2)
fprintf('\nAmount of Ti needed for the desired product size is %1.4f [g]\n', Ti_needed)

%Iron (Fe)
Fe_Desired = WtPct_FeO*product; %[g/mol]
FeO_MW = (Fe)+(O); %[g/mol]
Pct_Fe_FeO = (Fe)/FeO_MW; %[percent of FeO weight from Fe in decimal form]
Fe_needed = Pct_Fe_FeO*Fe_Desired; %amount of Fe needed for the desired product
size [g]
fprintf('\nAmount of FeO desired is %2.4f [g]', Fe_Desired)
fprintf('\nFeO Molecular Weight is %3.4f [g/mol]', FeO_MW)
fprintf('\nPercent of FeO weight from Fe in decimal form is %1.4f', Pct_Fe_FeO)
fprintf('\nAmount of Fe needed for the desired product size is %1.4f [g]\n', Fe_needed)
%%
```

```
%Calculated Elemental Composition of Tektite
Si_Pct = (Si_needed/product)*100; %[Percent]
Al_Pct = (Al_needed/product)*100; %[Percent]
K_Pct = (K_needed/product)*100; %[Percent]
Ca_Pct = (Ca_needed/product)*100; %[Percent]
Mg_Pct = (Mg_needed/product)*100; %[Percent]
Na_Pct = (Na_needed/product)*100; %[Percent]
Fe_Pct = (Fe_needed/product)*100; %[Percent]
Ti_Pct = (Ti_needed/product)*100; %[Percent]
O_Pct = 100-Si_Pct-Al_Pct-K_Pct-Ca_Pct-Mg_Pct-Na_Pct-Fe_Pct-Ti_Pct; %[Percent]
Less than or equal to this percent for Oxygen as there can also be many minor
constituants within the Tektite.
fprintf('\nCalculated Elemental Composition of Tektite as Percentages\n')
fprintf('\nElement         Percent')
fprintf('\nSilicon         %2.4f', Si_Pct)
fprintf('\nAluminum        %2.4f', Al_Pct)
fprintf('\nPotassium       %2.4f', K_Pct)
fprintf('\nCalcium         %2.4f', Ca_Pct)
fprintf('\nMagnesium       %2.4f', Mg_Pct)
fprintf('\nSodium          %2.4f', Na_Pct)
fprintf('\nIron           %2.4f', Fe_Pct)
fprintf('\nTitanium        %2.4f', Ti_Pct)
fprintf('\nOxygen        <=%2.4f\n', O_Pct)
%%
%Acid Solution Fabrication
%Calculations for the amount needed of each surrogate material to achieve
%desired output quantity with proportional elemental composition of Tektite
product = 13.1517; %Desired output quantity of Tektite [g]
fprintf('\nAcid Solution Fabrication\n')
fprintf('\nTarget quantity of Tektite is %2.4f [g]\n', product)

%SiO2 surrogate material C8 H20 O4 Si [TEOS]
S_Si_MW = (8*C)+(20*H)+(4*O)+Si; %[g/mol]
Pct_Si_S_Si = Si/S_Si_MW; %[percent of Si surrogate weight from Si in decimal form]
S_Si_needed = Si_needed/Pct_Si_S_Si; %amount of Si surrogate needed for the desired
product size [g]
%Using 35.5 [ml] for acid solution fabrication
p_TEOS = (S_Si_needed/S_Si_MW)*(S_Si_MW/1000)*(1e6/35.5); %TEOS density
[kg/m^3]
%(1/1000)[kg/g]*(1e6/1)[ml/m^3]*(1/density)[m^3/kg]
A_S_Si_needed = (1/1000)*((1e6)/1)*(1/p_TEOS)*S_Si_needed; %amount of Si
surrogate needed for the desired product size [ml]
fprintf('\nSiO2 surrogate material is Tetraethyl Orthosilicate [TEOS]')
fprintf('\nAmount of Si needed for the desired product size is %1.4f [g]', Si_needed)
fprintf('\nTEOS Molecular Weight is %3.4f [g/mol]', S_Si_MW)
```

```
fprintf('\nPercent of TEOS weight from Si in decimal form is %1.4f', Pct_Si_S_Si)
fprintf('\nBased on the Acid Solution formula using 35.5 [ml] of TEOS:')
fprintf('\nAmount of TEOS needed for the desired product size is %2.4f [g]',
S_Si_needed)
fprintf('\nTEOS density is %3.4f [kg/m^3]', p_TEOS)
fprintf('\nAmount of TEOS needed for the desired product size is %2.4f [ml]\n',
A_S_Si_needed)

%Al2O3 surrogate material N3 H18 O18 Al [Aluminum Nitrate Hydrate]
S_Al_MW = (3*N)+(18*H)+(18*O)+Al; %[g/mol]
Pct_Al_S_Al = Al/S_Al_MW; %[percent of Al surrogate weight from Al in decimal
form]
BW_S_Al_needed = Al_needed/Pct_Al_S_Al; %amount of Al surrogate needed for the
desired product size [g]
fprintf('\nAl2O3 surrogate material is Aluminum Nitrate Hydrate')
fprintf('\nAmount of Al needed for the desired product size is %1.4f [g]', Al_needed)
fprintf('\nAluminum Nitrate Hydrate Molecular Weight is %3.4f [g/mol]', S_Al_MW)
fprintf('\nPercent of Aluminum Nitrate Hydrate weight from Al in decimal form is
%1.4f', Pct_Al_S_Al)
fprintf('\nAmount of Aluminum Nitrate Hydrate needed for the desired product size is
%2.4f [g]\n', BW_S_Al_needed)

%K2O surrogate material K Br [Potassium Bromide]
S_K_MW = K+Br; %[g/mol]
Pct_K_S_K = K/S_K_MW; %[percent of K surrogate weight from K in decimal form]
A_S_K_needed = K_needed/Pct_K_S_K; %amount of K surrogate needed for the desired
product size [g]
fprintf('\nK2O surrogate material is Potassium Bromide')
fprintf('\nAmount of K needed for the desired product size is %1.4f [g]', K_needed)
fprintf('\nPotassium Bromide Molecular Weight is %3.4f [g/mol]', S_K_MW)
fprintf('\nPercent of Potassium Bromide weight from K in decimal form is %1.4f',
Pct_K_S_K)
fprintf('\nAmount of Potassium Bromide needed for the desired product size is %2.4f
[g]\n', A_S_K_needed)

%CaO surrogate material Ca Cl2 [Calcium Chloride]
S_Ca_MW = Ca+(2*Cl); %[g/mol]
Pct_Ca_S_Ca = Ca/S_Ca_MW; %[percent of Ca surrogate weight from Ca in decimal
form]
A_S_Ca_needed = Ca_needed/Pct_Ca_S_Ca; %amount of Ca surrogate needed for the
desired product size [g]
fprintf('\nCaO surrogate material is Calcium Chloride')
fprintf('\nAmount of Ca needed for the desired product size is %1.4f [g]', Ca_needed)
fprintf('\nCalcium Chloride Molecular Weight is %3.4f [g/mol]', S_Ca_MW)
```

```
fprintf('\nPercent of Calcium Chloride weight from Ca in decimal form is %1.4f',
Pct_Ca_S_Ca)
fprintf('\nAmount of Calcium Chloride needed for the desired product size is %2.4f
[g]\n', A_S_Ca_needed)

%MgO surrogate material Mg N2 O12 H12 (Mg(NO3)2+6*H2O) [Magnesium Nitrate
Hexahydrate]
S_Mg_MW = (12*H)+(12*O)+Mg+(2*N); %[g/mol]
Pct_Mg_S_Mg = Mg/S_Mg_MW; %[percent of Mg surrogate weight from Mg in
decimal form]
A_S_Mg_needed = Mg_needed/Pct_Mg_S_Mg; %amount of Mg surrogate needed for
the desired product size [g]
fprintf('\nMgO surrogate material is Magnesium Nitrate Hexahydrate')
fprintf('\nAmount of Mg needed for the desired product size is %1.4f [g]', Mg_needed)
fprintf('\nMagnesium Nitrate Hexahydrate Molecular Weight is %3.4f [g/mol]',
S_Mg_MW)
fprintf('\nPercent of Magnesium Nitrate Hexahydrate weight from Mg in decimal form is
%1.4f', Pct_Mg_S_Mg)
fprintf('\nAmount of Magnesium Nitrate Hexahydrate needed for the desired product size
is %2.4f [g]\n', A_S_Mg_needed)

%Na2O surrogate material Na N O3 [Sodium Nitrate]
S_Na_MW = (3*O)+N+Na; %[g/mol]
Pct_Na_S_Na = Na/S_Na_MW; %[percent of Na surrogate weight from Na in decimal
form]
A_S_Na_needed = Na_needed/Pct_Na_S_Na; %amount of Na surrogate needed for the
desired product size [g]
fprintf('\nNa2O surrogate material is Sodium Nitrate')
fprintf('\nAmount of Na needed for the desired product size is %1.4f [g]', Na_needed)
fprintf('\nSodium Nitrate Molecular Weight is %3.4f [g/mol]', S_Na_MW)
fprintf('\nPercent of Sodium Nitrate weight from Na in decimal form is %1.4f',
Pct_Na_S_Na)
fprintf('\nAmount of Sodium Nitrate needed for the desired product size is %2.4f [g]\n',
A_S_Na_needed)

%FeO surrogate material Fe N3 O9 9*(H2O) [Iron (III) Nitrate Nonahydrate]
S_Fe_MW = Fe+(3*N)+(18*O)+(18*H); %[g/mol]
Pct_Fe_S_Fe = Fe/S_Fe_MW; %[percent of Fe surrogate weight from Fe in decimal
form]
A_S_Fe_needed = Fe_needed/Pct_Fe_S_Fe; %amount of Fe surrogate needed for the
desired product size [g]
fprintf('\nFeO surrogate material is Iron (III) Nitrate Nonahydrate')
fprintf('\nAmount of Fe needed for the desired product size is %1.4f [g]', Fe_needed)
fprintf('\nIron (III) Nitrate Nonahydrate Molecular Weight is %3.4f [g/mol]', S_Fe_MW)
```

```
fprintf('\nPercent of Iron (III) Nitrate Nonahydrate weight from Fe in decimal form is %1.4f', Pct_Fe_S_Fe)
fprintf('\nAmount of Iron (III) Nitrate Nonahydrate needed for the desired product size is %2.4f [g]\n', A_S_Fe_needed)

%TiO2 surrogate material C12 H28 O4 Ti [Titanium Isopropoxide]
S_Ti_MW = (12*C)+(28*H)+(4*O)+Ti; %[g/mol]
Pct_Ti_S_Ti = Ti/S_Ti_MW; %[percent of Ti surrogate weight from Ti in decimal form]
S_Ti_needed = Ti_needed/Pct_Ti_S_Ti; %amount of Ti surrogate needed for the desired product size [g]
p_TiIso = 937; %TiIso density [kg/m^3]
A_S_Ti_needed = (1/1000)*((1e6)/1)*(1/p_TiIso)*S_Ti_needed; %amount of Ti surrogate needed for the desired product size [ml]
fprintf('\nTiO2 surrogate material is Titanium Isopropoxide')
fprintf('\nAmount of Ti needed for the desired product size is %1.4f [g]', Ti_needed)
fprintf('\nTitanium Isopropoxide Molecular Weight is %3.4f [g/mol]', S_Ti_MW)
fprintf('\nPercent of Titanium Isopropoxide weight from Ti in decimal form is %1.4f', Pct_Ti_S_Ti)
fprintf('\nAmount of Titanium Isopropoxide needed for the desired product size is %2.4f [g]', S_Ti_needed)
fprintf('\nTitanium Isopropoxide density is %3.4f [kg/m^3]', p_TiIso)
fprintf('\nAmount of Titanium Isopropoxide needed for the desired product size is %2.4f [ml]\n', A_S_Ti_needed)
```

THIS PAGE INTENTIONALLY LEFT BLANK

APPENDIX C. EDS ANALYSIS PROCESS (EXAMPLE)

A. EDS SPECTRA DATA FROM EDAX GENESIS SOFTWARE AND SEM

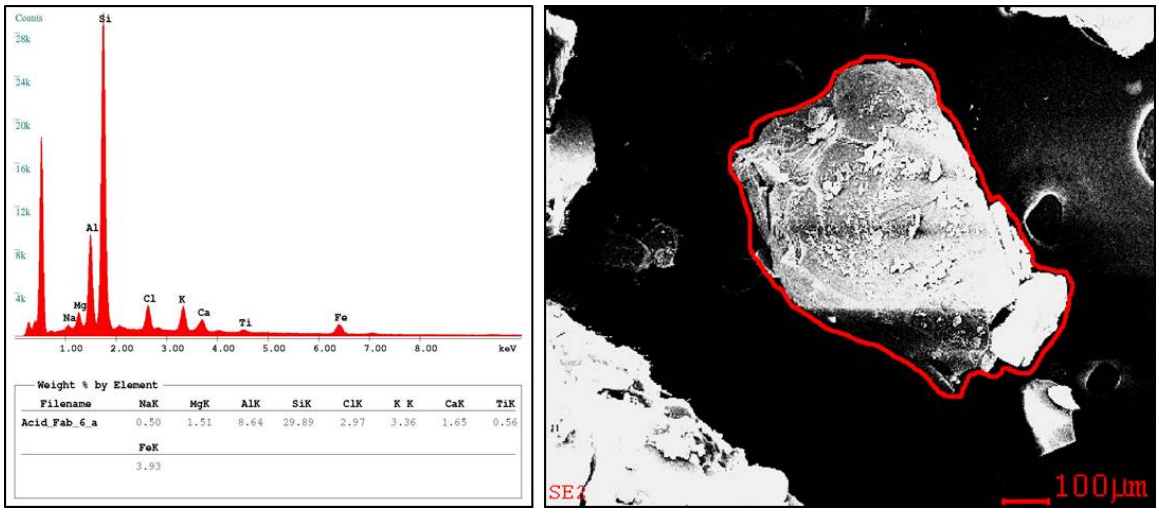

EDS spectra from acid solution thermal bath fabrication. Fifth area assessed from last fabrication performed. Data for all areas assessed was tabulated in Microsoft Excel (Figure 69).

Figure 69. EDS Spectra Data for One Area from Acid Solution Thermal Bath Fabrication, as Fabricated

B. TABULATION OF DATA AND STANDARD DEVIATION

EDS Composition Comparison for Acid Solution Synthesis with Fe and Ti added in Solution										
	Elemental Weight Percent from EDS									
Sample ID	Sodium	Magnesium	Aluminum	Silicon	Potassium	Calcium	Titanium	Iron	Chloride	Oxygen
Target	0.5638	1.4111	6.531	34.1414	2.1086	1.4651	0.5394	4.6483	0	48.5913
Acid_Fe_Ti_Salts_Fab_6_Area_1	0.45	1.53	10.72	26.44	3.76	1.86	0.77	5.75	2.79	48.72
Acid_Fe_Ti_Salts_Fab_6_Area_2	0.45	1.44	8.36	28.73	3.37	1.84	0.75	5.75	2.98	49.31
Acid_Fe_Ti_Salts_Fab_6_Area_3	0.6	1.71	10.77	27.17	3.45	1.79	0.53	4.52	3.16	49.46
Acid_Fe_Ti_Salts_Fab_6_Area_4	0.37	1.38	8.09	27.75	4.35	2.2	0.94	6.32	2.97	48.6
Acid_Fe_Ti_Salts_Fab_6_Area_5	0.5	1.51	8.64	29.89	3.36	1.65	0.56	3.93	2.97	49.96
Acid_Fe_Ti_Salts_Fab_6_Area_6	0.44	1.39	9.24	28.56	3.15	1.75	0.64	4.9	3.44	49.93
Acid_Fe_Ti_Salts_Fab_6_Area_7	0.56	1.52	8.17	30.16	3.25	1.61	0.64	4.25	2.82	49.84
Acid_Fe_Ti_Salts_Fab_6_Area_8	0.5	1.41	8.6	30.04	2.91	1.55	0.62	4.27	2.99	50.1
Acid_Fe_Ti_Salts_Fab_6_Area_9	0.51	1.54	10.18	28.56	3.05	1.59	0.58	4.11	3.03	49.88
Acid_Fe_Ti_Salts_Fab_6_Area_10	0.5	1.45	8.99	29.4	3.06	1.69	0.56	4.38	3.09	49.97
Acid_Fe_Ti_Salts_Fab_6_Area_2_map_a	0.44	1.39	8.09	29.4	3.35	1.77	0.85	5.17	2.95	49.54
Acid_Fe_Ti_Salts_Fab_6_Area_2_map_b	0.48	1.4	8.09	29.45	3.3	1.75	0.84	5.09	2.97	49.6
Acid_Fe_Ti_Salts_Fab_6_Area_2_map_c	0.49	1.42	8.08	29.45	3.27	1.78	0.81	5.1	2.96	49.6
Acid_Fe_Ti_Salts_Fab_6_Area_5_map	0.52	1.48	8.44	29.84	3.42	1.72	0.66	4.09	2.94	49.83
Acid_Fe_Ti_Salts_Fab_6_Area_6_map	0.48	1.42	8.95	29.19	3.09	1.62	0.62	4.63	3.25	50
Acid_Fe_Ti_Salts_Fab_6_Area_10_map	0.49	1.51	9.45	28.85	3.1	1.65	0.59	4.47	3.15	49.89

EDS composition comparison for acid solution synthesis with Fe and Ti added in solution, as fabricated. Fe content was added at 50% of target content to adjust for values observed in antecedent fabrications.

Figure 70. EDS Spectra Data for Thermal Bath Acid Fabrication

Standard Deviation	
Na	0.0524
Mg	0.0847
Al	0.9201
Si	1.0506
K	0.3398
Ca	0.1528
Ti	0.1243
Fe	0.6904
Cl	0.1607

Standard deviation calculated using standard software package of Microsoft Excel and EDS composition comparison data from acid solution synthesis with Fe and Ti added in solution (Figure 69).

Figure 71. Standard Deviation by Element from EDS Spectra Data for Thermal Bath Acid Fabrication

C. MATLAB CODE

```
%%Surrogate Material Composition Comparison to Target Composition
%Source data from EDS. Elemental weight percents are consolidated into
%excel file.

%Acid Solution Thermal Bath Fabrication

clear all
close all
clc

%Reference to source file
filename = 'Acid_Solution_TempBath_as_fabricated.xlsx';
%Elements and their order
Element = ['Na ' 'Mg ' 'Al ' 'Si ' 'K ' 'Ca ' 'Ti ' 'Fe ' 'Cl '];
%Element = [1 2 3 4 5 6 7 8 9];
%Target Weight Percents
Target = xlsread(filename,'B4:J4')
k = 9;
Acid_Fe_Ti_Salts_OvenDry_Area_Average = zeros(1,k);
Acid_Fe_Ti_Salts_Fab_6_Area_1 = zeros(1,k);
Acid_Fe_Ti_Salts_Fab_6_Area_2 = zeros(1,k);
Acid_Fe_Ti_Salts_Fab_6_Area_3 = zeros(1,k);
Acid_Fe_Ti_Salts_Fab_6_Area_4 = zeros(1,k);
Acid_Fe_Ti_Salts_Fab_6_Area_5 = zeros(1,k);
Acid_Fe_Ti_Salts_Fab_6_Area_6 = zeros(1,k);
Acid_Fe_Ti_Salts_Fab_6_Area_7 = zeros(1,k);
Acid_Fe_Ti_Salts_Fab_6_Area_8 = zeros(1,k);
Acid_Fe_Ti_Salts_Fab_6_Area_9 = zeros(1,k);
Acid_Fe_Ti_Salts_Fab_6_Area_10 = zeros(1,k);
Acid_Fe_Ti_Salts_Fab_6_Area_map_2a = zeros(1,k);
Acid_Fe_Ti_Salts_Fab_6_Area_map_2b = zeros(1,k);
Acid_Fe_Ti_Salts_Fab_6_Area_map_2c = zeros(1,k);
Acid_Fe_Ti_Salts_Fab_6_Area_map_5 = zeros(1,k);
Acid_Fe_Ti_Salts_Fab_6_Area_map_6 = zeros(1,k);
Acid_Fe_Ti_Salts_Fab_6_Area_map_10 = zeros(1,k);

%Area 1
Acid_Fe_Ti_Salts_Fab_6_Area_1 = xlsread(filename,'B5:J5')
%Area 2
Acid_Fe_Ti_Salts_Fab_6_Area_2 = xlsread(filename,'B6:J6')
%Area 3
Acid_Fe_Ti_Salts_Fab_6_Area_3 = xlsread(filename,'B7:J7')
%Area 4
Acid_Fe_Ti_Salts_Fab_6_Area_4 = xlsread(filename,'B8:J8')
%Area 5
Acid_Fe_Ti_Salts_Fab_6_Area_5 = xlsread(filename,'B9:J9')
%Area 6
Acid_Fe_Ti_Salts_Fab_6_Area_6 = xlsread(filename,'B10:J10')
%Area 7
Acid_Fe_Ti_Salts_Fab_6_Area_7 = xlsread(filename,'B11:J11')
%Area 8
Acid_Fe_Ti_Salts_Fab_6_Area_8 = xlsread(filename,'B12:J12')
```

```
%Area 9
Acid_Fe_Ti_Salts_Fab_6_Area_9 = xlsread(filename,'B13:J13')
%Area 10
Acid_Fe_Ti_Salts_Fab_6_Area_10 = xlsread(filename,'B14:J14')
%Area Map 2a
Acid_Fe_Ti_Salts_Fab_6_Area_map_2a = xlsread(filename,'B15:J15')
%Area Map 2b
Acid_Fe_Ti_Salts_Fab_6_Area_map_2b = xlsread(filename,'B16:J16')
%Area Map 2c
Acid_Fe_Ti_Salts_Fab_6_Area_map_2c = xlsread(filename,'B17:J17')
%Area Map 5
Acid_Fe_Ti_Salts_Fab_6_Area_map_5 = xlsread(filename,'B18:J18')
%Area Map 6
Acid_Fe_Ti_Salts_Fab_6_Area_map_6 = xlsread(filename,'B19:J19')
%Area Map 10
Acid_Fe_Ti_Salts_Fab_6_Area_map_10 = xlsread(filename,'B20:J20')

%Number of Areas
n = 16;
%Sample Average
for m = 1:k
    Acid_Fe_Ti_Salts_Fab_6_Average(m) =
(Acid_Fe_Ti_Salts_Fab_6_Area_1(m)+...

Acid_Fe_Ti_Salts_Fab_6_Area_2(m)+Acid_Fe_Ti_Salts_Fab_6_Area_3(m)+...

Acid_Fe_Ti_Salts_Fab_6_Area_4(m)+Acid_Fe_Ti_Salts_Fab_6_Area_5(m)+...

Acid_Fe_Ti_Salts_Fab_6_Area_6(m)+Acid_Fe_Ti_Salts_Fab_6_Area_7(m)+...

Acid_Fe_Ti_Salts_Fab_6_Area_8(m)+Acid_Fe_Ti_Salts_Fab_6_Area_9(m)+...

Acid_Fe_Ti_Salts_Fab_6_Area_10(m)+Acid_Fe_Ti_Salts_Fab_6_Area_map_2a(m)
+...

Acid_Fe_Ti_Salts_Fab_6_Area_map_2b(m)+Acid_Fe_Ti_Salts_Fab_6_Area_map_2
c(m)+...

Acid_Fe_Ti_Salts_Fab_6_Area_map_5(m)+Acid_Fe_Ti_Salts_Fab_6_Area_map_6(
m)+...
        Acid_Fe_Ti_Salts_Fab_6_Area_map_10(m))/n
    m = m+1;
end

fprintf('\nElement 1 = Na')
fprintf('\nElement 2 = Mg')
fprintf('\nElement 3 = Al')
fprintf('\nElement 4 = Si')
fprintf('\nElement 5 = K')
fprintf('\nElement 6 = Ca')
fprintf('\nElement 7 = Ti')
fprintf('\nElement 8 = Fe')
fprintf('\nElement 9 = Cl')
%%
%%
```

```
model_series = [Target;...
    Acid_Fe_Ti_Salts_Fab_6_Average]'
% model_error = [0 0.08773068; 0 0.560880261; 0 0.679337913; 0
1.096429812; 0 1.438304557; 0 0.79099094; 0 0.184282392; 0 2.21345582;0
1.159551637];
model_error = zeros(9,2);
model_error(:,2) = xlsread(filename,'N4:N12')
figure ;
bar(model_series)
set(gca,'XTickLabel',{'Na','Mg','Al','Si','K','Ca','Ti','Fe','Cl'})
set(gca,'GridLineStyle','-')
xlabel('Element'); %X Axis Label
ylabel('Elemental Weight Percent, [%]'); %Y Axis Label
%title('Acid Solution Fabrication 6 with Standard Deviation');
hold on;
numgroups = size(model_series, 1);
numbars = size(model_series, 2);
groupwidth = min(numbars/(numbars+1.5));
for i = 2
      x = (1:numgroups) - groupwidth/2 + (2*i-1) * groupwidth /
(2*numbars);  % Aligning error bar with individual bar
      errorbar(x, model_series(:,i), model_error(:,i), 'k',
'linestyle', 'none');
end
legend([],'Target',...
    'Sample Average','Location','NorthEast');
h = legend()
```

THIS PAGE INTENTIONALLY LEFT BLANK

LIST OF REFERENCES

[1] K. Stark et al., “Dose assessment in environmental radiological protection: State of the art and perspectives,” *J. Environ. Radioact.*, vol. 175, pp. 105–114, May 2017. Available: https://www.ncbi.nlm.nih.gov/pubmed/28505478

[2] International Atomic Energy Agency, “Advances in Nuclear Forensics: Countering the Evolving Threat of Nuclear and Other Radioactive Material out of Regulatory Control,” Vienna, Austria, 2015. Available: https://www.iaea.org/publications/10881/advances-in-nuclear-forensics-countering-the-evolving-threat-of-nuclear-and-other-radioactive-material-out-of-regulatory-control

[3] International Atomic Energy Agency, “Application of Nuclear Forensics in Combating Illicit Trafficking of Nuclear and Other Radioactive Material,” Vienna, Austria, Rep. TECDOC No. 1730, 2014. Available: http://www-pub.iaea.org/books

[4] *Radiological Worker Training*, Change Notice No. 2, U.S. Department of Energy, Washington, DC, USA, 2008. Available: https://www.standards.doe.gov/standards-documents/1100/1130-bhdbk-2008-cn2-2013-reaff-2013

[5] “Radiological Fundamentals,” class notes for Radiological Fundamentals, Naval Postgraduate School, Monterey, CA, USA, 2004.

[6] D. Kramer, “Nuclear forensics: Role, state of the art, program needs,” *Physics Today*, vol. 61, Issue. 6, Jun. 2008. [Online]. doi: 10.1063/1.2947644

[7] *Nuclear Forensics in Support of Investigations*, IAEA Nuclear Security Series No. 2-G, International Atomic Energy Agency, Vienna, Austria, 2015.

[8] N. Sharp et al., “Rapid analysis of trinitite with nuclear forensic applications for post-detonation material analyses,” *J. of Radioanalytical and Nucl. Chemistry*, vol. 302, no. 1, pp. 57–67, Oct. 2014.

[9] K. J. Moody, P. M. Grant, and I. D. Hutcheon, *Nuclear Forensic Analysis, Second Edition*. CRC Press, 2014.

[10] R. P. Mariella Jr. et al., “Laser comminution of submerged samples,” *J. of Appl. Physics*, vol. 114, no. 1, May 2013.

[11] R. P. Mariella Jr. et al., “Laser-Driven Hydrothermal Processing,” International Patent Application PCT/US2014/011120, Jan. 10, 2014.

[12] A. Camargo, “Characterization of particles created by laser-driven hydrothermal processing,” M.S. thesis, Dept. of Mechanical and Aerospace Engineering, NPS, Monterey, CA, USA, 2016.

[13] C. Koeberl, “Tektite origin by hypervelocity asteroidal or cometary impact: Target rocks, source craters, and mechanisms,” *Geological Society of America, Inc.*, Boulder, CO, Special Paper 293, 1992.

[14] G. N. Eby et al., “Trinitite redux: Mineralogy and petrology,” *Amer. Mineralogist*, vol. 100, no. 2–3, pp. 427–441, Feb. 2015.

[15] S. Menon, A. Camargo, C. Wu, R. Mariella and C. Luhrs, “Characterization of particles created by laser-driven hydrothermal processing,” *Materials Characterization*, vol. 133, pp. 1–9, Nov. 2017. [Online]. Available: https://doi.org/10.1016/j.matchar.2017.09.018

[16] R. P. Mariella Jr et al., “Laser-Driven Hydrothermal Process Studied with Excimer Laser Pulses,” *J. of Appl. Physics*, vol. 122, no. 7, Aug. 2017. [Online]. doi: 10.1063/1.4999306

[17] R. S. Dingus and R. J. Scammon. “Ablation of material by front surface spallation,” Los Alamos National Laboratory, Los Alamos, NM, USA, Rep. LA-UR--91-1911.

[18] R. A. Laudise, “Kinetics of hydrothermal quartz crystallization,” *J. Am. Chem. Soc.*, vol. 81, no. 3, pp. 562–566, Feb. 1959. [Online]. doi: 10.1021/ja01512a013

[19] R. P. Mariella Jr, private communication, Nov. 2017.

[20] C. Brinker and G. Scherer, *Sol-Gel Science: The Physics and Chemistry of Sol-Gel Processing*, San Diego, CA, USA, Academic Press, Inc, 1990.

[21] C. N. R. Rao and K. Biswas, “Soft chemistry routes,” *Essentials of Inorganic Materials Synthesis*, Hoboken, NJ: John Wiley & Sons, Inc, 2015, ch. 10. doi: 10.1002/9781118892671

[22] J. D. Wright and N.A.J.M. Sommerdijk, “Introduction,” *Sol-Gel Materials Chemistry and Applications*, CRC Press, 2000, ch. 1. pp. 2–8.

[23] A. E. Danks, S R Hall and Z Schnepp, “The evolution of ‘sol-gel’ chemistry as a technique for materials synthesis,” *Mater. Horiz.*, vol. 3, no. 2, pp. 91–112, Mar. 2016. [Online]. doi: 10.1039/c5mh00260e

[24] G. Schottner, “Hybrid sol−gel-derived polymers: Applications of Multifunctional Materials,” *Chem. Mater.*, vol. 13, pp. 3422–3435, Oct. 2001. [Online]. doi: 10.1021/cm011060m

[25] B. G. Trewyn et al., “Synthesis and functionalization of a mesoporous silica nanoparticle based on the sol–gel process and applications in controlled release,” *Acc. Chem. Res.*, vol. 40, no. 9, pp. 846–853, Jul. 2007. [Online]. doi: 10.1021/ar600032u

[26] G. Cao, *Nanostructures and Nanomaterials: Synthesis, Properties & Applications*. Covent Garden, London, UK: Imperial College Press, 2004.

[27] R. Akhter, N. Shirai and M. Ebihara, “Chemical characteristics of dalat tektites,” in 45th Lunar and Planetary Science Conference, Houston, TX, 2014.

[28] D. R. Chapman, “Australasian Tektite Geographic Pattern, Crater and Ray of Origin, and Theory of Tektite Events,” *J. of Geophysical Res.*, vol. 76, no. 26, pp. 6309–6338, Sep. 1971.

[29] W. D. Callister, Jr. and D. G. Rethwisch, *Materials Science and Engineering: An Introduction*, 9th ed. Hoboken, NJ, USA: John Wiley and Sons, 2014.

[30] M. R. Lindeburg , *Mechanical Engineering Reference Manual for the PE Exam*, 13th ed., Professional Publications Inc., 2013, ch. 20, pp. 1-24.

[31] O. A. Yakimenko, *Engineering Computations and Modeling in MATLAB/Simulink*. Reston, Virginia, USA: American Institute of Aeronautics and Astronautics, Inc., 2011.

[32] “Normality & Molarity Calculator,” Sigma Aldrich. [Online]. Available: https://www.sigmaaldrich.com/chemistry/stockroom-reagents/learning-center/technical-library/molarity-calculator.html

[33] J. O. Eckert Jr. et al., “Kinetics and mechanisms of hydrothermal synthesis of barium titanate,” *J. Am. Ceram. Soc.*, vol. 79, no. 11, pp. 2929–2939, Nov., 1996.

[34] F. M. White, *Fluid Mechanics*, 7th ed. New York, NY, USA: McGraw Hill, 2008, ch. 1, sec. 1.9, pp. 25–30.

[35] “NETZSCH Proteus Software for Thermal Analysis,”NETZSCH. Accessed November 17, 2017. [Online]. Available: https://www.netzsch-thermal-analysis.com/en/products-solutions/software/proteus/

[36] L. Esquivias, Ed., *Inorganic Dispersed-phase Composites by Sol-Gel Processing: An Update* (Key Engineering Materials). Durnten-Zurich, Switzerland: Trans Tech Publications Ltd, 2009, pp. 121–139.

[37] M. Yoshimura and K. Byrappa, “Hydrothermal processing of materials: past, present and future,” *J. Mater. Sci.*, vol. 43, pp. 2085–2103, Nov. 2017. [Online]. doi: 10.1007/s10853-007-1853-x

[38] “Chlorine (Cl),” *Encyclopædia Britannica, inc.* Accessed October 25, 2017. [Online]. Available: https://www.britannica.com/science/chlorine/Physical-and-chemical-properties

[39] “Properties of Salt,” Salt Association. Accessed November 13, 2017. [Online]. Available: http://www.saltassociation.co.uk/education/properties-of-salt/

[40] M. Perchacz et al., “Ionic Liquid-Silica Precursors via Solvent-Free Sol–Gel Process and Their Application in Epoxy-Amine Network: A Theoretical/Experimental Study,” *ACS App. Mat. Interfaces*, vol. 9, no. 19, pp. 16474–16487, Apr. 2017. [Online]. doi: 10.1021/acsami.7b02631

[41] C. N. R. Rao and K. Biswas, “Ceramic Methods,” in *Essentials of Inorganic Materials Synthesis*, Hoboken, NJ: John Wiley & Sons, Inc, 2015, ch. 3. doi: 10.1002/9781118892671

[42] J. I. Goldstein et al., *Scanning Electron Microscopy and X-ray Microanalysis.* New York, NY, USA: Plenum Press, 1992. [Online]. doi: 10.1 0071978-1-4613-0491-3

INITIAL DISTRIBUTION LIST

1. Defense Technical Information Center
   Ft. Belvoir, Virginia

2. Dudley Knox Library
   Naval Postgraduate School
   Monterey, California